Position Statement on the Use of Multiparametric Mapping for Advanced Tissue Characterization by Cardiovascular Magnetic Resonance – 2026

Developed by: Department of Cardiovascular Imaging of the Brazilian Society of Cardiology (in Portuguese: Departamento de Imagem Cardiovascular da Sociedade Brasileira de Cardiologia – DIC/SBC)

Position Statement Authors: *Isabela Bispo Santos da Silva Costa,[1,2] Jorge Andion Torreão,[3,4] Henrique Simão Trad,[5] Roberto Sasdelli Neto,[6] Gustavo Lemos Palandre,[7] Gabriel Cordeiro Camargo,[8,9] Rodrigo de Jesus Louzeiro Melo,[3] Luíz Flávio Galvão Gonçalves,[10,11,12,13,14] Fábio de Morais Medeiros,[15,16,17] Gilberto Szarf,[6,18] Guilherme Sant'Anna Antunes de Azevedo,[19,20] Eduardo Belisario Falchetto,[21] Tiago Augusto Magalhães,[22,23] Gabriela Liberato,[3,24] Renata Ávila Cintra,[25,26,27,28,29] Marly Maria Uellendahl Lopes,[18,30] Leonardo Sara da Silva,[31] Clério Francisco de Azevedo Filho,[32] Tiago Senra Garcia dos Santos,[24,33,34,35] Valéria de Melo Moreira,[3,22] Ariane Binoti Pacheco Leal,[36,37] Ludhmila Abrahão Hajjar,[38] Antônio Tito Paladino Filho,[33,39,40,41] Kevin Rafael de Paula Morales,[3] Fábio Fernandes,[3] Otavio Rizzi Coelho-Filho,[42]*

Universidade Federal do Maranhão,[1] São Luís, MA – Brazil
Instituto do Câncer do Estado de São Paulo,[2] São Paulo, SP – Brazil
Instituto do Coração do Hospital das Clínicas da Faculdade de Medicina da Universidade de São Paulo,[3] São Paulo, SP – Brazil
Santa Casa de Misericórdia da Bahia,[4] Salvador, BA – Brazil
Lotus Radiologia,[5] Ribeirão Preto, SP – Brazil
Hospital Israelita Albert Einstein,[6] São Paulo, SP – Brazil
Universidade Federal de Santa Catarina,[7] Florianópolis, SC – Brazil
Instituto Nacional de Cardiologia,[8] Rio de Janeiro, RJ – Brazil
Rede D'Or São Luiz,[9] Rio de Janeiro, RJ – Brazil
Hospital São Lucas — Rede D'Or São Luiz,[10] Aracaju, SE – Brazil
Clínica de Medicina Nuclear, Endocrinologia e Diabetes,[11] Aracaju, SE – Brazil
Clinradi Radioterapia e Imagem,[12] Aracaju, SE – Brazil
Hospital Decós,[13] Aracaju, SE – Brazil
Hospital Universitário da Universidade Federal de Sergipe,[14] Aracaju, SE – Brazil
Sabin Diagnóstico por Imagem,[15] Brasília, DF – Brazil
Grupo Santa,[16] Brasília, DF – Brazil
Rede D'Or São Luiz,[17] Brasília, DF – Brazil
Escola Paulista de Medicina da Universidade Federal de São Paulo,[18] São Paulo, SP – Brazil
Ecomax Diagnóstico por Imagem,[19] Blumenau, SC – Brazil
Hospital Unimed Blumenau,[20] Blumenau, SC – Brazil
Hospital Felício Rocho,[21] Belo Horizonte, MG – Brazil
Hospital do Coração,[22] São Paulo, SP – Brazil
Hospital de Clínicas da Universidade Federal do Paraná,[23] Curitiba, PR – Brazil
Hospital Sírio-Libanês,[24] São Paulo, SP – Brazil
Hospital Memorial Star — Rede D'Or São Luiz,[25] Recife, PE – Brazil
Hospital Esperança — Rede D'Or São Luiz,[26] Recife, PE – Brazil
Hospital Memorial — Rede D'Or São Luiz,[27] Recife, PE – Brazil
Hospital São Marcos — Rede D'Or São Luiz,[28] Recife, PE – Brazil
Hospital Esperança Olinda — Rede D'Or São Luiz,[29] Olinda, PE – Brazil
Diagnósticos da América (DASA),[30] São Paulo, SP – Brazil
Centro de Diagnóstico por Imagem Premium,[31] Goiânia, GO – Brazil
Duke University,[32] Durham, NC – United States
Instituto Dante Pazzanese de Cardiologia,[33] São Paulo, SP – Brazil
Hospital Vera Cruz,[34] Campinas, SP – Brazil
Alta Diagnósticos — Diagnósticos da América,[35] São Paulo, SP – Brazil
Bioscan Diagnóstico por Imagem,[36] Vitória, ES – Brazil
Hospital Estadual Infantil e Maternidade Alzir Bernardino Alves,[37] Vitória, ES – Brazil

DOI: https://doi.org/10.36660/abc.20260859i

Hospital das Clínicas da Faculdade de Medicina da Universidade de São Paulo,[38] São Paulo, SP – Brazil
Hospital Vila Nova Star,[39] São Paulo, SP – Brazil
Hospital e Maternidade Sepaco,[40] São Paulo, SP – Brazil
Rede D'Or São Luiz,[41] São Paulo, SP – Brazil
Disciplina de Cardiologia, Departamento de Clínica Médica, Faculdade de Ciências Médicas da Universidade Estadual de Campinas,[42] Campinas, SP – Brazil

SBC Clinical Practice Guidelines Committee: Humberto Graner Moreira (Chair), Félix José Alvarez Ramires, Helena Cramer Veiga Rey, José Augusto Soares Barreto Filho, Nadine Oliveira Clausell.

How to cite: Costa IBSS, Torreão JA, Trad HS, Sasdelli Neto R, Palandre GL, Camargo GC, et al. Position Statement on the Use of Multiparametric Mapping for Advanced Tissue Characterization by Cardiovascular Magnetic Resonance. Arq. Bras. Cardiol. 2026;123(10):e20260859.

Data Availability: all data supporting this Position Statement is contained in the manuscript.

Reviewing Editor: Humberto Graner Moreira

Note: These position statements are for information purposes and should not replace the clinical judgment of a physician, who must ultimately determine the appropriate treatment for each patient.

Correspondence: Sociedade Brasileira de Cardiologia – Av. Marechal Câmara, 360/330 – Centro – Rio de Janeiro, Brazil – Postal Code 20020-907. E-mail: diretrizes@cardiol.br.

Agradecimento aos Revisores

The authors thank the following reviewers for their invaluable contributions: Carlos Eduardo Rochitte, Cesar Higa Nomura, Ibraim Masciarelli Pinto, and Silvio Henrique Barberato.

Position Statement on the Use of Multiparametric Mapping for Advanced Tissue Characterization by Cardiovascular Magnetic Resonance – 2026

The report below lists the relationships existing or that occurred during the 12-month period preceding the start of the document preparation:

Expert	Type of relationship with industry
Antonio Tito Paladino Filho	Nothing to be declared
Ariane Binoti Pacheco Leal	Nothing to be declared
Clerio Francisco de Azevedo Filho	Nothing to be declared
Eduardo Belisario Falchetto	Nothing to be declared
Fabio Fernandes	Nothing to be declared
Fábio de Morais Medeiros	Nothing to be declared
Gabriel Cordeiro Camargo	Nothing to be declared
Gabriela Liberato	Nothing to be declared
Gilberto Szarf	Nothing to be declared
Guilherme Sant'Anna Antunes de Azevedo	Nothing to be declared
Gustavo Lemos Pelandré	Nothing to be declared
Henrique Simão Trad	Nothing to be declared
Isabela Bispo Santos da Silva Costa	Nothing to be declared
Jorge Andion Torreão	Nothing to be declared
Kevin Rafael de Paula Morales	Nothing to be declared
Leonardo Sara da Silva	Nothing to be declared
Ludhmila Abrahão Hajjar	Nothing to be declared
Luiz Flávio Galvão Gonçalves	Nothing to be declared
Marly Maria Uellendahl Lopes	Nothing to be declared
Otavio R Coelho-Filho	Financial Disclosure – Astra Zeneca: Consulting – Cardiology. – Pfizer: Consulting – Cardiology. – Viatris: Consulting – Cardiology. – Alnylam: Consulting – Cardiology. – GSK: Consulting – Cardiology.
Renata Ávila Cintra	Nothing to be declared
Roberto Sasdelli Neto	Nothing to be declared
Rodrigo de Jesus Louzeiro Melo	Nothing to be declared

Tiago Augusto Magalhães	Financial Disclosure – Novartis: Lectures – Training. – Eli Lilly: Lectures – Training. – Knight: Lectures – Training. – MSD: Lectures – Training. – Daiichi-Sankyo: Lectures – Training. – AstraZeneca: Lectures – Training. – Roche: Lectures – Training. – Gilead: Lectures – Training. – Pint Pharma: Lectures – Training. – Amgen: Lectures – Training.
Tiago Senra	Nothing to be declared
Valéria de Melo Moreira	Nothing to be declared

List of Abbreviations and Acronyms

[^{18}F]FDG	Fluorine-18-labeled fluorodeoxyglucose
2D	Two-dimensional
3D	Three-dimensional
4CH	Four-chamber
AC	Arrhythmogenic cardiomyopathy
ACC	American College of Cardiology
AHA	American Heart Association
AI	Artificial intelligence
ANCA	Antineutrophil cytoplasmic antibodies
AoS	Aortic stenosis
ARDs	Autoimmune rheumatic diseases
ATTR	Transthyretin
bSSFP	balanced steady-state free precession
CCTGA	Congenitally corrected transposition of the great arteries
CMR	Cardiac magnetic resonance imaging
CT	Computed tomography
CT-ECV	Extracellular volume by computed tomography
DM	Dermatomyositis
DSP	Desmoplakin
ECG	Electrocardiogram
ECV	Extracellular volume
EMF	Endomyocardial fibrosis
ERT	Enzyme replacement therapy
ESC	European Society of Cardiology
FLNC	Filamin C
GLS	Global longitudinal strain
GraSE	Gradient- and spin-echo
HCM	Hypertrophic cardiomyopathy
HF	Heart failure
ICD	Implantable cardioverter-defibrillator
ICI	Immune checkpoint inhibitor
IIM	Idiopathic inflammatory myopathies
LC	Light-chain
LGE	Late gadolinium enhancement
LMNA	Lamin A/C
LV	Left ventricle
LVEF	Left ventricular ejection fraction

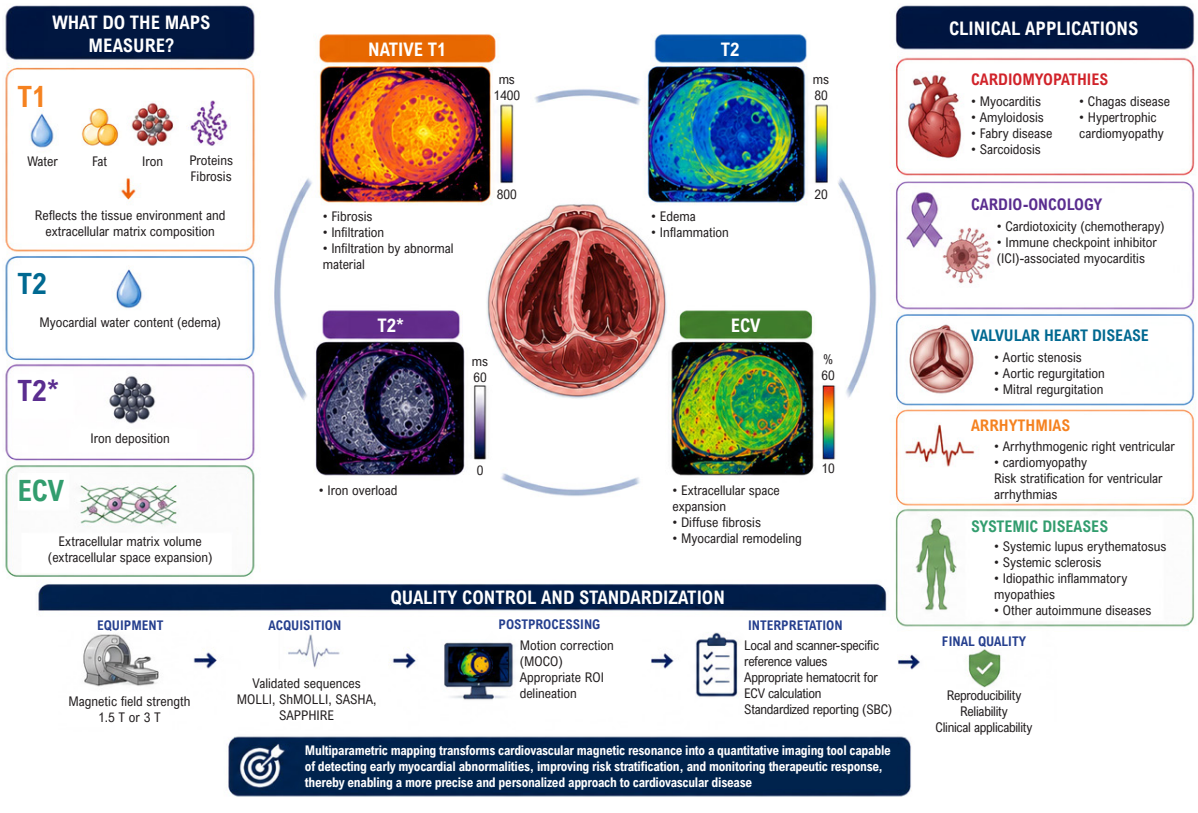
LVH	Left ventricular hypertrophy
mcLARO	Multi-contrast learned acquisition and reconstruction optimization
MESE	Multi-echo spin-echo
MOCO	Motion correction
MOLLI	Modified look-locker inversion recovery
MRI	Magnetic resonance imaging
MVP	Mitral valve prolapse
NDLVC	Non-dilated left ventricular cardiomyopathy
PLN	Phospholamban
PM	Polymyositis
ROC	Receiver operating characteristic
ROI	Region of interest
RV	Right ventricle
SAPPHIRE	Saturation-pulse-prepared heart-rate-independent inversion recovery
SASHA	Saturation recovery single-shot acquisition
SCMR	Society for Cardiovascular Magnetic Resonance
SD	Standard deviation
shMOLLI	Shortened modified look-locker inversion recovery
SLE	Systemic lupus erythematosus
SMART1Map	Saturation method using adaptive recovery times for cardiac T1 mapping
SNR	Signal-to-noise ratio
SSc	Systemic sclerosis
SSFP	Steady-state free precession
T	Tesla
T1M	T1 mapping
T2M	T2 mapping
T2-prep	T2 preparation
TE	Echo time
TI	Inversion time
VT	Ventricular tachycardia
WASOG	World Association for Sarcoidosis and Other Granulomatous Diseases

Table of Contents

1. Introduction 9
2. Key Concepts – Acquisition Techniques, Protocols, and Analysis/Post-Processing 9
2.1. T1 and ECV Mapping 9
2.1.1. Basic Physics Concepts 9
2.1.2. Myocardial T1 Map Acquisition Techniques 10
2.1.3. Saturation-Recovery Techniques 11
2.1.4. Extracellular Volume 11
2.1.5. Accuracy and Precision 12
2.1.6. Protocols 13
2.1.7. Analysis 13
2.1.8. Reference Values 14
2.1.9. Conclusion 16
2.1.10. Key Takeaways 16
2.2. T2 Mapping 16
2.2.1. Technical Concepts 17
2.2.1.1. Magnetic Resonance Imaging Scanners 17
2.2.1.2. T2 "Preparation" 17
2.2.1.3. Sequence Acquisition Type 17
2.2.1.4. Sequence Types 17
2.2.1.5. Image Acquisition Protocol 17
2.2.1.6. Postprocessing 17
2.2.1.7. Normal Values 18
2.2.1.8. Quality Control 19
2.2.1.9. Key Takeaways 19
2.3. T2* Quantification 19
2.3.1. Definitions and Objectives 20
2.3.2. Traditional (T2*) Quantification Technique 20
2.3.3. T2* Mapping 21
2.3.4. Advantages and Limitations of T2* Maps 21
2.3.5. Limitations 22
2.3.6. Conclusions 23
2.3.7. Key Takeaways 23
3. General Recommendations 23
3.1. Reporting of Results 23
3.1.1. Minimum Structure of Report 23
3.2. Normal Values 23
3.3. Clinical Interpretation 25
3.4. Conclusion 25
3.5. Key Takeaways 25
4. Ischemic Cardiomyopathy 25
4.1. Acute 25
4.2. Chronic 25
4.3. Key Takeaways 26
5. Non-Ischemic Cardiomyopathies 26
5.1 Dilated Phenotype 26
5.1.1. Chagas Disease 26
5.1.1.1. Clinical Applications in Chagas Disease 27
5.1.1.2. Key Takeaways 27
5.1.2. Myocarditis 27
5.1.2.1. Conclusion 28
5.1.2.2. Key Takeaways 28
5.1.3. Iron Overload 29
5.1.3.1. Conclusion 31
5.1.3.2. Key Takeaways 31
5.1.4. Sarcoidosis 31
5.1.4.1. Key Takeaways 32
5.2. Arrhythmogenic Phenotype 32
5.2.1. Conclusion 34
5.2.2. Key Takeaways 34
5.3. Hypertrophic Phenotype 34
5.3.1. Hypertrophic Cardiomyopathy 34
5.3.1.1. Myocardial Fibrosis Associated with Hypertrophic Cardiomyopathy and its Evaluation by Multiparametric Maps 34
5.3.1.2. Use of Multiparametric Maps in the Assessment of HCM 35
5.3.1.3. Differentiation of Hypertrophic Phenotypes 35
5.3.1.4. Native T1 Mapping as a Prognostic Tool in Patients with Hypertrophic Cardiomyopathy 35
5.3.1.5. Role of T2 Mapping in Hypertrophic Cardiomyopathy Diagnosis and Prognosis 35
5.3.1.6. Impact of Multiparametric Maps on Clinical Evaluation of Patients with Hypertrophic Cardiomyopathy 36
5.3.1.7. Limitations 36
5.3.1.8. Conclusion 36
5.3.1.9. Key Takeaways 36
5.3.2. Amyloidosis 36
5.3.2.1. Key Takeaways 37
5.3.3. Fabry Disease 37
5.3.3.1. Morphofunctional Characterization by Cardiac Magnetic Resonance Imaging 37
5.3.3.2. T1 and T2 Mapping 38
5.3.3.3. Extracellular Volume 38
5.3.3.4. Late Enhancement 38
5.3.3.5. Diagnostic Strategy Based on Multiparametric Maps 38
5.3.3.6. Diagnostic Flowchart 39
5.3.3.7. Clinical Applications and Treatment Monitoring 39
5.3.3.8. Limitations and Challenges 39
5.3.3.9. Conclusion 39
5.3.3.9. Key Takeaways 39
5.3.4. Others (Danon, Pompe, Glycogen Storage Diseases) 39
5.3.4.1. Danon Disease 39
5.3.4.2. Pompe Disease 40
5.3.4.3. Type III and IV Glycogen Storage Diseases 41
5.3.4.4. PRKAG2 41
5.3.4.5. Limitations 42
5.3.4.6. Conclusion 42
5.3.4.7. Key Takeaways 42
5.4. Restrictive Phenotype 42
5.4.1. Endomyocardial Fibrosis 42
5.4.1.1. Conclusion 43
5.4.1.2. Key Takeaways 43
5.5. Non-Dilated Phenotype 43
5.5.1. Genetic Cardiomyopathy 43
5.5.1.1. Conclusion 44
5.5.1.2. Key Takeaways 44
5.6. Other 45
5.6.1. Athlete's Heart 45
5.6.2. Hypertensive Cardiomyopathy 45
6. Valvular Heart Disease 46
6.1. Aortic Stenosis 46
6.2. Aortic Regurgitation 46
6.3. Mitral Regurgitation 46

6.3.1. Conclusion 47
6.3.2. Key Takeaways 47
7. Takotsubo Syndrome 47
7.1. Limitations 51
7.2. Key Takeaways 51
8. Congenital Heart Disease 51
8.1. Tetralogy of Fallot 52
8.2. Systemic Right Ventricle 52
8.3. Univentricular Heart 53
8.4. Other Congenital Heart Diseases 53
8.5. Conclusion 53
8.6. Key Takeaways 53
9. Cardio-Oncology 54
9.1. Anthracycline- and Trastuzumab-Induced Cardiotoxicity 54
9.2. Cardiotoxicity from Immune Checkpoint Inhibitors 54
9.3. Radiotherapy-Induced Cardiotoxicity 55
9.4. Key Takeaways 55
10. Systemic Conditions 55
10.1. The Need for Advanced Diagnostic Tools in the Context of Autoimmune Rheumatic Diseases 55
10.2. The Value of Parametric Maps in Myocardial Tissue Characterization 55
10.3. Systemic Lupus Erythematosus 55
10.4. Systemic Sclerosis 56
10.4.1. Correlations and Prognosis 56
10.5. Rheumatoid Arthritis 56
10.6. Idiopathic Inflammatory Myopathies 57
10.7. Antineutrophil Cytoplasmic Antibody-Associated Vasculitis 58
10.8. Detection of Arrhythmogenic Substrates 58
10.9. Implications for Monitoring and Therapy 59
10.10. Conclusions 59
10.11. Key Takeaways 59
11. Masses 59
11.1. Cardiac Tumors 59
11.2. Cardiac Magnetic Resonance Imaging and Parametric Maps 61
11.3. Challenges and Future Prospects 61
11.4. Conclusion 61
11.5. Key Takeaways 61
12. Final Considerations 62
References 64

Central Illustration: Position Statement on the Use of Multiparametric Mapping for Advanced Tissue Characterization by Cardiovascular Magnetic Resonance – 2026



Arq. Bras. Cardiol. 2026;123(10):e2026085

Basic concepts and clinical applicability of multiparametric maps in cardiac magnetic resonance imaging. ECV: extracellular volume; MOLLI: modified look-locker inversion recovery; ROI: region of interest; SAPPHIRE: saturation-pulse prepared heart-rate-independent inversion recovery; SASHA: saturation recovery single-shot acquisition.

1. Introduction

Cardiovascular diseases continue to be the leading cause of morbidity and mortality in Brazil, having a significant impact on both public health and socioeconomic costs. Among these conditions, cardiomyopathies – both ischemic and non-ischemic – stand out for their high prevalence, etiological diversity, and diagnostic complexity. Early and accurate recognition of these diseases is essential for guiding appropriate treatment interventions, improving prognosis, and reducing adverse outcomes.

In this context, cardiac magnetic resonance (CMR) imaging has established itself as one of the primary tools for evaluating patients with cardiomyopathies. In addition to providing detailed anatomical and functional information, CMR plays an increasingly important role as a multiparametric imaging method, allowing for the noninvasive, highly accurate characterization of myocardial tissue. International and national guidelines highlight the importance of CMR and computed tomography (CT) in the diagnosis of ischemic and non-ischemic cardiomyopathies, as well as congenital heart diseases, reinforcing the relevance of these methods in contemporary clinical practice.[1-4]

Among the most significant advances in the field of CMR is multiparametric mapping, which has revolutionized diagnostic capabilities by quantifying intrinsic properties of the myocardium, such as T1 and T2 relaxation times, as well as calculating extracellular volume (ECV). This technique originated in the early relaxation studies of the 1980s, which demonstrated the potential of CMR parameters to distinguish normal from abnormal tissue. Systematic application of multiparametric maps began in earnest in the 2000s, with the development of rapid acquisition sequences and more robust reconstruction algorithms.[5,6] Today, this technique continues to evolve, with increasing international standardization, establishment of reference values for age groups and specific populations, and incorporation into large multicenter cohorts.

Multiparametric mapping allows objective, quantitative, and reproducible assessment of myocardial tissue, overcoming the limitations of qualitative methods such as late gadolinium enhancement (LGE), especially in scenarios involving diffuse myocardial involvement.[7] T1 analysis allows for the early identification of fibrosis and infiltration, T2 reflects edema and inflammatory activity, ECV indirectly quantifies extracellular matrix deposition, and T2* mapping plays a key role in the analysis of myocardial iron deposition.[5] Taken together, these parameters enhance the sensitivity and specificity of CMR in detecting inflammatory and infiltrative cardiomyopathies (such as amyloidosis and Fabry disease), chemotherapy-induced cardiotoxicity, and viral myocarditis, as well as help refine risk stratification in ischemic heart disease.

In addition to their role in early diagnosis, multiparametric maps hold promise for use in longitudinal follow-up, allowing noninvasive monitoring of disease progression and assessment of treatment efficacy. This makes them an essential tool not only for clinical practice but also for translational research, by providing biomarkers of response in clinical trials. Thus, the progressive incorporation of multiparametric mapping into routine practice in specialized centers represents a milestone in the care of cardiomyopathies and points toward an increasingly personalized medicine, based on quantitative, high-precision imaging.

This position statement was developed in accordance with the recommendations of the Brazilian Society of Cardiology (SBC), following a structured methodology to ensure scientific rigor and clinical applicability. A careful selection of the available literature was conducted, prioritizing domestic and international guidelines, consensus documents, original studies with robust methods, systematic reviews, and meta-analyses relevant to the topic. The recommendations contained herein are based on the best available scientific evidence and discussed by experts in the field; they are presented at the end of each section and highlighted as key messages.

This SBC position statement aims to synthesize current knowledge on multiparametric mapping in CMR, contextualize its applicability within the Brazilian setting, standardize information on image acquisition and analysis, and provide guidance on the use and application of this technique for the benefit of patients with cardiomyopathies (Central Illustration).

2. Key Concepts – Acquisition Techniques, Protocols, and Analysis/Post-Processing

2.1. T1 and ECV Mapping

2.1.1. Basic Physics Concepts

T1 refers to the recovery of the longitudinal magnetization of tissues following the application of a radiofrequency pulse. Within a magnetic field, the protons in the tissues excited by that field form a net magnetization vector that can be shifted by radiofrequency pulses. The rate at which the longitudinal component of this magnetization vector recovers after a radiofrequency pulse is called the T1 time, and it is generally exponential.

T1 mapping (T1M) refers to the process of fitting a curve to this exponential function based on different time measurements of the recovery of longitudinal magnetization in the tissues of interest, which is subsequently rendered as an image. Each point in the image corresponds to the T1 value of that tissue, provided that all time measurements refer to the same tissue, highlighting the need for proper registration of the structures to be measured. In the heart, measurements must be acquired while accounting not only for variations imparted by respiratory movement but also for the cardiac cycle, in order to accurately reflect the T1 value of the myocardium.

The assessment of myocardial T1 time and the creation of reliable parametric maps first became possible in 2004, with the modified look-locker inversion-recovery (MOLLI) technique, which combines an inversion recovery sequence with rapid cardiac-gated image acquisition.[8]

Several factors influence the recovery of longitudinal magnetization, including technical factors – such as the magnetic field and acquisition parameters – and tissue-related factors, which ultimately reflect the energy exchange capacity of tissue protons and thus offer the potential for tissue

characterization, allowing for the quantitative representation of normal tissues and pathological processes. Conditions that facilitate such energy exchange in tissues, and thus accelerate the recovery of longitudinal magnetization, result in shorter T1 values. This includes the magnetic field itself, with T1 values being shorter in 1.5-Tesla (T) compared to 3.0-T scanners. The presence of paramagnetic substances also reduces T1 time, as occurs in conditions involving iron infiltration in myocardial tissue and following the injection of gadolinium contrast – an effect that can be used to measure the extracellular space volume, as discussed below.

Excess adipose tissue in the myocardium, by reducing the movement of protons in lipid molecules and cell walls, also shortens T1 time – an effect observed in post-myocardial infarction adipose metaplasia, as well as in sphingolipid deposition in Fabry disease. On the other hand, processes that increase the motion of water molecules reduce T1 relaxation capacity, increasing the recovery time of longitudinal magnetization – an effect observed in myocardial edema and in conditions involving an increase in extracellular matrix volume, such as amyloidosis.

A detailed discussion of the physical principles involved in the creation of myocardial T1 maps would fall outside the scope of this paper; however, it is important to highlight the technical complexity involved so that the reader is aware of the precautions necessary when using this technique. More in-depth information is available elsewhere in the literature.[5,9-14]

2.1.2. Myocardial T1 Map Acquisition Techniques

There are two main techniques for acquiring myocardial T1 maps currently in use: those based on inversion-recovery, i.e. the MOLLI sequences and their variations, and those based on saturation-recovery, which also have variants and adaptations depending on the equipment and manufacturer. These variations and optimizations are distinguished by different acquisition sequences (number of radiofrequency pulses, readout times, pauses, and readout parameters, such as flip angle) and are constantly evolving. Table 1 presents an overview of the main sequences, while Figure 1 shows images acquired using the different techniques.

Inversion-recovery techniques: the MOLLI technique introduced image acquisition from each Look-Locker set using the single-shot technique (one image per radiofrequency pulse), with selective acquisition at the same points in the cardiac cycle and varying inversion times (TIs), allowing for the acquisition of a T1 map slice during a single breath hold. The original MOLLI sequence, however, uses at least 17 heartbeats to complete all the acquisition sets necessary to create the map, with an acquisition protocol described as 3(3)3(3)5 (the numerical sequence refers to the number of inversion pulses, reads, and recovery pauses),[10] requiring a long breath-hold and thus more susceptible to respiratory movement artifacts. The sequence has also been shown to be heart rate-dependent, with a T1 measurement bias, particularly for longer T1 times and higher heart rates. Variants have been proposed to address these shortcomings.

One of the most common such variants is MOLLI with a 5(3)3 acquisition protocol, which shifts acquisition of the first five images to the first inversion pulses, allowing for a longer myocardial recovery time and using only 11 heartbeats for acquisition. Another variation is the ShMOLLI ("shortened" modified Look-Locker imaging) sequence[13] with a 5(1)1(1)1 acquisition protocol, which is less heart rate- dependent and requires only a short breath hold. For post-contrast imaging, the 4(1)3(1)2 protocol is used over 11 heartbeats, improving estimation of T1 time, which is shortened after contrast administration.

Despite these variations and optimizations, inversion-recovery-based sequences such as MOLLI and ShMOLLI

Table 1 – Main acquisition sequences for T1 maps

	T1 Preparation	Acquisition Time	T1 Precision	T1 Accuracy	Comments
MOLLI	IR	17 beats	++	++	Measurement bias, underestimating T1 (T2 effect and magnetization transfer); dependent on heart rate
MOLLI 5(3)3	IR	9–12 beats	++	++	
ShMOLLI 5(1)1(1)1	IR	9 beats	++	++	
SASHA	SR	11 beats	+	+++	No dependence on T2, magnetization transfer, or heart rate. Increased noise, loss of precision
SAPPHIRE	IR/SR	9 beats	++	+++	Improved accuracy

Source: after Moon et al.[6] IR: inversion recovery; MOLLI: Modified Look-Locker Inversion Recovery; SAPPHIRE: Saturation pulse prepared heart rate independent inversion recovery; SASHA: saturation-recovery single-shot acquisition; ShMOLLI: Shortened Modified Look-Locker Inversion Recovery; SR: saturation recovery.

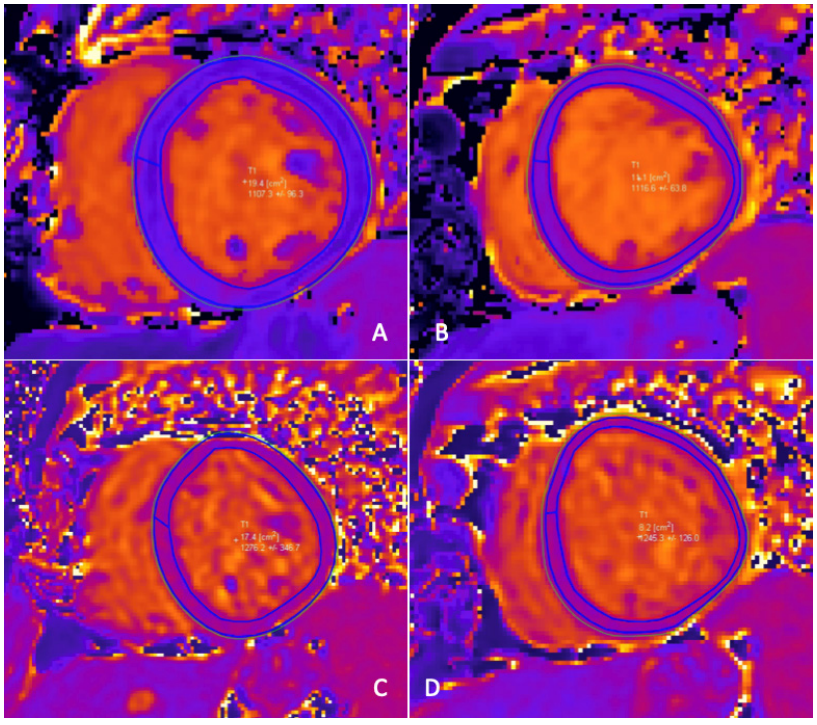


Figure 1 – *Representative images of the Modified Look-Locker Inversion Recovery (MOLLI) technique with 5(3)3 protocol (A and B) and the SmartMapT1 (C and D) technique. Global myocardial measurement, same time point, patient with aortic regurgitation.*

always carry a potential bias toward underestimating T1, due to factors such as dependence on transverse magnetization loss or the T2 factor, "off-resonance" effects, and magnetization transfer. These limitations notwithstanding, they are highly reproducible and accurate sequences, with a large body of published studies on their utility in various pathological states.

2.1.3. Saturation-Recovery Techniques

Saturation-recovery sequences cancel out the longitudinal magnetization, making image acquisition independent of heart rate by eliminating the need to wait for T1 recovery. Although they offer greater accuracy in determining T1 time, they have lower precision and a lower signal-to-noise ratio (SNR) than inversion-recovery techniques. The evolution of steady-state free-precession (SSFP) techniques, as used in the saturation recovery single-shot acquisition (SASHA) sequence, has mitigated the issue of low SNR. Another variant of this technique is SMART1Map (saturation method using adaptive recovery times for cardiac T1M). Unlike SASHA, where each saturation and acquisition pulse occurs during the same heartbeat, the SMART1Map sequence uses saturation and acquisition pulses during different heartbeats. Finally, a hybrid technique has been developed which employs saturation pulses followed by inversion pulses prior to image acquisition (saturation pulse prepared heart rate independent inversion recovery, SAPPHIRE), thereby improving accuracy.[13,15]

2.1.4. Extracellular Volume

ECV is a quantitative biomarker of the fraction of myocardium corresponding to the extracellular compartment. An increase in ECV reflects expansion of this compartment, which can occur through various mechanisms, such as interstitial fibrosis, edema, or infiltration by abnormal material, including amyloid deposits. Therefore, ECV is not a specific histological marker of fibrosis and should be interpreted in correlation with the clinical context, other CMR findings and, when available, local reference values. In patients with heart disease, ECV exceeds 28–30% (depending on the magnetic field strength), and may even reach values above 40% in infiltrative conditions such as amyloidosis.

Following intravenous (and, therefore, extracellular) administration, paramagnetic contrast medium distributes throughout both the intravascular space and the extracellular space of tissues, including the myocardium. It is well known that gadolinium contrast shortens the T1 time in proportion to its concentration in different tissues, allowing for a comparative evaluation of pre- and post-contrast T1 maps, thereby generating an estimate of gadolinium concentration based on the pre- and post-contrast 1/T1 ratio in myocardium and blood – the latter measured in the ventricular cavity. Correction for hematocrit is required, as well as comparison with the intravascular concentration of the paramagnetic agent, thereby excluding the cellular component of the intravascular compartment and generating an estimate of plasma T1. It is

then assumed that gadolinium has distributed itself evenly between the intravascular and extracellular compartments, which has been shown to occur with relative certainty approximately 10 minutes after intravenous injection of the contrast agent. There is a constant shift in this distribution of gadolinium following intravenous administration, as a result of variations in tissue perfusion and renal filtration of the contrast agent; however, from a clinical standpoint, a measurement obtained 10 minutes after contrast injection has proven sufficient for calculating the ECV. The formula for ECV estimation is:

		Post-contrast 1/T1 in myocardium	-	Native 1/T1 in myocardium
ECV =	(1 - Hematocrit) *	Post-contrast 1/T1 in blood	-	Native 1/T1 in blood

Values should be expressed and interpreted as a fraction of volume rather than an absolute measurement. Normal values have been reported in several studies, some of which even record variations with age and sex.

It is important to keep in mind that the technical considerations applicable to native T1, as well as any measurement biases of pre-contrast T1, will also apply to post-contrast measurements. Other variables also come into play, including positioning errors. The volume and type of contrast agent used can also influence the measurements, as can renal function, which affects the rate of contrast filtration in blood plasma. It also bears stressing that the dependence of ECV measurement on magnetic field strength, sequence types, and imaging parameters is less pronounced than for native or post-contrast T1 measurements, given the nature of the measurement.

At many facilities, incorporating hematocrit measurement into the routine outpatient CMR workflow can be a challenge; in addition to laboratory variables inherent to the measurement itself, this can also cause delays in signing off the report. In light of these considerations, a technique for synthetic hematocrit estimation has also been developed, based on the relationship between the T1 value of the pre-contrast (native) blood pool and the relationship between that value and the patient's hematocrit, which has come to be known as the synthetic ECV.[16]

The recommended contrast dose is 0.1 to 0.2 mmol/kg/body weight. Post-contrast T1 maps should be acquired 10 to 30 minutes after contrast injection; standardization of this timing is recommended. When the contrast dose is divided into more than one injection – e.g. in pharmacological stress tests – the timer should start once the final dose is injected. Hematocrit should be measured no later than 24 hours after the scan; ideally, the blood sample should be drawn at the time of the scan (Chart 1).

2.1.5. Accuracy and Precision

Accurate, precise, and reproducible measurements of myocardial T1 and ECV are the goal of the technique, but physical and biological variables are diverse. Accuracy errors refer to systematic bias in the measurement. Precision, on the other hand, refers to random, noise-related errors. These and other biases affect the reproducibility of the technique and the determination of normal values. Multiple technical factors influence these values, such as T2 sensitivity, off-resonance, flip angle, spatial resolution (matrix), partial volume, and magnetization transfer, among others. Changes in acquisition parameters can strongly influence these measurements, and standardization of parameters for each scanner is essential. Once reference values have been established for a given scanner, the sequence parameters should no longer be altered. Patient-

Chart 1 – Potential implications of conventional (hematocrit-based) extracellular volume, synthetic extracellular volume, and paramagnetic contrast on interpretation of T1 maps

	Potential technical limitations	Clinical impact
Laboratory hematocrit	Sample drawn at any time other than simultaneously with the CMR scan, hemodilution, hemoconcentration, recent transfusions, laboratory error.	May result in incorrect estimation of ECV, even when T1 maps are of good quality.
Gadolinium contrast	Differences among contrast agents, the dose administered, time after contrast administration, and renal function.	Directly influences contrast distribution and ECV values.
Synthetic ECV	Based on estimating hematocrit from native-blood T1, using equations specific to each scanner, sequence, and magnetic field.	May reduce the need for blood draws, but is less accurate in certain populations.
	Performs less well in patients with anemia, polycythemia, renal insufficiency, hematologic disorders, inflammatory conditions, or abnormalities of blood composition. Lack of universal standardization among manufacturers.	May introduce systematic bias and reduce the reliability of ECV estimation when compared to the method based on actual measured hematocrit.

RMC: ressonância magnética cardíaca; VEC: volume extracelular.

related factors, such as heart rate, respiratory movements, hematocrit, and renal function, also affect measurements.[10]

The decision regarding which sequence and protocol to employ should be guided by clinical context. Correct positioning of the tissue to be measured between images is essential. Automatic motion correction (MOCO) protocols have been developed for this purpose and should be used when available.[17,18] The use of such automatic corrections does not eliminate the need for a breath hold. Free-breathing, navigator-based techniques are also available, but clinicians should bear in mind that they increase acquisition time and are reliant on the patient's breathing pattern; therefore, a breath hold is preferable. An understanding of the variables involved and an ability to recognize artifacts are essential for the proper use of the method.

2.1.6. Protocols

For diffuse cardiomyopathies, two-chamber short-axis views at the base and middle third are sufficient; acquisition of a long-axis view is optional. Caution is required when obtaining measurements in slices where the structure being measured is not orthogonal to the acquisition plane, such as short-axis slices of the cardiac apex, where a partial-volume effect is present. In diseases with irregular distribution, a long-axis view should be included, such as the four-chamber (4CH) view for amyloidosis and the three-chamber view for Fabry disease; however, the choice of plane should take into account the findings on cine and T2/STIR sequences. Evaluation of cine and T2/STIR images is also essential in determining the mapping protocol in focal and acute diseases; in this context, coverage should include areas of maximum and minimum abnormalities visualized in the other sequences (or, ideally, the entire length of the left ventricle [LV]). Care should be taken not to prolong the scan too much, to prevent undue patient discomfort and fatigue.

For ECV measurement, the technique and parameters should be the same as for native T1 acquisition, except for the MOLLI protocol. The same views and phase of the cardiac cycle phase should be imaged.

2.1.7. Analysis

It is essential that clinicians understand the technique being analyzed and the type of acquisition. Some analysis software may require manual entry of certain parameters, even if only the sequence type. Prior to map analysis, the raw images should be assessed for motion artifacts and other artifacts. This understanding is essential for subsequent evaluation of the map and identification of artifacts and areas from which measurements should or should not be taken (Figures 2 and 3; Videos 1 and 2). A visual qualitative analysis should be performed before any quantitative analysis to ensure confidence in the measured values.

For evaluation of diffuse cardiomyopathies, a single region of interest (ROI) covering the mid-septum should be sufficient for analysis (Figure 4), and the value can be validated with measurements of the basal septum. Obtaining measurements from the lateral walls is best avoided, to prevent artifacts related to the lung parenchyma and venous contamination. A global measurement of the entire slice may also be used.

Focal conditions can be assessed using specific ROIs in the affected areas; visual evaluation of the color map may be helpful. Always remember to assess for artifacts and avoid areas where abnormalities in the map appear unreliable. Generating a value and/or color map using the 16-segment model outlined in the American Heart Association (AHA) guidelines is also an interesting and effective technique to

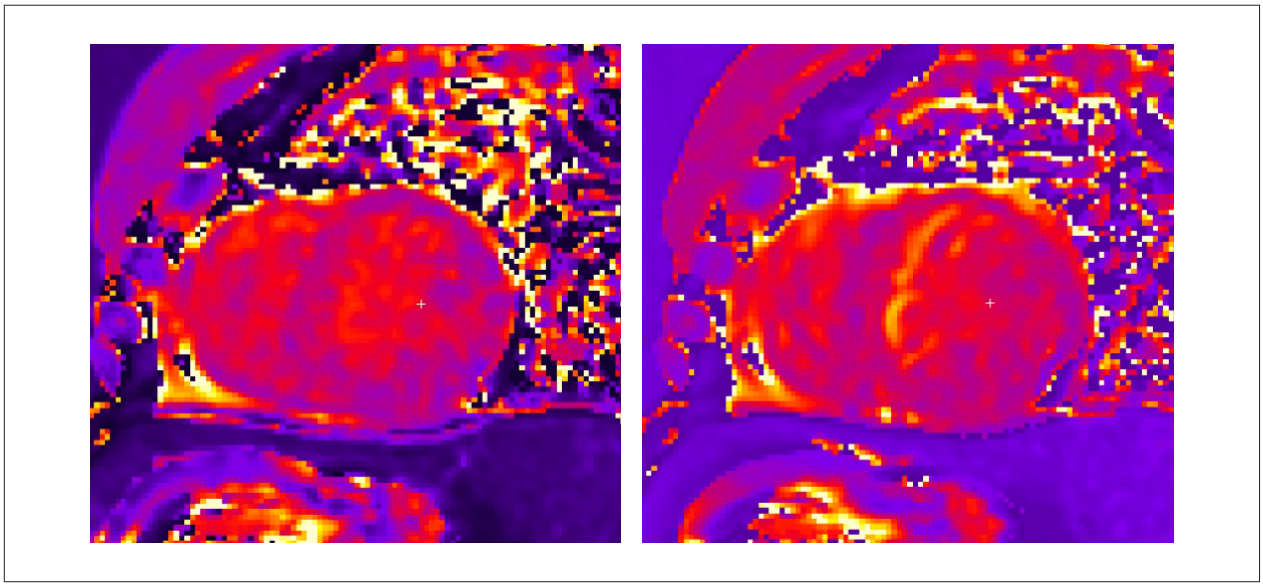


Figure 2 – *Motion correction (MOCO) absent in image A and present in image B, with respective maps. Analysis is compromised in the map without MOCO.*

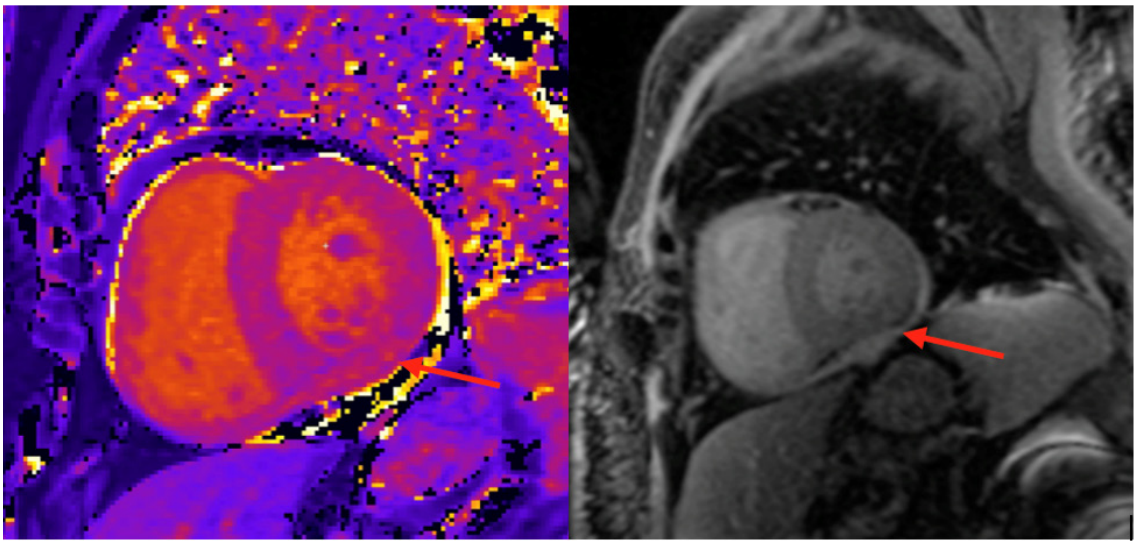
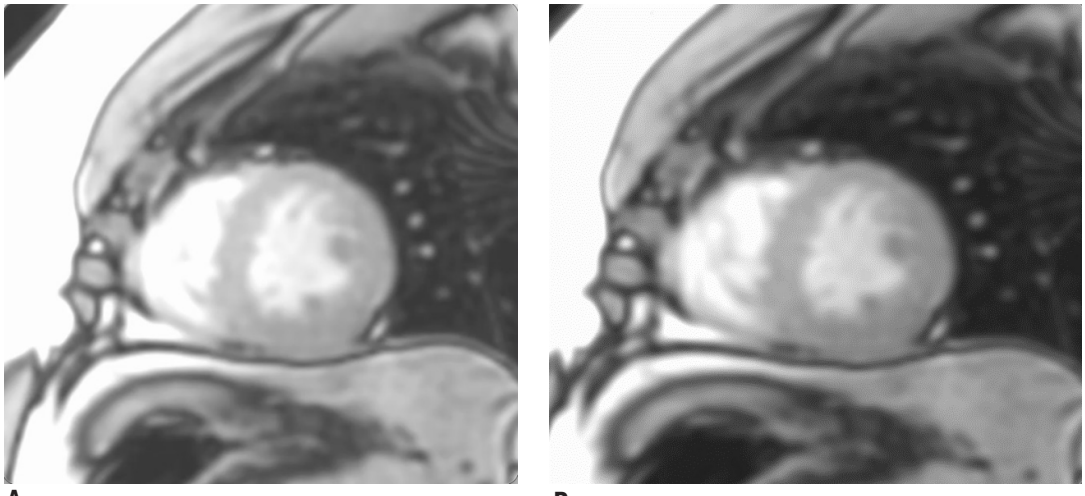


Figure 3 – *Motion correction: the image shows an area on the inferior wall with a positional artifact despite the correction technique. The corresponding T1 map shows an area of compromised analysis on the inferior wall.*

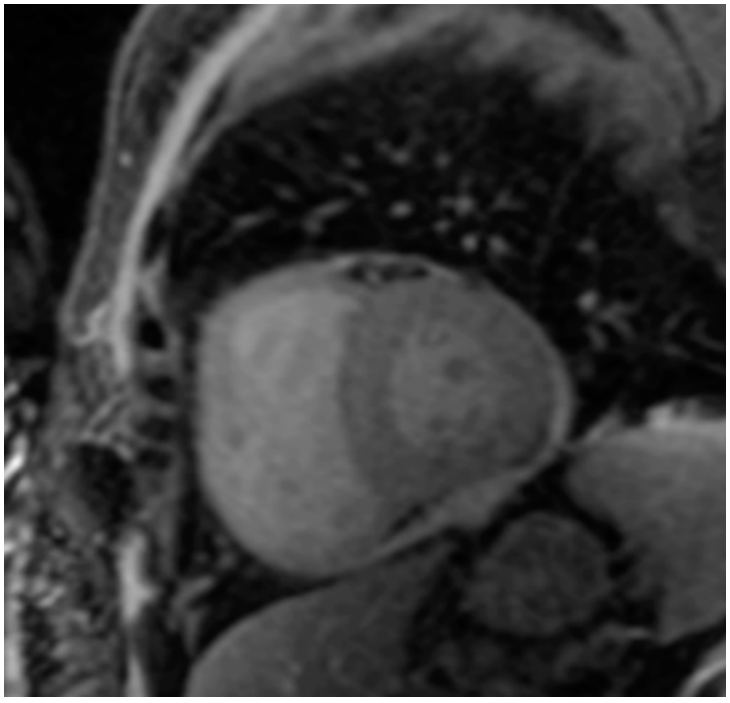


Video 1 – *Motion correction (MOCO) is absent in cine A and applied in cine B, with the corresponding maps. Analysis of the map without motion correction is limited.*
Link: http://abccardiol.org/supplementary-material/2026/12310/pos_mapa_vid_01a.mp4
Link: http://abccardiol.org/supplementary-material/2026/12310/pos_mapa_vid_01b.mp4

assess the entire myocardium at a glance and easily compare segments (Figure 5). Small ROIs (i.e. less than 20 pixels) should be avoided. Various automatic or semi-automatic analysis software programs are available on the market, and there is no specific recommendation regarding which to use. What is essential, however, is understanding how these tools work and performing a visual assessment of any automatically generated ROIs.

2.1.8. Reference Values

Significant progress has been made in standardization and matters of technical quality; nevertheless, significant differences still persist among platforms, sequences, and centers. Therefore, clinical interpretation continues to depend on validated, local (facility-specific) reference values and rigorous quality control, in accordance with published consensus recommendations.[5] When establishing local



Video 2 – *Motion correction (MOCO): the cine demonstrates a positional artifact in the inferior wall despite application of the correction technique. The corresponding T1 map shows limited interpretability in this region.*
Link: http://abccardiol.org/supplementary-material/2026/12310/pos_mapa_vid_02.mp4

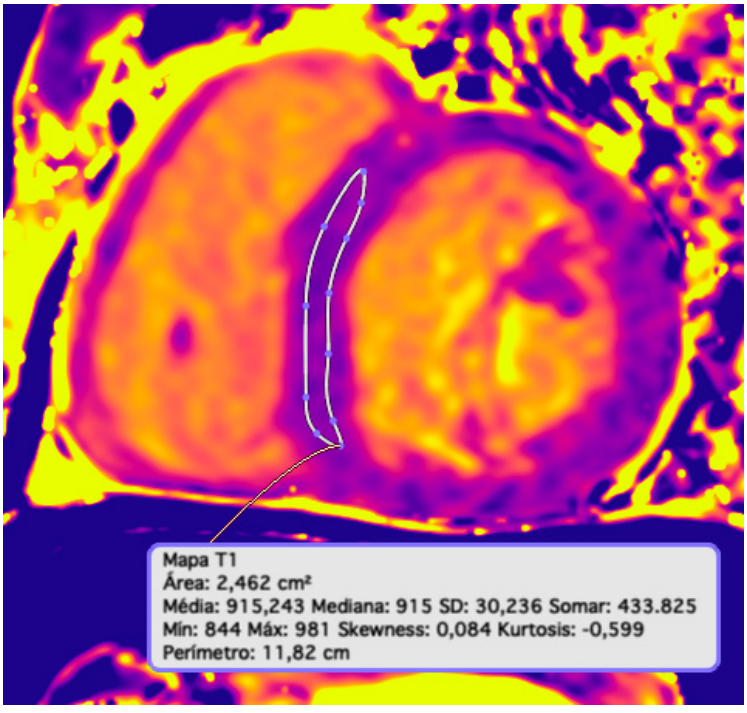


Figure 4 – *Short-axis Modified Look-Locker Inversion Recovery (MOLLI) technique with region of interest in the septal position.*

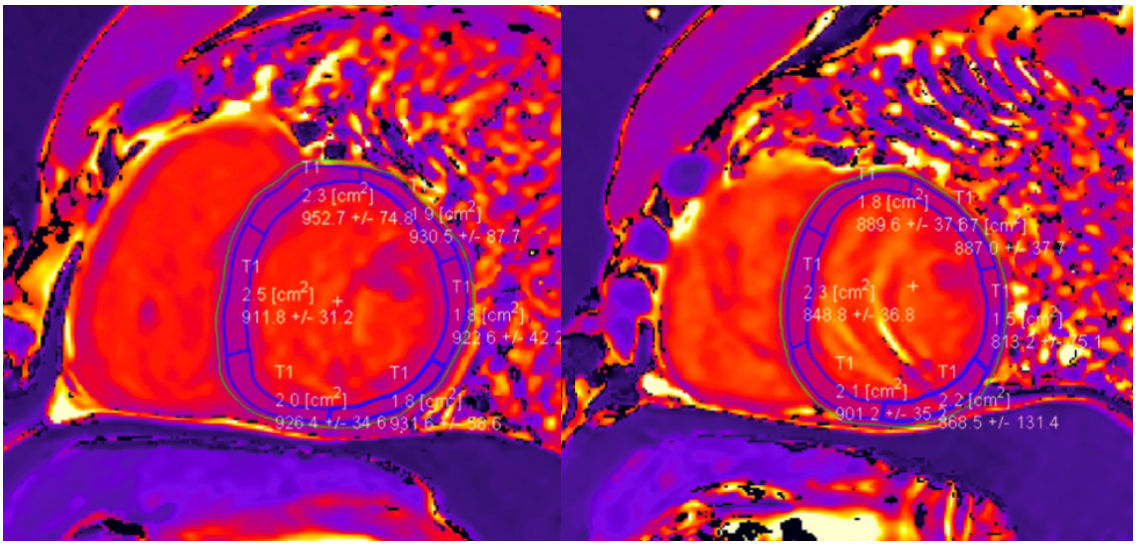


Figure 5 – *Modified Look-Locker Inversion Recovery (MOLLI) technique with 5(3)3 sequence showing basal and mid two-chamber views, with measurements adapted to the respective American Heart Association segments.*

reference values, technical parameters must strictly mirror those that will subsequently be used in daily clinical practice. Local reference values are then defined as the mean plus or minus two standard deviations from the normal sample acquired at the facility. Other approaches have included the creation of standard normal tables based on Z-scores and demonstrated the possibility of analysis across different magnetic fields, scanners, and acquisition schemes other than MOLLI.[19]

2.1.9. Conclusion

T1M and ECV calculation are powerful quantitative tools for noninvasive tissue characterization, but require rigorous standardization, quality control, and integrated clinical interpretation. MOLLI and SASHA are the most widely used sequences, and ECV adds prognostic and diagnostic value in the assessment of fibrosis, infiltration, and myocardial edema.

2.1.10. Key Takeaways

- T1 represents the time to recovery of longitudinal magnetization in tissues following a radiofrequency pulse;
- T1M generates quantitative parametric images that reflect tissue properties (water, fat, iron, collagen, protein content);
- Low T1 values → iron, fat, sphingolipids (e.g. Fabry disease);
- High T1 values → edema, diffuse fibrosis, infiltration, increased extracellular space (e.g. amyloidosis);
- Inversion-recovery techniques → MOLLI, ShMOLLI (high accuracy, but dependent on heart rate and prone to artifacts). MOLLI (5[3]3) is the most widely used protocol; ShMOLLI reduces dependence on heart rate;
- Saturation-recovery techniques → SASHA, SMART1Map, SAPPHIRE (greater accuracy, lower precision);
- ECV: calculated as the difference between pre- and post-contrast T1 values, corrected for hematocrit; reflects the expanded extracellular space (fibrosis, edema, infiltration/amyloid protein). Optimal timing for post-contrast T1 measurement: 10–30 min after contrast administration, at a dose of 0.1–0.2 mmol/kg;
- The hematocrit must be drawn on the day of the scan; a synthetic hematocrit may be used when necessary;
- Technical variables (magnetic field, flip angle, motion correction, resolution, heart rate, respiration) influence measurements;
- Automatic MOCO is strongly recommended;
- Standardize protocols and do not change settings after local validation;
- Diffuse cardiomyopathies: basal and middle short-axis slices; ROI in the mid-septum;
- Focal lesions: ROIs in the affected areas; avoid regions with artifacts;
- ROIs < 20 pixels should be avoided; always review raw images before analysis;
- Normal = mean ± 2 SD of healthy sample.

2.2. T2 Mapping

T2 mapping (T2M) of the myocardium using CMR is performed by pixel-by-pixel fitting to a transverse magnetization decay curve from a series of T2-weighted (T2W) images. This technique allows direct quantification of myocardial T2 values and is used to detect changes in myocardial T2 relaxation time. Such changes reflect alterations in the amount of water present in the myocardial tissue, a parameter directly associated with

various clinical conditions, such as ischemic heart disease (acute myocardial infarction),[20] acute inflammatory processes such as myocarditis,[21] takotsubo cardiomyopathy,[23] chemotherapy-induced cardiotoxicity,[24] and heart transplant rejection,[25,26] among others.[27,28] T2M mapping entails acquiring a specific sequence during CMR, followed by post-processing of the images to generate the T2 map. Precise measurements of T2M values can then be obtained. The technical aspects involved will be detailed below, while clinical applications will be discussed in their respective sections.

2.2.1. Technical Concepts

2.2.1.1. Magnetic Resonance Imaging Scanners

In current clinical practice, magnetic resonance imaging (MRI) scanners with magnetic field strengths (B0) of 1.5 T and 3.0 T are used, in accordance with Society for Cardiovascular Magnetic Resonance (SCMR) recommendations.[5,29] Systems with a B0 of 3.0T provide a higher SNR and may allow greater spatial and temporal resolution, but are more susceptible to artifacts.[30] The use of a dedicated cardiac imaging coil is recommended to reduce artifacts and increase the SNR. All MRI system manufacturers provide pulse sequences for T2M acquisition.

2.2.1.2. T2 "Preparation"

Preparation for T2 magnetization in T2M uses a T2 preparation module (T2-prep) followed by rapid image acquisition, typically using balanced steady-state free precession (bSSFP) or gradient-echo (GRE) sequences. T2-prep consists of a 90° pulse, followed by 180° pulses to refocus the transverse magnetization, and a final 90° pulse to restore longitudinal magnetization, as described by Huang et al.[31] This preparation can be applied selectively or non-selectively and combined with other pulse techniques to acquire a single or multiple images.

Conversely, T2M techniques without magnetization preparation are generally based on multi-echo spin-echo (MESE) sequences, in which multiple images with different echo times (TEs) are acquired to generate maps with varying T2 sensitivity.[30]

2.2.1.3. Sequence Acquisition Type

Image acquisition for T2M can be "single-shot" or segmented. "Single-shot" acquisitions are faster, performed during a single R-R interval and a single breath-hold, and are most commonly used for two-dimensional (2D) sequences. Segmented acquisitions require multiple R-R intervals, which increases the breath-hold duration needed for acquisition, but they can be used for three-dimensional (3D) sequences.

Currently, 2D T2M sequences are those most widely available in daily practice and, consequently, most commonly used. The main difference between 2D and 3D images is isotropy: in 3D, the images are isotropic, whereas in 2D they are non-isotropic, making them susceptible to the partial-volume effect and areas of low resolution.[30]

A proper patient breath-hold at the time of acquisition remains the best method for minimizing artifacts in CMR. MOCO techniques should be used if available.[5,32]

2.2.1.4. Sequence Types

There are many sequences under development for T2M acquisition that still require clinical validation. Table 2 lists the commercially available 2D T2M sequences offered by manufacturers in Brazil at the time of writing.

2.2.1.5. Image Acquisition Protocol

For T2M imaging, the acquisition protocol will depend on the suspected clinical condition:

- Diffuse cardiomyopathies (e.g., amyloidosis): a single short-axis image may be sufficient; addition of a 4CH image may aid in diagnosis;
- Focal conditions (e.g., myocardial infarction, myocarditis): one or more images in the short-axis plane, the location of which may be guided by cine MRI and T2-weighted imaging; addition of a 4CH image or one obtained in a plane orthogonal to the affected segment may aid in diagnosis;
- Slice thickness: 6 to 8 mm, with in-plane spatial resolution of at least 1.6 to 2.0 mm.[29]

The current recommendation is to acquire electrocardiogram (ECG)-gated images during mid-diastole to minimize cardiac motion artifacts.[5] If acquisition "accelerators" such as "parallel imaging" are compatible with the sequence employed, they should be used, provided that image quality is maintained.

2.2.1.6. Postprocessing

Postprocessing of T2M images must quantify the mono-exponential T2 decay of the myocardium to obtain the native T2M value. In current daily practice, such postprocessing can be performed automatically by the acquisition system and, consequently, is specific to the manufacturer of the MRI scanner employed; it consists of automatic generation of color and grayscale maps of the acquired slice(s). In this modality, to obtain the native T2 value of the myocardium, the professional must draw an ROI on the LV myocardium displayed on the map (usually the grayscale map); the value obtained will correspond to the T2M[35] (Figure 6).

Alternatively, manual postprocessing can be performed by the professional, using dedicated software or manual calculation. In this case, the ROI must be positioned on the LV myocardium in the same location across all images from the specific sequence acquisition so that the T2M can be calculated by the software (Figure 7) or manually.

It is important to note that the ROI must be positioned within the myocardium, avoiding partial-volume interference from intraventricular blood or extracardiac tissues.[35] T2M measurement for diffuse myocardial involvement can be performed using a single mid-septal ROI.[5,35] For diseases with focal myocardial involvement, the ROI should be positioned in the areas identified as abnormal.[34,35]

Table 2 – Cardiac magnetic resonance imaging sequence types for myocardial T2 mapping

Sequence type	2D/3D	Blood signal	Description
"Single-shot T2-prep bSSFP" (Huang et al., 2007)[31]	2D	"Bright"	This T2M technique uses T2-prep in a non-selective manner, followed by "single-shot" bSSFP image acquisition. Typically, 3 images are acquired at different T2 preparation times, and the bSSFP scan is programmed to occur during the same phase of the cardiac cycle (either mid-diastole or end-systole). The pulse sequence parameters are chosen so that the total acquisition time remains within the duration of a single breath-hold for most patients.
DIR-prepared FSE or TSE (Baeßler et al., 2015)[33]	2D	"Dark"	These are MESE-based T2M techniques that generate T2-weighted images with a desired effective TE within a breath hold, with blood signal suppression, resulting in "dark-blood" T2-weighted images. Multiple such "dark-blood" T2-weighted images can be acquired at different TE values and then aligned pixel-by-pixel to create a T2 map.
GraSE (Baeßler et al., 2015,[33] Sprinkart et al., 2015)[34]	2D	"Dark"	GraSE-based T2M combines an FSE pulse sequence with EPI, producing "dark-blood" images. GraSE pulse sequences generally yield significantly higher T2 values than T2-prep bSSFP pulse sequences. In addition, the longer echo spacing and EPI readout used in GraSE may increase susceptibility to motion blur and in-plane motion, introducing partial-volume effects.

2D: two-dimensional; 3D: three-dimensional; bSSFP: balanced steady-state free precession; DIR: double inversion recovery; EPI: echoplanar imaging; FSE: fast spin echo; GraSE: gradient- and spin-echo; T2M: T2 mapping; T2-prep: T2 preparation; TE: echo time; TSE: turbo spin echo.

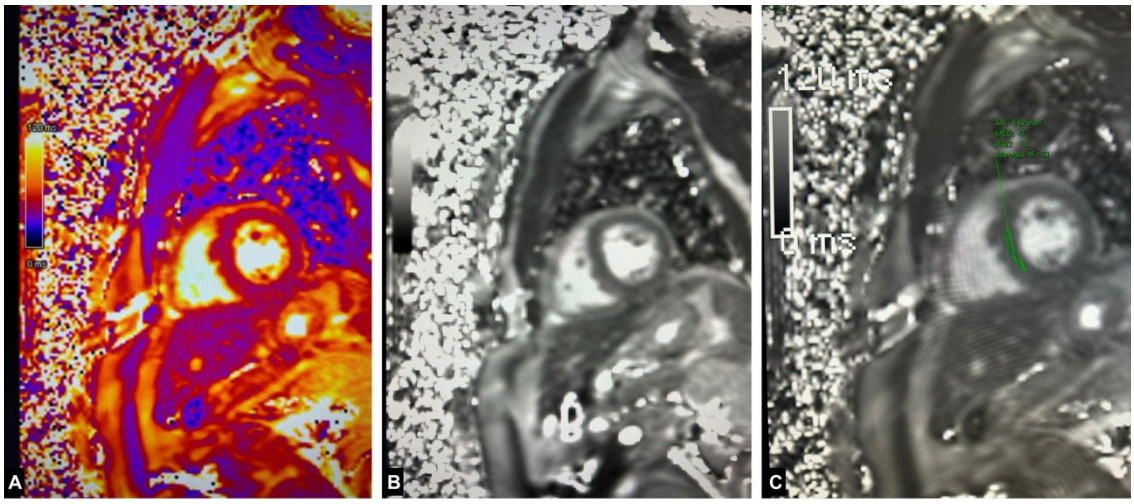


Figure 6 – *T2 mapping (T2M) after automatic postprocessing by the acquisition system software. Color (A) and grayscale (B) maps are shown, both with value scales related to color or grayscale intensity displayed on the left side of the image. In (C), the region of interest was positioned over the interventricular septum, and the obtained value ("MED", in green) corresponds to the native T2M value.*

2.2.1.7. Normal Values

In healthy individuals, myocardial tissue has a uniform composition and, therefore, exhibits consistent magnetic properties. As a result, normal native T2 values of the myocardium are highly reproducible and exhibit relatively narrow ranges when acquired under the same conditions,[36] ranging from 40 to 60 ms for most sequences obtained on 1.5-T MRI scanners.[37] However, there are no *in vitro* normal values that can be applied to *in vivo* T2M.

Furthermore, individual T2M can be affected by various factors, some intrinsic (such as hydration status and body temperature) and others extrinsic (environmental ones, such as ambient temperature; those related to image acquisition, including B0, sequence type, apnea, and motion; and those related to postprocessing).

For T2M to be applicable in clinical practice, the current recommendation is that reference or normal values be obtained in each MRI scanner from a sample of the local population,

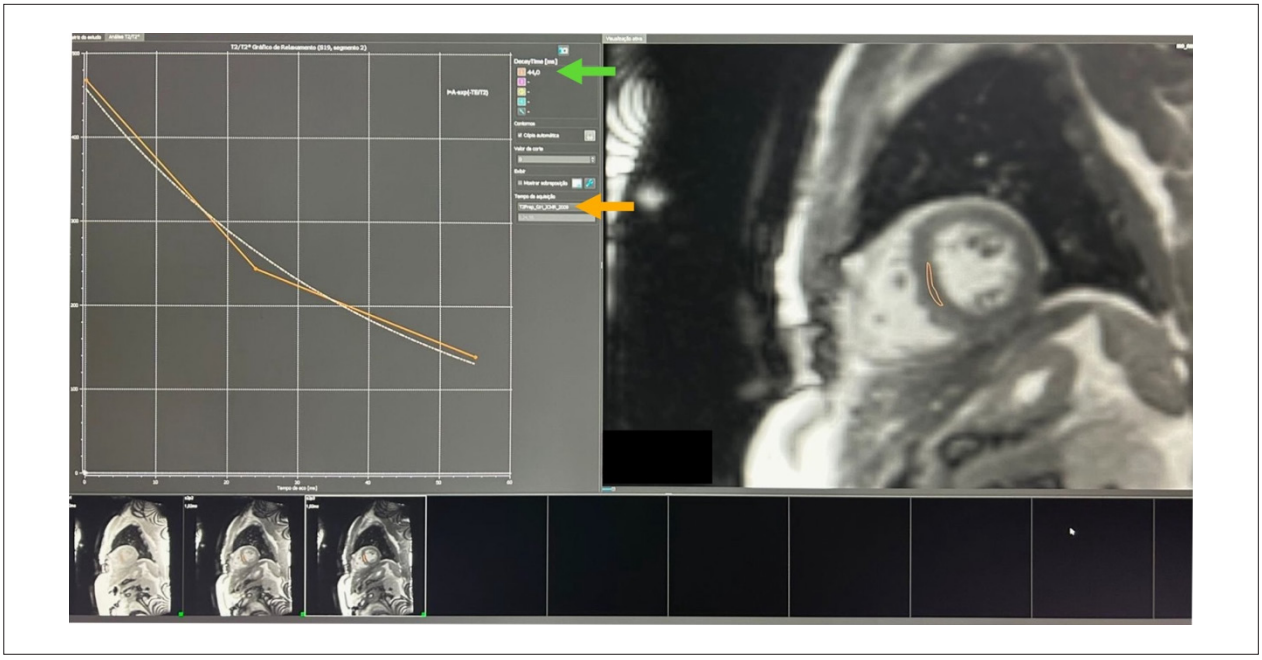


Figure 7 – *Software-processed T2 mapping (T2M). At the bottom of the screenshot, the three images obtained in the balanced steady-state free precession sequence with motion correction are shown, with the region of interest positioned over the interventricular septum, as evident in the upper right panel. The graph in the upper left panel shows the T2 decay of the myocardium, with the selected calculation protocol (orange arrow) and the actual value obtained (green arrow), corresponding to the native T2M value.*

always using the same acquisition and postprocessing parameters. The SCMR recommends obtaining reference values from at least 15 healthy individuals or 20 individuals with a normal CMR for the study of major myocardial changes (e.g. amyloidosis and acute myocardial infarction); and from at least 50 healthy individuals for subtle myocardial changes (e.g. diffuse fibrosis). These reference values which will be more accurate if stratified by sex.[5]

2.2.1.8. Quality Control

For T2M measurements to be reliable, image acquisition and postprocessing must be performed in the same manner as for the images of healthy individuals used to establish the reference/normal values for that particular MRI scanner. If these conditions change, it becomes impossible to assess whether changes in tissue parameter results are due to pathology or simply to a change in how the measurement was obtained.

In addition, image quality control must be performed using acquisitions of the sequence(s) on a phantom – the same one used as a quality benchmark for other sequences obtained in that particular scanner – whenever there is a change in system hardware, a software upgrade or update, and every 3 months even if no such changes have occurred.[5] Also regarding image quality control, it is important to note the interference caused by magnetic field inhomogeneity (which is most significant in 3.0T MRI systems, and which can be minimized through the use of shimming and adiabatic pulses) as well as motion artifacts (e.g. cardiac or respiratory), mitigation of which requires proper patient instruction and cooperation during image acquisition.[5,29]

2.2.1.9. Key Takeaways

- T2M of the myocardium can be used in daily practice, with sequences available on 1.5-T and 3.0-T MRI scanners;
- Proper calibration of software and hardware (coil/scanner) parameters for the desired sequence is recommended, followed by data acquisition from local volunteers and patients to establish normal reference ranges, without modifying any pre-set parameters;
- When acquiring T2M images, control for respiratory (breath-hold) and cardiac (R-R phase) artifacts, as well as magnetic field inhomogeneity (shimming);
- During postprocessing (automatic or manual), check the color and grayscale maps;
- Position the ROI for T2M measurement according to the indication for the scan (diffuse cardiomyopathies: mid-septum; focal conditions: ROI at the affected site or sites).

2.3. T2* Quantification

Myocardial iron overload represents a serious and potentially life-threatening complication of a wide range of clinical conditions, but is particularly prominent in patients with thalassemia major, chronic hemolytic anemias, hereditary hemochromatosis, and myelodysplastic syndromes with a high transfusion burden.

Excessive iron deposition in the myocardium has several effects: changes in molecular structure and cellular homeostasis, increased production of reactive oxygen species, increased oxidative stress, mitochondrial damage, interstitial fibrosis, and progressive ventricular dysfunction.[38,39] Clinically, these mechanisms translate into an increased risk of heart failure (HF), complex arrhythmias, and sudden death, making early diagnosis and monitoring of iron overload essential for reducing morbidity and mortality.[38,40]

In this context, CMR has established itself as the most robust noninvasive method for quantifying myocardial iron. The advent of the T2* quantification technique – initially based on the acquisition of multiple TEs and analysis of a ROI in the interventricular septum – represented a milestone in the management of these patients. With subsequent advances, the technique has evolved to allow construction of parametric T2* maps, which provide a voxel-by-voxel representation of the actual transverse relaxation time. Recent studies have stressed that T2* maps not only maintain the diagnostic accuracy of the conventional method but also expand its clinical applicability.[41-44]

2.3.1. Definitions and Objectives

The **T2*** parameter corresponds to the actual transverse relaxation time observed in tissues. Unlike "pure" T2, which reflects only the loss of phase coherence (dephasing) caused by intrinsic spin–spin interactions, T2* also incorporates the effects of local inhomogeneities in the magnetic field.[29,45] In other words, T2* is more sensitive to microscopic changes in the magnetic environment, such as those caused by the presence of iron. The result is a faster exponential decay of the signal, which translates into reduced T2* values.[40]

Reduced T2* values are directly related to the degree of iron deposition and correlate robustly with ventricular function and the risk of adverse clinical events.[38,39]

The primary purpose of quantifying myocardial T2* is to detect, stratify, and monitor iron overload in the heart. It is an objective marker that allows radiologist and cardiologist to integrate functional, prognostic, and therapeutic information into a single measurement, with a direct impact on clinical management of the patient.

One of the greatest advances brought about by T2* was the ability to diagnose iron overload before the onset of clinical manifestations or echocardiographic abnormalities.[38,39] Patients with T2* values that are still only slightly reduced may have preserved ventricular function but are already at risk of progressive deterioration if their chelation therapy is not adjusted. This subclinical nature of the technique makes it essential for monitoring of high-risk populations, such as patients undergoing periodic blood transfusions for thalassemia major.

Prognostic stratification is another core purpose of T2* quantification. Reduced values are strongly associated with development of HF and sudden death and are considered one of the best predictors of events in patients with thalassemia.[40,42]

T2* is also indispensable for monitoring the response to iron chelation therapy. Changes in values over time reliably reflect the efficacy of the established therapeutic regimen, allowing for individualized dose adjustments, changes in chelation agents, or intensification of a combination strategy.[40] Furthermore, the possibility of serial measurement, with high reproducibility across scans, gives T2* a central role in clinical practice, and it has been incorporated into international consensus statements and guidelines.[29]

It is important to note that, although the cutoff values were originally established using the traditional mid-septum ROI method, T2* maps preserve this applicability while also offering the possibility of assessing regional heterogeneity and providing additional information on iron distribution.[41,43,44] Thus, the ultimate goal of quantification remains the same, but the modern method broadens the range of information available to the treating physician.

2.3.2. Traditional (T2*) Quantification Technique

The traditional T2* quantification technique laid the foundation for CMR diagnosis of iron overload.[39,40,42,46] The protocol is based on a multi-echo GRE sequence, typically ECG-gated to reduce motion artifacts. The scan is performed during a brief breath-hold, usually lasting 8 to 12 seconds, ensuring that multiple TEs are obtained within the same respiratory cycle.[39,40,42,46] These TEs are selected so as to capture both the initial points (when the signal is still elevated) and the final points of decay (near the noise level), allowing for precise fitting of the mono-exponential curve (Figure 8).

The most commonly used image is a short-axis view at the mid-level of the LV, with a single ROI positioned mid-septum. This is not an arbitrary choice: the septum is relatively thick, less prone to susceptibility artifacts originating from the lungs or intracavitary blood and exhibits excellent inter-scan and inter-observer reproducibility.[39,40,42,46]

The mean signal of the ROI is plotted as a function of TE to yield a decay curve. This behavior is described mathematically by a simple mono-exponential function:

$$S(TE) = S_0 \cdot e^{-TE/T2*}$$

Where *S(TE)* is the signal intensity at a given TE, S_0 is the initial signal, and T2* is the actual relaxation time.[45]

This was the technique used to establish clinical reference values. Several studies have shown that healthy individuals have T2* values in the interventricular septum equal to or greater than 20 ms when imaged on 1.5-T scanners. Values between 10 and 20 ms indicate moderate iron overload, and values below 10 ms correlate with a high risk of HF and sudden death.[39,40,42,46] This categorization is still widely used today, and serves as a benchmark for comparison even when more advanced techniques are employed.

Despite its robustness, this method has significant limitations. The main limitation is that it provides only an overall, averaged value for the interventricular septum, without capturing regional variations across the myocardium. This means that areas with heterogeneous iron deposition may have their overload underestimated. In addition, the technique is sensitive to susceptibility artifacts, particularly near blood or

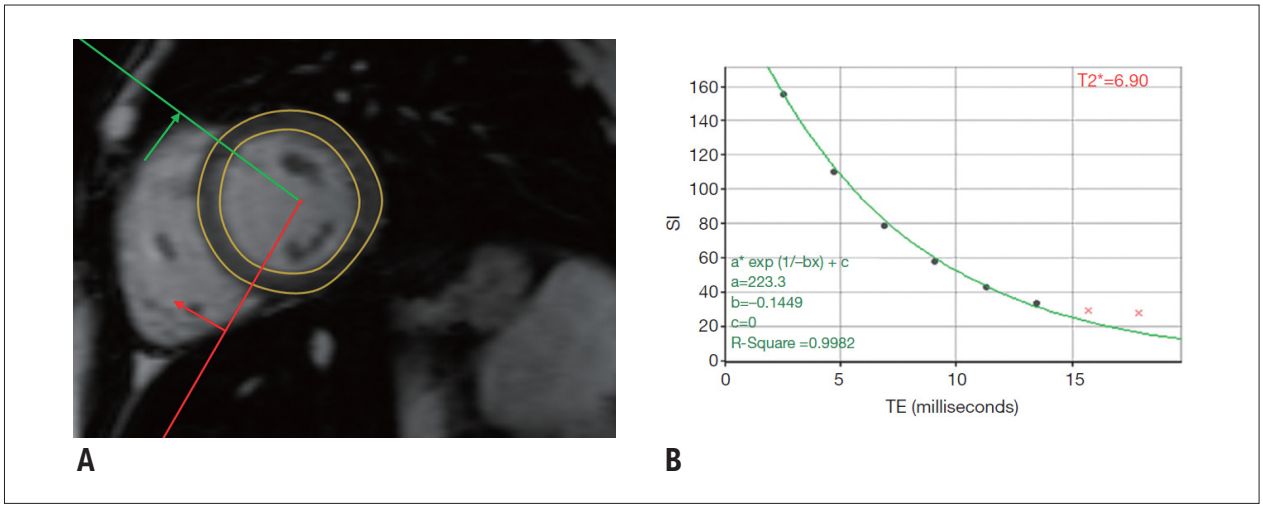


Figure 8 – *Example of the traditional T2 quantification technique: region of interest in the mid-ventricular septum (A) and a mono-exponential curve fitted to signals from multiple echo times (B). Adapted from He et al.*[46]

the lungs, and relies on the patient's cooperation and ability to perform an adequate breath hold. Nevertheless, due to its simplicity and longstanding clinical validation, the traditional technique remains the benchmark and is considered the historical gold standard against which new methods, such as T2* mapping, are compared.[41,43]

2.3.3. T2* Mapping

The development of parametric T2* maps was another milestone in the quantification of myocardial iron overload. Building on the same principles as the traditional method, this technique overcame previous limitations by enabling voxel-by-voxel assessment, generating a color image that depicts the distribution of cardiac iron intuitively and in minute detail.[41,43,44]

Image acquisition for generating T2* maps continues to be based on multi-echo GRE sequences, typically ECG-gated and performed during a short breath-hold. However, instead of analyzing the average signal from a single ROI, the software processes each pixel individually. For each voxel, the signal obtained at different TEs is fitted to a mono-exponential curve and assigned a specific T2* value. The result is a color-coded parametric map: high T2* values appear in cool tones (blue, green), while low values – which indicate iron overload – are represented by warm tones (yellow, orange, red).[41,43,44]

This approach eliminates the limitation of relying solely on a single ROI, expanding the analysis to the entire myocardium and allowing for the detection of **spatial heterogeneity in iron deposition**, which is impossible with the traditional method. In clinical practice, T2* maps can be analyzed in two ways:

1. Septal ROI on the map – this remains the most widely used method, as it maintains direct comparability with historical reference values (≥ 20 ms: normal; < 10 ms: severe);[38]

2. Segmental analysis – evaluation of the myocardium following the AHA 16- or 17-segment model, allowing for regional characterization and identification of areas with greater iron overload.[41,43,44]

The second strategy is particularly useful for patients with non-homogeneous deposition, in whom the septal average could preclude identification of regions with significant overload.

2.3.4. Advantages and Limitations of T2* Maps

T2* maps offer a number of practical and scientific benefits:

- Intuitive visualization: color-coded maps allow near-immediate interpretation, facilitating communication among radiologists and cardiologists;
- Detection of heterogeneity: regional analysis increases sensitivity for identifying areas with higher iron deposition;
- Multicenter standardization: facilitates reproducibility across clinical studies and research, reducing inter-examiner variability;
- Integration with postprocessing software: voxel-by-voxel analysis paves the way for automated segmentation algorithms, artificial intelligence (AI), and machine learning;
- Broader clinical applicability: this method allows not only absolute quantification but also qualitative assessment of the iron distribution pattern.

Despite their advantages, T2* maps still carry some limitations. The analysis is more susceptible to **noise**, especially in longer echoes, when the signal is close to the background level. Susceptibility artifacts at interfaces with blood or lung tissue can generate spurious values in peripheral regions of the myocardium.[41,43,44] To address these issues, modern algorithms include automatic rejection of noisy echoes or employ noise-offset adjustments.

Another challenge is magnetic field- related variability. At 1.5 T, cutoff values are well established, but at 3 T there are still uncertainties, and standardization of protocols is essential to ensure comparability.[29,42,43] Furthermore, analysis requires

dedicated software which may not be available at all centers, posing a barrier to widespread adoption of the technique in less specialized settings.

In recent years, several developments have expanded the applicability of T2* maps:

- Free-breathing T2* – techniques employing respiratory motion correction allow acquisition during free breathing, thus benefiting patients who cannot tolerate a prolonged breath-hold[44] (Figure 9);
- Multiparametric mapping – integrating T1, T2, T2*, and quantitative susceptibility mapping (QSM) into a single protocol increases diagnostic accuracy and provides a more comprehensive view of cardiac pathophysiology;[43]
- Advanced deep learning-based reconstructions – approaches such as multi-contrast learned acquisition and reconstruction optimization (mcLARO) reduce acquisition time and increase robustness, allowing simultaneous generation of multiple quantitative maps more efficiently.[47]

These innovations suggest that T2* mapping is on track to not only become established as a clinical standard but also integrate into a broader ecosystem of multiparametric mapping, where different contrasts are combined into more comprehensive and informative protocols.

2.3.5. Limitations

Despite technical advancements and robust clinical impact, T2* mapping has limitations that can be grouped into three categories: technical, interpretive, and logistic.

The first challenge is sensitivity to noise, especially in longer echoes, when the signal is already close to the background level. Voxel-by-voxel analysis, a defining characteristic of T2* mapping, is more vulnerable to noise variations than the average obtained from a septal ROI.[41]

Another critical issue is the presence of magnetic susceptibility artifacts, particularly in regions near blood, the lungs, or air-tissue interfaces. These artifacts can distort T2* values in certain regions of the myocardium, limiting reliable interpretation across the entire ventricular circumference.[41,43,46,48,49]

In addition, there is the issue of magnetic field dependence. The classic cutoff values were defined for 1.5-T systems and cannot be directly applied to 3-T scans, where absolute T2* values tend to be lower due to increased field inhomogeneity.[29,42,43] This demands added caution in interpretation and highlights the need for field-specific protocols.

Even under ideal conditions, interpretation of T2* values must take into account factors such as regional heterogeneity of iron deposition, which can make it difficult to define a single representative value. Although the maps allow segmental analysis, there is still debate regarding which segments are most relevant for clinical prognosis. The interventricular septum remains the reference, but examination of other segments may provide additional information in specific cases.[41,43,44]

Furthermore, the technique is not entirely iron-specific. Local susceptibility changes, fibrosis, or edema can influence T2* values, albeit to a lesser extent. This highlights the importance of interpreting the findings within the patient's clinical context and, ideally, in conjunction with other CMR parameters, such as T1 and T2 maps.[43,47]

Finally, there are barriers related to routine implementation. Postprocessing requires dedicated software, which may not be available in all facilities, especially those not affiliated with large academic centers. The need for adequate training for technicians and physicians is also an important factor, as errors in acquisition or analysis can compromise the reliability of the results.

Another logistic consideration is the duration of the scan. Although relatively short, the multi-echo sequence still requires patients to hold their breath. In individuals with dyspnea, children, or critical illness, this may not be feasible. New motion-corrected free-breathing acquisition techniques represent a promising solution, but are not yet widely available.[44] Chart 2 summarizes the main limitations.

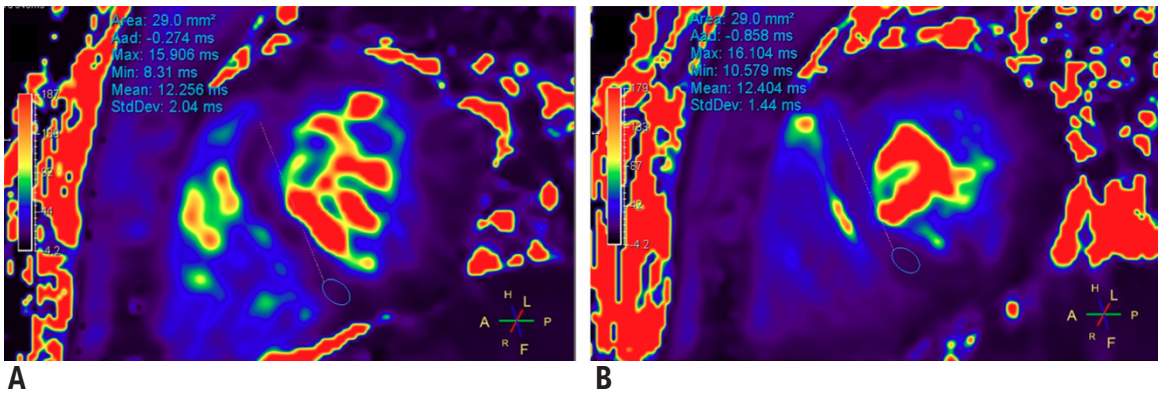


Figure 9 – *T2* parametric maps obtained during breath-hold (A) and during free breathing with motion correction (B) in a patient with myocardial iron overload. Excellent agreement is observed between the two techniques, demonstrating the clinical feasibility of the free-breathing approach. Adapted from Nazarova et al.[44]*

Chart 2 – Potential limitations of T1, T2, and T2* mapping sequences

Technique/parameter	Potential technical limitations	Clinical impact
Native T1 (MOLLI)	Sensitivity to off-resonance effects, magnetization transfer, high heart rate, variability among manufacturers and magnetic field strengths (1.5 T vs. 3 T).	May result in overestimation or underestimation of T1 values and hinder comparisons between centers.
Native T1 (ShMOLLI/SASHA/SAPPHIRE)	Methodological differences between sequences, lower precision, lower signal-to-noise ratio (in some techniques).	Values are not interchangeable between sequences.
T2 mapping	Sensitive to respiratory motion, arrhythmias, partial volume effects, and heterogeneity across sequences.	May result in falsely increased or decreased myocardial T2.
T2* mapping	Susceptible to magnetic field artifacts, especially in regions adjacent to the lungs or coronary vessels.	May compromise the quantification of iron overload.
ECV	Depends on the accurate determination of hematocrit and the quality of pre- and post-contrast T1 maps.	Errors in hematocrit may be amplified in the final ECV calculation.

ECV: extracellular volume; MOLLI: Modified Look-Locker Inversion Recovery; SAPPHIRE: saturation pulse prepared heart rate independent inversion recovery; SASHA: saturation-recovery single-shot acquisition; ShMOLLI: shortened modified look-locker technique.

2.3.6. Conclusions

T2* mapping is the most important tool for the noninvasive assessment of myocardial iron overload. Although the traditional septal ROI technique still guides cutoff values, maps offer the possibility of detailed regional analysis and integration with automated software. Two decades of evidence confirm that reduced T2* correlates with HF, arrhythmias, and mortality, providing high prognostic value in the follow-up of transfusion-associated cardiomyopathies (such as in thalassemia major and hemochromatosis). In the future, innovations such as free breathing, multiparametric protocols, and use of deep learning methods are expected to establish the T2* map as the universal standard for analysis.

2.3.7. Key Takeaways

- T2* quantification has revolutionized the management of patients with myocardial iron overload, enabling early diagnosis, risk stratification, and monitoring of treatment response;
- The traditional septal ROI method was essential for establishing the reference values used to this day, but is limited to an overall measurement and does not capture the heterogeneity of myocardial iron deposition;
- T2* maps represent the natural evolution of the technique, allowing voxel-by-voxel analysis, detailed segmental assessment, and intuitive visualization that facilitates communication with the treating physician;
- The prognostic value of T2* is well established: values below 10 ms at 1.5 T are strongly associated with risk of HF and sudden death and are considered one of the most robust markers for risk stratification in thalassemia major and other transfusion-dependent conditions;
- Recent advances, such as free-breathing imaging, multiparametric protocols (T1, T2, T2*, QSM), and AI-based reconstructions (e.g. mcLARO) suggest greater accuracy, speed, and standardization in future.

3. General Recommendations

3.1. Reporting of Results

To ensure that multiparametric (T1, T2, T2*, and ECV) CMR mapping results are useful and comparable across centers, report standardization is mandatory, including the format in which results are presented, the definition of normal ranges, and a description of the limitations of the technique. These recommendations are in line with recent national and international guidelines.[1,2,5,29,33,50,51]

3.1.1. Minimum Structure of Report

The report must contain:

- Magnetic field strength (1.5 T or 3 T), make, and model of the scanner;
- Sequence employed (e.g. MOLLI, ShMOLLI, or SASHA for T1; GraSE or T2-prep bSSFP for T2; multi-echo GRE for T2*);
- Software (including version) used for postprocessing;
- Anatomic region(s) of interest (mid-septum, global average of the LV, or segmental analysis);
- Absolute values obtained (in ms for T1/T2/T2*; as % for ECV);
- Reference ranges used (specifying whether they are based on international consensus and/or local validation).

3.2. Normal Values

The interpretation of multiparametric maps depends on well-defined reference values. At the time of writing, the

SCMR Normal Values 2025 review[51] is the most current international reference, featuring a large sample and stratification by age, sex, and ethnicity; the 2017 SCMR/EACVI consensus[5] remains a key document for technical standardization; and the most recent Brazilian guideline[2] provides reference ranges adapted to the national context.

Examples of reference ranges in healthy adults are given in Tables 3 and 4. The following values with reference ranges are for guidance only. Due to the various influencing factors described above, site-specific reference ranges must be established in accordance with the current SCMR consensus guidelines.

- Native T1: ~950–1050 ms at 1.5 T; ~1100–1250 ms at 3 T;
- ECV: ~24–29% (regardless of field strength), calculated from same-day hematocrit;
- T2: ~45–55 ms at 1.5 T; ~40–50 ms at 3 T;
- T2*: ≥ 20 ms, normal; 10–20 ms, moderate iron overload; < 10 ms, severe iron overload (preferably always evaluated at 1.5 T).

To ensure robust and clinically useful reference ranges for multiparametric maps, the SCMR recommends that each facility derive its own values from carefully characterized local samples. For scenarios involving large-scale myocardial changes – in which the effect on T1, T2, T2*, or ECV is extensive, such as in amyloidosis or myocardial infarction – relatively smaller samples are sufficient to define normal limits with acceptable precision: at least 15 healthy individuals or 20 individuals with a normal CMR.[5] However, for conditions with subtle effects, such as diffuse fibrosis or other diseases with low tissue contrast, the sample size must be increased to narrow reference ranges and reduce measurement variability; therefore, a minimum of 50 healthy individuals is recommended, stratified by sex when possible, given the known influence of sex on T1/ECV and other parameters.[5]

In all cases, data collection must follow standardized protocols (same magnetic field strength, sequence, manufacturer, software version, and ROI method), with explicit quality control (e.g. artifact exclusion, motion correction, same-day hematocrit for ECV) and publication of the mean, SD, and 2.5–97.5% reference interval. In addition, it is strongly recommended that each center establish and maintain its own reference ranges, based on local healthy cohorts, updating them whenever there are relevant changes in hardware, software, or protocol, since the direct transfer of "normal values" between platforms can introduce systematic bias and compromise clinical interpretation.[29]

Table 3 – Summary of native T1 and extracellular volume values

Technique/field strength	Native T1 (ms)	ECV (%)	Notes
MOLLI/1.5 T	950–1050	24–28	Most commonly used method; high reproducibility; sequence-dependent (e.g., 5(3)3, 4(1)3(1)2).
MOLLI/3 T	1100–1250	24–29	Values increase by ~150–200 ms compared to 1.5 T; greater susceptibility to field artifacts.
ShMOLLI/1.5 T	930–1000	23–27	Shorter acquisition time; values slightly lower than MOLLI; good clinical agreement.
ShMOLLI/3 T	1050–1200	24–28	Range similar to 3 T MOLLI, but slightly lower.
SASHA/1.5 T	1050–1150	25–29	Higher values compared to MOLLI; lower sensitivity to heart rate variability.
SASHA/3 T	1200–1300	25–30	Consistent, but less commonly used in routine clinical practice.
StarMap/1.5 T	960–1020	24–28	Close agreement with MOLLI; fast acquisition; requires local validation.
StarMap/3 T	1150–1250	24–28	Equivalent to MOLLI at 3 T; depends on the reconstruction algorithm.

ECV: extracellular volume; MOLLI: Modified Look-Locker Inversion Recovery; SASHA: saturation-recovery single-shot acquisition; ShMOLLI: Shortened Modified Look-Locker technique; T: Tesla.

Table 4 – Summary of T2 and T2* map values

Parameter	1.5 T (mean [SD]/range)	3 T (mean [SD]/ range)	Notes
T2 (ms)	45–55	40–50	Varies with technique (GraSE or T2-prep bSSFP).
T2* (ms)	≥ 20, normal; 10–20, moderate overload; < 10, severe overload	Not standardized**	Myocardial iron assessment validated only at 1.5 T.

bSSFP: balanced steady-state free precession; GraSE: gradient and spin echo; T: Tesla; T2-prep: T2 preparation.

3.3. Clinical Interpretation

- Results should not be interpreted in isolation, but rather integrated with clinical, laboratory, and other imaging data;
- When available, age- and sex-adjusted reference values should be used;
- Discrepancies between parameters (e.g., elevated T1 with normal ECV) should be discussed in the report, including possible pathophysiological explanations and recommendations for clinical correlation;
- The European Society of Cardiology (ESC) guidelines on cardiomyopathies[1] emphasize that multiparametric mapping is an essential tool in the differential diagnosis of infiltrative, inflammatory, and hereditary cardiomyopathies.

3.4. Conclusion

Standardized reporting of CMR multiparametric maps, including absolute values, normal ranges, and technical limitations, is essential to ensure quality of care and scientific comparability. These recommendations are in line with national[2] and international[5,51] guidelines and should inform clinical practice and research in Brazilian centers.

3.5. Key Takeaways

The report should follow a standardized format, including information on the magnetic field, equipment manufacturer and model, sequence employed (MOLLI, ShMOLLI, SASHA, etc.), and postprocessing software and version;

- Anatomic ROI (septum, global average, or segmental);
- Preference for septal measurement;
- Absolute values (in ms for T1/T2/T2*; as % for ECV);
- Reference ranges and their source (international or local);

International reference: SCMR Normal Values 2025[51] (stratified by age, sex, and ethnicity);

- Examples in healthy adults: Native T1 ≈ 950–1050 ms (1.5 T) | 1100–1250 ms (3 T), ECV ≈ 24–29%, T2 ≈ 45–55 ms (1.5 T) | 40–50 ms (3 T), T2* ≥ 20 ms = normal | 10–20 ms = moderate overload | < 10 ms = severe overload;
- Each center should establish its own reference ranges, using homogeneous protocols (same field, sequence, software, ROI) and same-day hematocrit for ECV;
- Recommended sample size: ≥ 15 individuals for conditions with a large effect (abnormal tissue), ≥ 50 healthy individuals for conditions involving subtle changes (diffuse fibrosis).

4. Ischemic Cardiomyopathy

Multiparametric maps are useful in the myocardial tissue assessment of patients with suspected or established ischemic cardiomyopathy. In cases where the etiology of myocardial damage is not yet known, they aid in the differential diagnosis with non-ischemic causes (as will be discussed in other sections); in cases where an ischemic origin of the cardiomyopathy has already been established, they provide additional diagnostic and prognostic information in both the acute and chronic phases, as discussed below.

4.1. Acute

The identification of myocardial edema in a coronary artery territory may indicate acute or recent ischemic damage[52] and is an important finding for the differential diagnosis with chronic cardiomyopathies, including ischemic heart disease, when myocardial fibrosis may be present but without attendant tissue edema. Traditionally studied using T2-weighted sequences,[53] myocardial edema can also be assessed using T1M and T2M sequences, which offer improved accuracy and reproducibility in patients with acute coronary syndrome.[54,55]

In distinguishing between acute and chronic myocardial infarction, Tahir et al. demonstrated that myocardial T1 and T2 times, quantified using parametric sequences, are increased in the acutely infarcted area, and were the best parameters to make this distinction (area under the receiver operating characteristic [ROC] curve of 0.975 and 0.979, respectively), outperforming evaluation with T2-weighted sequences, whether analyzed visually or semiquantitatively.[54] In the same study, the authors found that T1 and T2 values in the infarcted area decrease over a 6-month period following the acute event, yet remain higher than those in non-infarcted myocardium throughout this time (Figure 10).

In identifying the culprit artery in patients with non-ST-segment elevation myocardial infarction, Layland et al. also demonstrated greater accuracy of T1M and T2M sequences, with lower interobserver variability, compared to the T2-weighted sequence.[55] In addition to indicating the presence of acute ischemic myocardial damage, the area of edema extending beyond the area of necrosis – which represents potentially reversible tissue injury – can be used as a marker of the area of myocardium at risk.[56] T1M and T2M sequences have also demonstrated their utility for this purpose, with similar performance between them.[57]

Still regarding the reversibility of myocardial injury, the T1 values observed acutely in the infarct area are highly accurate in predicting irreversible damage.[58] Furthermore, because they show an inverse linear relationship with the potential for functional recovery, myocardial T1 measurements may be more useful than LGE when assessed acutely for this purpose, due to the nonlinear behavior of the latter.[59]

Microvascular obstruction and intramyocardial hemorrhage – conditions that may be seen in the acute phase of myocardial infarction following reperfusion – are indicative of worse prognosis when present.[60] Both can be accurately detected on T1M and T2M sequences as regions of lower signal intensity within the infarct area.[61] Intramyocardial hemorrhage is also detectable and quantifiable on T2* mapping sequences.[62]

4.2. Chronic

In the chronic phase of ischemic cardiomyopathy, the presence and extent of ischemia and myocardial fibrosis are highly relevant factors for prognostic assessment and clinical decision-making.[63] Techniques based on perfusion and late

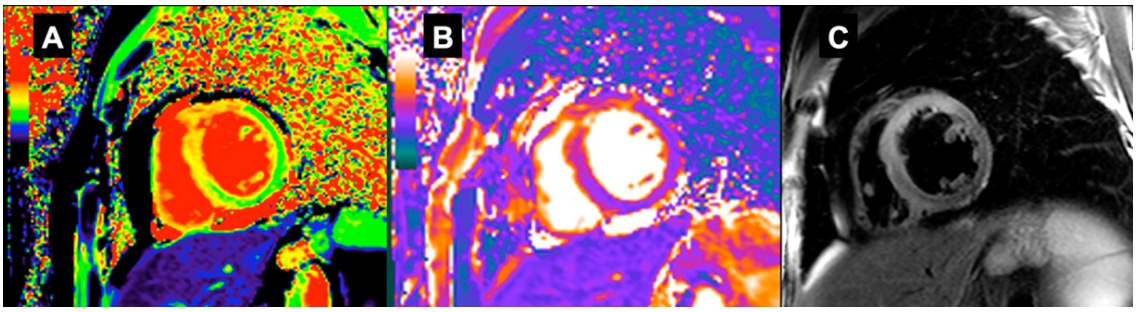


Figure 10 – *T1 map (A), T2 map (B), and fat-saturated T2-weighted sequence (C) images (short-axis view), showing increased signal intensity in the mid-anterior-septal and mid-anterior segments of the left ventricle, consistent with myocardial edema, 3 days after an acute ST-segment elevation myocardial infarction involving the left anterior descending artery and treated with primary percutaneous coronary intervention. Although the signal change is noticeable in all sequences, the contrast between the affected and remote regions is greater in the parametric sequences.*

myocardial enhancement in CMR have well-documented performance[64] and are the gold standard for this type of assessment, although T1M sequences may be helpful in some specific scenarios and provide additional information in some specific scenarios.

The presence of post-infarction myocardial fibrosis increases T1 time in the affected region, a finding that can be detected in non-contrast images, which makes it especially useful in the assessment of patients with contraindications to contrast administration.[65] However, given that several clinical studies have demonstrated reduced sensitivity of native T1 for detecting and quantifying infarct area in the chronic setting,[65-67] this technique cannot be considered a substitute for the standard LGE-based assessment.[68] In future, technologies that use AI to generate virtual contrast images based on native myocardial T1 maps and cine images may improve the accuracy of this type of analysis, enhancing its clinical utility.[69]

On the other hand, the quantification of native T1 and ECV in remote (non-fibrotic) myocardium in patients with chronic ischemic cardiomyopathy has established utility in predicting mortality, major cerebrovascular events, and hospitalization for HF, which may be independent of and superior to other established methods for this purpose.[70,71] In a prospective, observational study conducted exclusively in patients with chronic coronary artery disease, an increase in native T1 exceeding two SDs from normal in the remote myocardium showed the largest area under the ROC curve for predicting all-cause mortality (0.729), outperforming assessment of the extent of late enhancement (0.539) and the presence of LV ejection fraction (LVEF) equal to or less than 35% (0.527).[70]

For the assessment of myocardial ischemia, considering that myocardial blood volume increases during stress[72] and that this increase causes a change in the native myocardial T1 value,[73] studies have demonstrated that areas of ischemia[74,75] and microvascular dysfunction[76] can be identified on stress CMR scans with T1M, obviating the need for contrast. However, given the small number of patients included in clinical studies, the lack of a standard protocol, and several technical considerations still under debate,[77] stress studies based on T1M remain an investigational technique.

4.3. Key Takeaways

- T1M and T2M sequences are superior to T2-weighted sequences for detecting myocardial edema in the acute phase of myocardial infarction;
- Measurements of native myocardial T1 can identify regions of infarction in the chronic post-myocardial infarction phase without the need for contrast, but are inferior to assessment with LGE sequences, especially due to low sensitivity;
- Assessment of myocardial areas free of fibrotic scarring (remote myocardium) through quantification of native T1 and myocardial ECV has high prognostic value in patients with chronic coronary artery disease.

5. Non-Ischemic Cardiomyopathies

5.1 Dilated Phenotype

5.1.1. Chagas Disease

CMR provides a noninvasive means of assessing myocardial inflammation, fibrosis, and edema in Chagas cardiomyopathy. Conventional techniques such as LGE are able to identify focal fibrosis, but more recent parametric mapping techniques, such as T1M and T2M, allow quantification of diffuse and often microscopic myocardial changes. Native T1 values reflect fibrosis and inflammation, while T2 values are markers of edema.

These mapping techniques have gained prominence in the evaluation of Chagas cardiomyopathy, particularly due to their ability to characterize myocardial tissue changes in a quantitative, noninvasive, and sensitive manner, even in subclinical stages of the disease.[78-80]

5.1.1.1. Clinical Applications in Chagas Disease

Recent studies have demonstrated the utility of T1 and T2 maps in the evaluation of Chagas cardiomyopathy in the following scenarios:

Early detection of fibrosis: patients with Chagas cardiomyopathy exhibit elevated native T1 and ECV values, even in the absence of LGE, indicating diffuse fibrosis undetected by conventional techniques.[78]

Assessment of inflammation: increased signal intensity on T2-weighted images can be detected in all stages of Chagas disease, including the indeterminate stage, and correlates well with the extent of myocardial fibrosis assessed by LGE. The presence of myocardial edema, identified by T2, correlates with the clinical severity of the disease and may indicate persistent inflammatory activity, even in asymptomatic patients or those with mild ventricular dysfunction.[79]

Disease staging: native T1 and ECV values correlate with the clinical severity of Chagas cardiomyopathy and may aid in disease staging and risk stratification. In a prospective study, overall native T1 and ECV values were significantly higher in patients with more advanced Chagas cardiomyopathy (slightly reduced LVEF and reduced LVEF) compared with those with the indeterminate form of the disease, those with preserved LVEF, and healthy controls. This finding suggests that T1M and ECV can detect diffuse myocardial changes that correlate with disease severity. Another striking finding was the observation of an increased mean global ECV (above 30%) in approximately 12% of patients with the indeterminate form of the disease. In contrast, only 3% of patients in this group showed detectable LGE. These results may suggest that global ECV is a more sensitive marker than LGE for identifying early extracellular matrix abnormalities in this setting, and may even help identify patients requiring earlier initiation of cardioprotective therapy.[78]

Therapeutic monitoring: changes in T1 and T2 values following benznidazole therapy suggest that these techniques may be useful in monitoring treatment response. Sousa et al. described a case report of acute Chagas disease presenting with nonspecific symptoms but without clinical evidence of Chagas cardiomyopathy and demonstrated via CMR that, despite the absence of LGE, the T2 map was diffusely abnormal in a manner characteristic of myocardial edema. Subsequent scans obtained during treatment identified a progressive reduction in T2 values until they returned to normal. Throughout the follow-up period, scans showed no evidence of LGE.[80]

According to current guidelines,[81] there is no evidence to suggest any benefit from routine use of antiparasitic agents in patients with chronic Chagas cardiomyopathy. However, a recent prospective study evaluated the behavior of CMR findings after 60 days of benznidazole treatment in this setting. There were no significant changes in cavity diameters (LV diastolic and systolic volumes) or LVEF; however, reductions were observed in native T1, T2, and ECV values.[82] These findings suggest that there may be an opportunity to reduce fibrosis/inflammation in patients with chronic Chagas cardiomyopathy using this therapeutic approach and thereby slow the rate of disease progression.

Integration with other imaging modalities: native T1 map values obtained by CMR also correlate with another early marker of myocardial damage routinely used to detect subclinical signs of ventricular dysfunction: global longitudinal strain (GLS), assessed by echocardiography. Lima et al. demonstrated, in mild forms of Chagas cardiomyopathy with preserved LVEF, a moderate correlation between native T1 map values and GLS ($r = 0.634$; $p = 0.015$).[83]

Prognostic marker for major cardiovascular events: studies show that T1 map parameters, such as global ECV, are elevated from the early stages of chronic Chagas cardiomyopathy and correlate with an increased risk of ventricular arrhythmias, such as non-sustained ventricular tachycardia (VT), regardless of LVEF and the extent of fibrosis detected by LGE. This suggests that ECV may serve as an early marker of arrhythmia risk and disease progression, with potential prognostic value and utility for risk stratification.[84]

To minimize the effect of late enhancement on the increase in overall ECV, another study evaluated the prognostic value of native T1 in non-enhancing areas, i.e., areas where no LGE is detectable. When these values exceed 1100 ms, there appeared to be an independent predictive association with major cardiovascular events (a composite of defibrillator implantation, heart transplantation, or death), highlighting the prognostic utility of T1M in Chagas cardiomyopathy, even in areas without detectable macroscopic fibrosis.

5.1.1.2. Key Takeaways

- T1M (including ECV) and T2M techniques represent significant advances in CMR and are emerging as valuable tools in the evaluation of chronic Chagas cardiomyopathy, enabling early detection and quantification of myocardial fibrosis and inflammation, with prognostic implications and the potential to guide therapeutic strategies and risk stratification;
- Clinical use of these methods can improve disease staging, risk stratification, and treatment monitoring. However, efforts are needed to standardize protocols and expand access to these techniques, especially in regions where Chagas disease is endemic.

5.1.2. Myocarditis

Myocarditis is an inflammatory disease of the myocardium that may be of infectious, autoimmune, or toxic etiology. Its main pathophysiological mechanism involves damage to and necrosis of cardiomyocytes, which triggers an inflammatory response and perpetuates the process.[85]

The course of myocarditis is traditionally divided into three phases:

1. Acute phase (lasting a few days);
2. Subacute phase (lasting weeks to months);
3. Chronic phase (scarring or related to dilated cardiomyopathy).

Given the risk of progression to HF or sudden death – which occurs in up to 12% of cases – accurate diagnosis is essential. However, endomyocardial biopsy is generally reserved for

specific situations, such as giant cell myocarditis, eosinophilic myocarditis, or severe cases with refractory HF.

Since 2009, CMR, due to its ability to characterize tissue at different stages of the disease, has been incorporated into the Lake Louise criteria, in accordance with an American College of Cardiology (ACC) position statement.[86] The recommended diagnostic sequences originally included:

- T2-weighted images for detection of edema (which can be performed qualitatively, by identifying localized areas of hyperintensity, or quantitatively, by comparing myocardial signal to that of skeletal muscle);
- Early enhancement (to assess hyperemia);
- Late enhancement (indicative of necrosis or fibrosis).

These recommendations were largely based on qualitative criteria.

In 2018, a new ACC position statement[87] updated the criteria to incorporate parametric maps (T1, T2, and ECV).

The main concept behind T2 map assessment is the detection of myocardial edema, which translates into elevated T2 values. Compared to traditional T2-weighted sequences, T2M offers such advantages as:

- Less subjectivity (lower inter- and intra-observer variability);
- Faster acquisition and lower susceptibility to artifacts;
- Better SNR;
- Greater sensitivity in diffuse edema.

Overall, the sensitivity and specificity of this technique are approximately 91% and 79%, respectively, with an overall accuracy of 79%.[88] Although some authors have suggested values above 65 ms, the 60-ms threshold appears to represent a more sensitive cutoff point while maintaining good specificity.[89,90]

Elevated native T1 and ECV values are also present in the acute phases, indicating myocardial injury (inflammation and cellular necrosis), but they are nonspecific, as they may remain elevated in scar tissue from previous events.[1] Although these values tend to decrease as the acute phase resolves, there are still no defined parameters to confirm inflammatory activity based solely on these data. As additional information, in a recent study of patients with acute myocarditis, the T1 map demonstrated ability to identify inflammation even in segments without LGE, albeit to a lesser degree, suggesting diffuse involvement – a capability not demonstrated by T2M.[49]

Based on these data, the new Lake Louise criteria (Table 5) now define the diagnosis of myocarditis as follows:

- At least one criterion for edema (regional or global hyperintensity on T2-weighted sequences or elevation on T2M) plus one criterion for myocardial injury (LGE, elevated native T1, or elevated ECV).

The following are also considered supporting criteria, although they are neither mandatory nor exclusionary:

- Global or regional wall motion abnormalities;
- Evidence of pericarditis (effusion, edema, or pericardial enhancement).

Table 5 – New Lake Louise criteria (3), now incorporating parametric maps. Diagnosis requires the presence of one criterion for edema and one criterion for non-ischemic myocardial injury

2018 Lake Louise Criteria	
Major criteria	Localized T2 hyperintensity (visual analysis)
	Global increase in signal intensity on T2-weighted sequences
	Increased T2 map
	Late gadolinium enhancement with a non-ischemic pattern
	Increased T1/extracellular volume
Supporting criteria	Global or regional wall motion abnormalities
	Pericarditis (effusion, edema, or pericardial enhancement)

Data from the literature suggest that incorporating parametric maps into the new criteria has increased diagnostic sensitivity from 72% (previous criteria) to 88%, while maintaining specificity at around 96%.[92]

Parametric maps appear to play an even more important role in cases of myocarditis with atypical presentations, such as those related to the use of immunotherapy agents of the immune checkpoint inhibitor (ICI) class. Of these patients, only 28% exhibit LGE and 48% exhibit T2 hyperintensity.[93] When parametric maps are used, T1 prolongation is observed in 78% of cases and T2 prolongation in 43%. Furthermore, when applying the Lake Louise criteria, 95% of patients meet the criteria for myocardial injury (T1 enhancement or late enhancement), significantly increasing diagnostic accuracy.[93]

Regarding prognosis, evidence in the literature demonstrates an independent association between T1 and ECV values and the prediction of adverse cardiovascular events (death, hospitalization, HF, heart transplantation, and recurrence of myocarditis).[94,95]

Based on the data described above and following the SCMR recommendations,[29] we propose a protocol for the use of T1M and T2M in the investigation of acute myocarditis (Table 6) and present a summary of the method's main characteristics and advantages (Table 7).

5.1.2.1. Conclusion

Multiparametric CMR (T1, T2, ECV + LGE) is currently the noninvasive gold standard for the diagnosis, stratification, and follow-up of acute myocarditis and its variants, combining high diagnostic accuracy with proven prognostic value.

5.1.2.2. Key Takeaways

- Myocarditis is an inflammatory disease of the myocardium of infectious, autoimmune, or toxic etiology;

Table 6 – Recommended sequences for myocarditis

Sequences	Recommendations
1. Cine MRI	– Acquired in the standard planes (long-axis and short-axis with complete coverage of both ventricular cavities).
2. Anatomic ("black blood") T2-weighted sequences	– Acquired in the same radial slices as cine imaging and 3 short-axis slices (basal, mid, and apical) – Mandatory if parametric maps are not available; optional when they are available – Recommended if associated pericarditis is suspected (in which case, use fat-saturated sequences).
3. Native T1 map	– Acquired in 3 short-axis views (basal, mid, and apical). – The upper limit varies depending on the magnetic field strength, manufacturer, and local factors, and should be established by each facility.
4. T2 map	– Acquired in 3 short-axis views (basal, mid, and apical). – There may be limitations in patients with a high heart rate.
5. Late enhancement (10 to 15 minutes after gadolinium injection)	– Acquired in the same views as cine imaging (long-axis and short-axis).
6. Post-contrast T1 map (at least 10 min after gadolinium injection)	– Performed on views identical to those used for T1 maps. – Calculation of extracellular volume must use a hematocrit obtained within 24 hours of the scan.

Table 7 – Characteristics and advantages of parametric maps in myocarditis

1. T2 mapping	– Related to myocardial edema. – Specific for the acute phase. – Less subjectivity, greater robustness, and higher accuracy than T2-weighted sequences. – Best cutoff point above 60 ms.
2. T1 mapping/extracellular volume	– Related to myocardial injury (inflammation and necrosis). – Nonspecific for the acute phase, although values decrease as the disease progresses. – May be increased, albeit to a lesser degree, in areas without late gadolinium enhancement, reflecting its ability to identify diffuse involvement. – Established association with prognosis. – Particularly useful in identifying myocarditis induced by immune checkpoint inhibitors.

• It is classically divided into three phases: acute, subacute, and chronic (fibrosis/dilated cardiomyopathy);

• HF or sudden death may occur in up to 12% of cases;

Endomyocardial biopsy is reserved for severe or specific forms (e.g. giant cell, eosinophilic);

• T2M detects myocardial edema (increased T2). Sensitivity ≈ 91%, specificity ≈ 79%; cutoff: T2 ≥ 60 ms;

• Native T1 and ECV are increased in the acute phases (inflammation/necrosis) but are nonspecific (may remain elevated in chronic fibrosis);

• Increased T1 can detect inflammation in segments without late enhancement, indicating diffuse involvement;

• In 2018, the new Lake Louise criteria incorporated parametric maps (T1, T2, ECV), increasing diagnostic sensitivity. At least one criterion for edema (increased T2 or T2 hypersignal) and one criterion for myocardial injury (increased T1/ECV or late enhancement) are required;

• Including these maps has increased diagnostic sensitivity from 72% to 88%, while maintaining specificity at ≈ 96%;

• Particularly useful in ICI-induced myocarditis, in which late enhancement may be absent;

• Increased T1 and ECV are associated with a higher risk of adverse cardiovascular events (death, HF, transplantation, recurrence).

5.1.3. Iron Overload

Assessment of myocardial iron deposition can be performed using CMR with the T2* technique.[96] Because iron behaves as a paramagnetic agent, its presence can be detected by the shortening effect it causes in myocardial T2*.

Myocardial iron overload can occur due to repeated blood transfusions for the treatment of anemia or due to increased intestinal absorption resulting from genetic causes. Since HF is the most common cause of death in patients with iron overload, this method is highly relevant in this setting, especially given that treatment with chelating agents is effective and reduces mortality.[39,97]

This technique has been validated through quantitative iron studies in human hearts, confirming that the iron concentration in the mid-septum is representative of the overall iron concentration in the myocardium.[38] It has been demonstrated that 98% of patients with thalassemia major who went on to develop HF had a myocardial T2* value of less than 10 ms (Figures 11 and 12).[98] Furthermore, treatment progress can be monitored with this technique.[99]

Although it is possible to assess myocardial iron deposition using 3-T scanners, it is recommended that scans for this indication be performed on 1.5-T equipment, which tends to produce fewer artifacts and offer greater data reproducibility.[100]

It is recommended that images be acquired in the short-axis plane, in the mid- LV region, with a gradient-echo sequence.[41] Multi-echo acquisitions should be used,

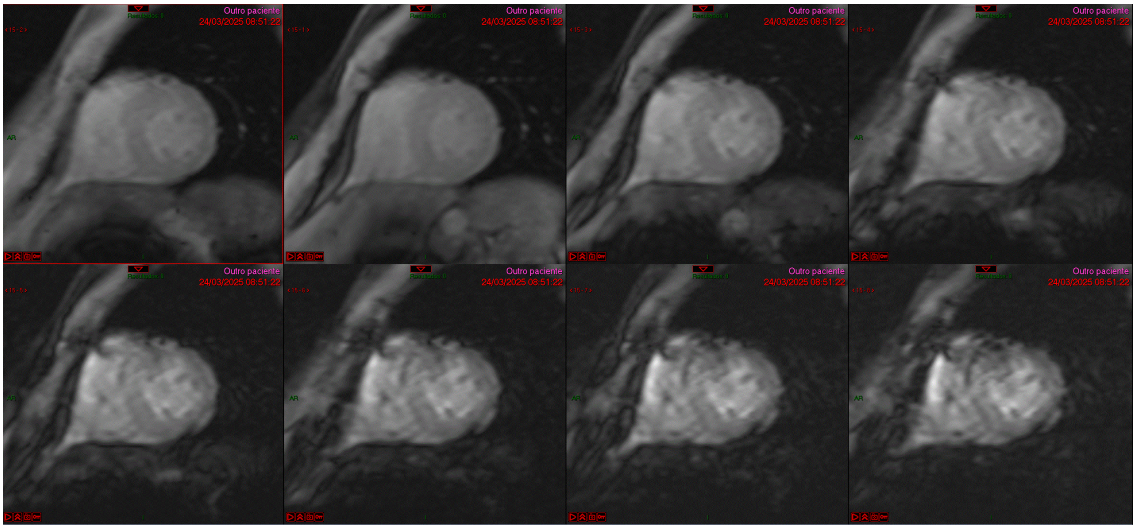


Figure 11 – *Example of T2* mapping in a healthy patient.*

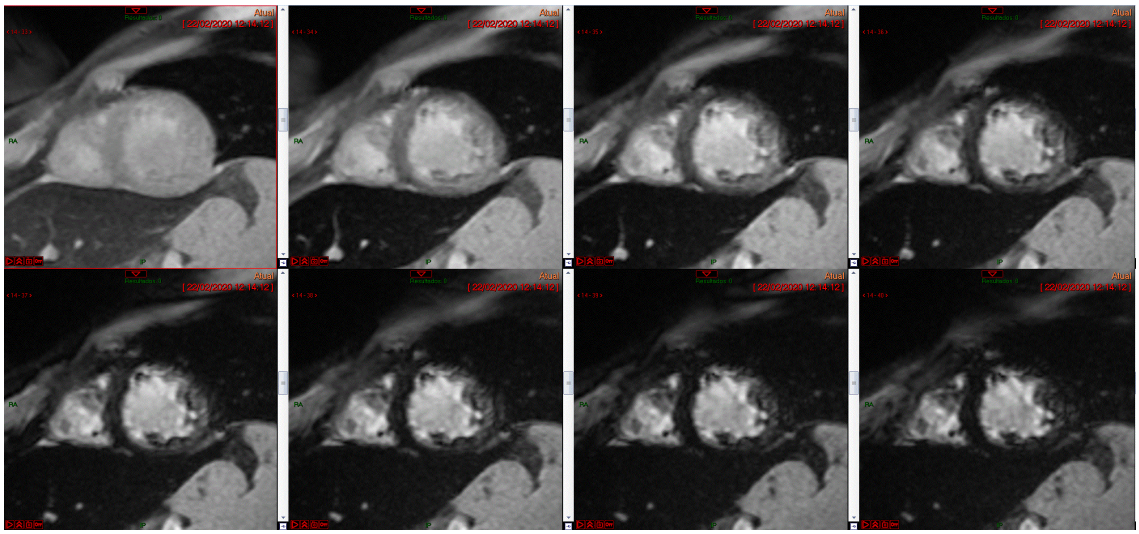


Figure 12 – *Example of T2* mapping technique in a patient with myocardial iron overload and a T2* < 10 ms.*

employing 8 echoes with equal intervals ranging from 2 to 18 ms, in a single breath-hold, using "dark-blood" imaging if possible, although "white-blood" images are also validated. Measurements should be obtained with the ROI positioned in the septum, encompassing both the subendocardial and subepicardial regions.

It is important to note that native myocardial T1 is expected to be reduced in patients with myocardial iron deposition; however, this technique is less well-validated for this application, and while it may offer advantages in terms of reproducibility in cases of low-level myocardial iron deposition, it is unlikely to be relevant in situations where myocardial iron deposition poses a risk of HF and is clinically significant.[101,102]

5.1.3.1. Conclusion

Myocardial T2* is a fundamental tool for the diagnosis, stratification, and treatment monitoring of iron overload and should be performed in a standardized manner, ideally at 1.5 T and using a septal ROI.

5.1.3.2. Key Takeaways

- T2* mapping is the gold-standard noninvasive method for detecting and quantifying iron overload in the myocardium;
- Iron acts as a paramagnetic agent, shortening the T2* time – the shorter the T2*, the higher the iron load;
- **Iron overload** occurs primarily due to **repeated blood transfusions** (thalassemia major, chronic anemias) or **increased intestinal absorption** (genetic causes, such as hemochromatosis);
- **The mid-septum T2* value** is a good indicator of total myocardial iron content (In thalassemia major, **a T2* value < 10 ms** is strongly associated with HF, in 98% of cases);
- T2* allows for **monitoring of the response to chelation therapy** over time;
- Prefer 1.5 T for this application, due to lower susceptibility to artifacts and greater reproducibility compared to 3 T;
- Patients with iron overload exhibit **r**educed T1 values; however, this technique is less well-validated and has limited clinical utility.

5.1.4. Sarcoidosis

Sarcoidosis is a systemic granulomatous disease of undetermined etiology[2] and a challenging diagnosis. Diagnostic criteria have been established by three different societies: the Japanese Circulation Society (JCS), the Heart Rhythm Society (HRS), and the World Association for Sarcoidosis and Other Granulomatous Diseases (WASOG).

Clinical cardiac manifestations occur in 5–10% of all cases,[103,104] but autopsies reveal cardiac involvement in up to 58% of cases.[105,106]

The condition behaves as an inflammatory cardiomyopathy. Diagnosis is challenging, especially given that 49 to 65% of cases present with cardiac symptoms as the initial manifestation, without evidence of extracardiac involvement. Another challenging scenario is when involvement is exclusively cardiac, which occurs in 3 to 5% of cases.[107] It is the second leading cause of mortality in sarcoidosis, after pulmonary involvement.[108]

Endomyocardial biopsy was long considered the gold standard for diagnosis; however, even when guided by imaging, its sensitivity is limited to 20–50%.[109] Thus, most cases are currently diagnosed based on a combination of clinical data, evidence of extracardiac involvement (lungs, lymph nodes, skin, eyes), and imaging studies, with cardiac MRI currently considered the first-line choice, combined with [^{18}F]FDG PET in some settings.[110] CMR is the gold standard among imaging modalities.[111]

LGE is positive for fibrosis in approximately one-third of cases and is the best predictor of mortality and ventricular arrhythmias, even in patients diagnosed with sarcoidosis but who are asymptomatic from a cardiovascular standpoint.[110,112] It is considered a diagnostic criterion in all classifications of the medical societies mentioned above. Its pattern may vary, with meso-/epicardial or even transmural involvement, typically of the basal interventricular septum (especially the basal anterolateral segment, near the right ventricle [RV]) and the lateral wall (more commonly in the basal inferolateral segment).[113]

LGE is highly effective for detecting focal fibrosis but is limited in assessing diffuse or early involvement – situations in which multiparametric mapping sequences have recently made a greater contribution. The assessment of edema using T2-weighted sequences (T2-STIR and T2M) is included as a diagnostic criterion only in the WASOG classification,[109] with concurrent use of both techniques recommended.

Native T1, T2, and ECV maps have emerged as extremely useful tools for quantitative tissue characterization in cardiac sarcoidosis, supplementing conventional LGE evaluation. Their use is recommended by the SCMR in cases of suspected sarcoidosis, as outlined in its 2020 publication on standard protocols.[29] Parametric maps are particularly useful in cases where echocardiography is negative or inconclusive, and the use of combined techniques is recommended over the isolated use of any single technique.

According to a preliminary study of patients with cardiac sarcoidosis, measurement at the mid-septum showed similar performance to measurement of all mid-third segments in distinguishing healthy from affected myocardium, which facilitates standardization and speeds up analysis.[114]

The use of T2M increases the sensitivity of edema detection from 88% to 99%.[115] Increased T2 values are consistently found in cases of myocardial inflammation,[116] and studies have shown that T2M is superior to LGE for identifying active lesions in patients who initially show no LGE.[115,117,118]

Native T1M has debatable added value over LGE,[111] but it can also be used for treatment monitoring.[119] T1 and ECV values have demonstrated the ability to aid in the differential diagnosis of similar inflammatory conditions, with lower T1 map values and higher ECV values in areas of LGE in sarcoidosis and the acute and chronic phases of myocarditis. The mean (SD) values obtained for native T1 maps were 1157 (54) ms in sarcoidosis, 1196 (63) ms in acute myocarditis, and 1215 (74) ms in chronic myocarditis. The values for ECV

were 0.65 versus 0.45 and 0.47, respectively, with an ECV cutoff value of 0.57 corresponding to an accuracy of 0.87 for diagnosis of sarcoidosis.[120]

Recently, multiparametric imaging – particularly T2M – has been used to monitor disease activity and response to immunotherapy.[121-123]

Native T1 map:

• Consistently elevated in cardiac sarcoidosis when compared to those of healthy patients;

• Provides information complementary to LGE, particularly in detecting diffuse forms of the disease;

• Useful for early disease detection in patients with suspected cardiac sarcoidosis.

Post-contrast T1 map and ECV:

• Quantification of ECV is less dependent on technical factors related to the MRI scanner compared to absolute T1 values;

• Regional analysis of ECV in areas with positive LGE findings may help differentiate sarcoidosis from other forms of myocarditis;

• Provides prognostic information regarding clinical outcomes.

T2 map:

• Elevated T2 values correlate with active myocardial inflammation;

• Useful for monitoring the response to anti-inflammatory therapy and may even guide timing of its initiation;

• Correlates with myocardial activity on [^{18}F]FDG PET;

Values return to normal with successful treatment.

Limitations: multiparametric maps are nonspecific, and findings may overlap with those of other conditions. Validation in large, prospective cohorts is pending. Its prognostic role is still unclear pending further evaluation, unlike that of LGE. The use of maps has stronger evidence in the context of investigation of arrhythmia risk.

Advances and prospects: becoming quantitative biomarkers, adjuncts to LGE and GLS. Reductions in T2 map values and LGE following immunotherapy have already been demonstrated. Use of AI and automation for better detection and quantification of subtle changes and reduced variability.[113,124]

5.1.4.1. Key Takeaways

• Quantification of T1 maps (native and ECV) is a sensitive marker for detecting diffuse infiltration and fibrosis in cardiac sarcoidosis, particularly in cases with no LGE;

• The T2 map is a biomarker of active myocardial inflammation and can be used to monitor the response to immunosuppressive treatment;

• The combined use of PET/CMR with multiparametric maps increases diagnostic confidence and provides supplemental information for risk stratification;

• Regional analysis of the native T1 map and ECV in areas with positive LGE improves the ability to discriminate cardiac sarcoidosis from other inflammatory myocardial conditions.

5.2. Arrhythmogenic Phenotype

Arrhythmogenic cardiomyopathy (AC) is a cardiac disease characterized by the progressive replacement of myocardial tissue with fibro-adipose tissue, predisposing patients to life-threatening arrhythmias and sudden death.[125] Diagnostic criteria for AC were first proposed in 1994[126] and revised in 2010 by an international task force.[127] Subsequent studies have demonstrated frequent LV involvement in this disease, primarily based on CMR findings in these patients showing the presence of fibrosis in both the RV and LV on LGE imaging. Autopsy studies have also shown that 87% of cases of sudden death diagnosed with AC at autopsy had histological involvement of the LV, and that biventricular involvement in the disease is much more common than univentricular involvement.[128]

Consequently, in 2020, new diagnostic criteria were published (the Padua criteria), which now include left-sided involvement and emphasize morphofunctional and structural findings as markers of the disease.[129] Recently, changes to the diagnostic criteria were reaffirmed and refined through an international consensus, corroborating the understanding of the importance of morphofunctional findings and imaging methods in defining AC.[125] An innovative aspect of this latest definition is the primary characterization of AC as a disease of myocardial "scarring", resulting from myocyte death and fibro-adipose repair processes. This leads to scarring-related ventricular arrhythmias and progressive impairment of ventricular systolic function, with systolic dysfunction correlating with the extent of scarring. This characteristic is consistent across all phenotypic variations of the disease (LV, RV, or biventricular involvement).[125,130]

AC manifests in three main phenotypes: RV-dominant (the classic form), biventricular, and LV-dominant. CMR plays a key role in its diagnosis and is considered the gold standard for:

• Biventricular morphofunctional assessment: cine-CMR sequences allow detailed analysis of the function and volumes of both ventricles.

• Assessment of myocardial fibrosis: uses the LGE technique to identify and quantify the presence of myocardial fibrosis, a disease-defining finding in AC.

According to the latest guidelines,[125] the diagnosis of AC is based on the evaluation of the morphofunctional and structural criteria described below.

a) Morphofunctional criteria:

• RV:

◦ Presence of regional wall motion abnormalities;

◦ Volume enlargement – indexed end-diastolic volume (EDV) greater than:

- > 112 mL/m² in women;
- > 121 mL/m² in men;
- > 130 mL/m² in athletes;

◦ Systolic dysfunction – ejection fraction less than:

- < 51% in women;
- < 52% in men;
- < 52% in athletes;

- LV:
  - Systolic dysfunction – ejection fraction less than:
    - < 57% in women;
    - < 57% in men;
    - < 58% in athletes;
  - Volume enlargement – indexed end-diastolic volume greater than:
    - > 96 mL/m² in women;
    - > 105 mL/m² in men;
    - > 122 mL/m² in athletes.

b) Structural criteria (LGE)

- Myocardial fibrosis: primary evidence, based on LGE findings, of fibrosis in the myocardium;
  - RV: unequivocal late enhancement, confirmed in two orthogonal views and in more than one region;
  - LV: "ring-like" pattern confirmed in two orthogonal views, or involvement of one or two segments with a meso- or subepicardial pattern.

Given the importance of myocardial fibrosis in the pathophysiology of AC and in the mechanism of reentrant ventricular arrhythmias, obtaining late-enhancement images is essential in the evaluation of these patients. However, this technique identifies only focal, reparative fibrosis. In this regard, parametric maps could expand the scope of CMR in AC, as they are capable of assessing diffuse, interstitial fibrosis and allow detection of increased ECV. Due to these characteristics, parametric maps are capable of identifying early structural changes or changes in affected family members, enabling earlier diagnosis.[131] T2M, in turn, would be capable of identifying acute changes in inflammatory states already recognized as possible manifestations of AC. One limitation to the applicability of such maps in these patients is their primary utility in evaluating the LV, given the susceptibility of this technique to partial-volume artifacts when applied to the thin-walled RV myocardium. Despite these possibilities, data are still preliminary, and few studies have been conducted to demonstrate the applications of parametric maps in the assessment of patients with AC.

Bourfiss et al. evaluated T1-mapping CMR in 43 individuals, including patients with AC, genotype-positive relatives, and controls. Patients with AC had significantly higher global T1 values than controls, while relatives did not differ significantly from controls. In contrast, T1 dispersion (the SD of T1 values among LV segments) was higher in both patients and relatives, particularly in the inferolateral and inferior regions. A T1 dispersion cutoff of > 77 ms demonstrated good diagnostic ability (AUC 0.80), identifying abnormalities in 65% of family members, many of whom lacked late enhancement or other structural or electrical manifestations of the disease. These findings suggest that increased T1 primarily reflects myocardial fibrosis and that T1 dispersion may be an early marker of myocardial involvement in individuals with AC-associated mutations before the development of an overt clinical phenotype.[132]

Georgiopoulos et al. evaluated T1M in 30 patients with AC and 59 first-degree relatives who did not meet diagnostic criteria for the disease. Elevated native T1 values were identified in 37% of the patients, including nearly one-third of those with an apparently normal LV according to conventional criteria. There was no association between elevated T1 and the presence of late enhancement. Among the relatives, only 5% showed late enhancement, while 37% exhibited increased native T1, substantially increasing the detection of abnormalities by CMR. These results suggest that T1M is capable of identifying early interstitial fibrosis in patients with AC and in mutation-carrying relatives, even in the absence of evident structural changes, and may contribute to diagnosis and monitoring in the early stages of the disease.[133]

Although data in the literature are still scarce, T1 map findings may help assess the prognosis of patients with AC, in addition to serving as a tool for early diagnosis. Lu G et al. conducted a prospective study of 91 patients with AC (mean age 36 years; 95%CI 27–50 years) who underwent CMR between November 2010 and March 2022.[134] The diagnosis of AC was established based on the revised 2010 task force criteria. LV involvement was considered if LVEF was < 50%, or if there were abnormalities in LV wall motion or LV LGE affecting more than one segment. CMR examinations were performed using T2-weighted, LGE, and T1M sequences, with estimation of ECV. The primary outcome was the first occurrence of sustained VT after CMR. During a mean follow-up of 55 months, 36 of 91 (40%) patients experienced sustained VT. Although there was no difference in native T1 values between patients who experienced the outcome and the control group ($p = 0.09$), the ECV was significantly increased in patients with sustained VT. In addition, LGE was more frequently present in these patients (50% vs. 29%; $p = 0.045$). However, after multivariate analysis, only the ECV value continued to show a statistically significant difference in predicting arrhythmic events. Each 1% increase in ECV was associated with a 13% higher risk of sustained VT (HR 1.13; 95%CI 1.08–1.18).

A rare but documented presentation of AC is an acute episode of chest pain with elevated cardiac enzymes and no evidence of stenosis on cine coronary angiography. The diagnosis is based on meeting the criteria for AC and on genetic testing. Also known as a "hot phase", this presentation may lead to the primary diagnosis and should therefore be included in the differential diagnosis of young patients presenting with chest pain of no obvious coronary cause. Bariani R et al. reported the hot-phase presentation in 5% of patients with AC followed at their institution.[135] Histological and cellular analysis of myocardial biopsy specimens revealed a mononuclear inflammatory infiltrate with edema and necrosis of cardiomyocytes and a predominance of T cells. In this study, CMR findings were consistent with those of acute myocarditis; however, the presence of subepicardial LGE in the vast majority of cases and findings of fibro-fatty infiltration were notable. In this clinical presentation, the T2 map can be a useful tool to supplement conventional CMR, characterize the acuity of the condition, and aid in distinguishing it from other, more common causes of acute chest pain with elevated myocardial necrosis markers.

Considering the potential applications of tissue characterization by CMR – which includes the use of parametric maps – for the diagnostic and prognostic assessment of AC, it is evident that T1M and ECV estimation

can provide significant additional information to supplement morphofunctional assessment and detection of fibrosis by LGE. Consequently, this will further enhance the capabilities of CMR in tissue characterization and expand the already recognized role of this modality in the assessment of patients with suspected or known AC.[130,136,137]

International guidelines on the indications and clinical applicability of CMR list assessment of patients with AC as a Class I recommendation.[138] However, due to the scarcity of studies using parametric maps in this population, these sequences were not included in the recommended CMR protocol for evaluation of these patients, not even as optional sequences.[29] CMR has proven essential for the reclassification and better understanding of cardiomyopathies, including AC.[139] Its ability to detail structural changes in the myocardium is crucial for defining the specific disease type (phenotype), identifying its cause (etiology), and informing the most appropriate treatment. In AC, specifically, structural assessment by CMR has revolutionized our understanding of this disease, providing essential information on its pathophysiology, aiding in diagnosis, and improving prognostic stratification.

Given the value of CMR in the evaluation of cardiomyopathies, and especially in AC, the use of all tools available in CMR protocols – including parametric maps – appears to be the most effective strategy for studying these patients. Although further research is needed to consolidate the applicability of parametric maps in AC, their incorporation into current clinical protocols is recommended. This would allow use of CMR to its fullest possible extent as a method of structural assessment, optimizing the diagnosis and management of AC.

5.2.1. Conclusion

Arrhythmogenic cardiomyopathy is a structural heart disease characterized by myocardial scarring, and CMR has become a key element in its diagnosis, phenotyping, and prognostic stratification. The integration of morphofunctional assessment, fibrosis detection (by LGE), and tissue characterization (especially by T1/ECV) enhances diagnostic capabilities and enables earlier identification of ventricular involvement, including in asymptomatic family members. Although evidence in support of parametric maps in this setting is still lacking, their gradual incorporation is likely to further expand the role of CMR in AC.

5.2.2. Key Takeaways

- Myocardial scarring: fibro-fatty replacement → ventricular arrhythmias and risk of sudden death;
- Evolving criteria: 1994 → 2010[140] → Padua 2020[129] and recent consensus: incorporates LV phenotype and emphasizes morphofunctional/structural findings;
- LV involvement is frequent; biventricular involvement is more common than isolated involvement;
- Phenotypes: RV-dominant (classic), biventricular, and LV-dominant;
- CMR is key (Class I): the gold standard for biventricular function/volumetric assessment (cine) and fibrosis (LGE);
- CMR criteria – morphofunctional:
  - RV: increased volumes and reduced EF, plus regional wall motion abnormalities;
  - LV: enlargement/decreased EF with specific cut-off points (sex/athlete);
- Structural criteria (LGE):
  - LV: unequivocal LGE in ≥ two planes and > one region;
  - VE: meso-/subepicardial ("ring-like") pattern in ≥ 2 planes;
- Parametric maps (T1/ECV/T2):
  - May detect diffuse interstitial fibrosis (earlier diagnosis, especially in family members);
  - Limitations in the RV (thin wall/artifacts); evidence is still preliminary;
- Key findings:
  - Increased native T1 and greater T1 dispersion in AC; dispersion may identify genotype-positive relatives without LGE;
  - Increased ECV predicts sustained VT; LGE is an additional factor, but on multivariate analysis, ECV stands out;
- "Hot phase": myocarditis-like presentation (pain, troponin, normal coronary arteries); T2M helps identify acute inflammatory activity;
- Practice: integrate cine + RT + (T1/ECV/T2) for phenotyping, risk stratification, and follow-up.

5.3. Hypertrophic Phenotype

5.3.1. Hypertrophic Cardiomyopathy

Hypertrophic cardiomyopathy (HCM) is the most common genetic heart disease, with an estimated prevalence of 1 in 500 individuals; it is characterized by LV hypertrophy (LVH) not explained by hemodynamic overload.[141] Although the prognosis is generally favorable, a small proportion of individuals experience an unfavorable course, with events including sudden death, HF, and stroke.

Risk stratification for events in patients with HCM has made significant progress with the use of CMR. LGE imaging has made it possible to identify disease-related patterns of myocardial fibrosis, as well as to quantify the absolute values and percentage of the myocardium affected, which closely correlates with arrhythmic events during follow-up of patients with this disease.[142]

The advent of multiparametric mapping in CMR (T1 and T2) has refined the assessment of patients with HCM, allowing absolute quantification of relaxation times and, consequently, a more robust evaluation of the possible presence of interstitial fibrosis and edema potentially related to this condition.

5.3.1.1. Myocardial Fibrosis Associated with Hypertrophic Cardiomyopathy and its Evaluation by Multiparametric Maps

Myocardial fibrosis in HCM manifests primarily as hyperplasia and disorganization of collagen fibers and bundles, as well as derangement and necrosis of myocardial cells.

Although some degree of myocardial fibrosis may occur in LVH due to other causes, the distinct histopathological mechanisms of hypertrophy observed lead to a greater development of myocardial fibrosis in HCM.[143] Although late myocardial enhancement can distinguish between most clinical scenarios, more refined measures of interstitial fibrosis (such as those provided by T1M and ECV estimation) can differentiate between adaptive forms of hypertrophy (e.g. athlete's heart, hypertension) and those related to storage diseases (e.g. Fabry disease, cardiac amyloidosis) when compared to HCM.[144]

T2M quantifies transverse relaxation, which is sensitive to water content. Although it is a technique traditionally used to measure myocardial inflammatory activity, it can serve as a marker of microvascular ischemia or hemodynamic overload in the context of HCM.

5.3.1.2. Use of Multiparametric Maps in the Assessment of HCM

Myocardial fibrosis is one of the markers most closely associated with clinical outcomes in the follow-up of patients with HCM. Although late enhancement plays a significant role in its identification, more recent studies have focused on identifying diffuse (interstitial) myocardial fibrosis, which often cannot be detected by the traditional LGE technique.

Puntmann et al.[145] evaluated T1M and ECV as markers of diffuse interstitial fibrosis using 3-T equipment. In this study, the parameters of 25 patients diagnosed with HCM were compared to those of patients with hypertension.

Myocardial T1M mean (SD) values were lower in hypertensive patients compared to patients with HCM: 1070 (55) ms vs. 1254 (43) ms, respectively ($p < 0.001$); as were ECV values: 0.26 (0.07) ms vs. 0.38 (0.11) ms, respectively ($p < 0.001$). This demonstrates the ability to identify diffuse myocardial fibrosis based on parameters provided by multiparametric maps.

Subsequent studies investigated the value of T1M in patients without identifiable late enhancement. Xu et al. evaluated 258 patients with HCM but without late enhancement or LV outflow tract obstruction and found a significant increase in native T1 and ECV compared to controls without the disease (mean [DP] T1: 950 [48] ms vs. 913 [46]; mean [DP] ECV: 24.5% [2.8%] vs. 23.0% [2.7%]; both $p < 0.001$, respectively), suggesting diffuse fibrosis even in the absence of focal scarring.[141]

5.3.1.3. Differentiation of Hypertrophic Phenotypes

Distinguishing hypertensive hypertrophy from HCM can be challenging. In this context, Hinojar et al.[146] conducted a comparative analysis of native T1 map values among patients with HCM, patients carrying the HCM gene mutation but without phenotypic manifestations (G+/P-), and a third group consisting of patients with hypertension. All groups were compared to disease-free controls. Patients with HCM had significantly higher mean (SD) native T1 map values than those observed in patients with hypertension: 1102 (58) vs. 1033 (68) ms ($p < 0.0001$). Interestingly, the group of patients carrying a HCM gene mutation (G+/P-) showed significant elevations in T1 map values when compared to the control group: 1055 (55) vs. 1023 (44) ms ($p < 0.0001$).

This finding demonstrated that myocardial structural disruption in patients with HCM may precede the development of hypertrophy and suggests it has potential as an early marker of disease progression.[146]

5.3.1.4. Native T1 Mapping as a Prognostic Tool in Patients with Hypertrophic Cardiomyopathy

Although less studied than late enhancement as a prognostic tool, T1M has shown promising results in risk stratification for patients with HCM. Since these methods assess the same biological phenomenon – expansion of the extracellular space resulting from myocardial replacement by fibrosis – there is a certain degree of collinearity between the two. However, recent studies have reported findings that may be useful in the application of T1M as a prognostic tool, particularly because it detects early changes in myocardial architecture (secondary to the onset of interstitial myocardial fibrosis).

Wang et al. evaluated 663 patients referred for CMR and followed them prospectively for 44 months. In this group of individuals, global native T1 and ECV were independent predictors of HF-related death and hospitalization for HF, even after adjusting for extent of LGE and ESC risk score.[147] Furthermore, an increase in the C-index (from 0.52 to 0.72) was observed when the results of the T1 map or ECV were added to clinical models based on risk factors, reinforcing the incremental value of these biomarkers.

Ventricular arrhythmias are one of the leading causes of adverse clinical outcomes in the follow-up of patients with HCM. In this regard, O'Hara et al. combined late enhancement and T1M in a hybrid model (LGE-T1) to predict ventricular arrhythmias. The LGE-T1-based model was able to accurately predict the risk of ventricular arrhythmias for this cohort and improved risk stratification for sudden cardiac death, thereby better identifying patients with HCM. This approach has significant potential to better select patients for primary preventive implantation of an implantable cardioverter-defibrillator (ICD).[148,149]

5.3.1.5. Role of T2 Mapping in Hypertrophic Cardiomyopathy Diagnosis and Prognosis

Although not as widely studied as T1M in the context of HCM, T2M is gaining ground in evaluation of patients with this condition. The presence of myocardial damage due to microcirculatory changes and imbalances between myocardial oxygen supply and demand are potential mechanisms involved in the pathophysiology of HCM, and both can be identified through myocardial T2M. Huang et al.[150] proved this concept in 47 patients with HCM. When compared to the control group, patients with HCM had increased native T1 values, as expected, but also had significantly higher T2 map values compared to the control group, even when considering non-hypertrophied segments.

More recently, Xu et al.[151] prospectively evaluated 674 patients diagnosed with HCM. During a 36-month follow-up, they observed that patients with HCM, late enhancement,

and a maximum T2 value ≥ 44.9 ms had a higher risk of cardiovascular events ($p < 0.001$). Furthermore, multivariate regression analysis showed that T2 values provided significant prognostic value for predicting cardiovascular events (defined in this study as a combination of cardiovascular death and appropriate shock from an ICD) ($p < 0.001$). Similar to T1M, T2M also plays a role in predicting arrhythmic events during follow-up of patients with HCM.

In another study, 57 patients referred for 3-T CMR were prospectively followed. The third tertile of T2 values (48 [8] ms) was an independent predictor of a composite outcome of VT on Holter monitoring and/or exercise testing, hospitalization for arrhythmias, ICD activation, and all-cause mortality (OR = 22.8, 95%CI 1.4–361.6, $p = 0.026$).[152]

5.3.1.6. Impact of Multiparametric Maps on Clinical Evaluation of Patients with Hypertrophic Cardiomyopathy

The incorporation of multiparametric maps into the routine assessment of patients with cardiomyopathies provides accuracy gains for assessing different conditions, particularly in cases where traditional techniques reveal subtle findings or where there is phenotypic overlap with other cardiomyopathies. This scenario is commonly observed in the hypertrophic phenotype, where various conditions with similar morphological characteristics can provide valuable information for determination of etiology through multiparametric imaging. Warnica et al.[153] conducted an interesting study that investigated the impact of T1 and T2 maps on the differential diagnosis of cardiomyopathies. In patients with HCM, there was a marginal increase in sensitivity and specificity, from 95% to 98% and from 99% to 100%, respectively (not statistically significant; $p = 0.08$ for both parameters), when these maps were added to HCM assessment.

However, the same study noted that adding mapping to routine protocols improved diagnostic sensitivity for infiltrative diseases that are phenocopies of HCM (Fabry disease, amyloidosis), resulting in a relative 24% reduction in subsequent cardiac scans over a 12-month period. Therefore, the implementation of these techniques is not only welcome in terms of improving diagnostic and prognostic accuracy but also potentially in terms of cost-effectiveness.

It is likely that the combination of tissue characterization techniques and multiparametric imaging (T1/T2 maps, EF, and late enhancement) acts synergistically in the risk stratification of patients with HCM. Further studies are needed before the latest techniques can be definitively incorporated into assessment protocols for these patients.

5.3.1.7. Limitations

From a practical standpoint, there is a lack of studies that would allow for the assessment of disease progression using these techniques (e.g., serial T1M/T2M to monitor disease progression). Furthermore, the possibility of using the results of multiparametric mapping to guide decisions regarding interventions (e.g. whether to implant an ICD to prevent future arrhythmic events), although desirable, is not yet a reality.

5.3.1.8. Conclusion

Multiparametric myocardial maps have established themselves as important tools in the evaluation of patients with HCM. The native T1 map and ECV quantify diffuse fibrosis, distinguish etiologies of hypertrophy, and predict clinical outcomes. T2M adds to the analysis by identifying residual edema and has prognostic value by correlating with ventricular arrhythmias during follow-up. The routine incorporation of these parameters into CMR improves diagnosis and risk stratification. However, further advances are still needed to enhance their integration into clinical decision making.

5.3.1.9. Key Takeaways

- Multiparametric maps are useful tools in the evaluation of patients with HCM, especially when applied to the differential diagnosis of phenocopies;
- Because they are quantitative measures of interstitial myocardial fibrosis, T1M and ECV estimation are important tools in the evaluation of these patients, especially in those without identifiable LGE;
- T1 and T2 maps have independent prognostic value in predicting events (especially arrhythmias) during follow-up of patients with HCM.

5.3.2. Amyloidosis

T1M by CMR has established itself as one of the most relevant tools in the evaluation of cardiac amyloidosis (CA). More than just characterizing the myocardium, it allows detection of early involvement, estimation of amyloid burden, and monitoring of disease progression over time. In this context, native T1 and ECV should be understood as complementary parameters with implications for diagnosis, prognosis, and follow-up. Native T1 is elevated in both light-chain (LC) and transthyretin (ATTR) cardiac amyloidosis. One of the most important aspects is the ability to perform the scan without contrast, with high diagnostic accuracy demonstrated in consistent clinical studies.[154,155] Extreme native T1 values allow the clinician to rule out or confirm CA with high confidence,[155] reducing the need for gadolinium. This point is particularly important in patients with renal dysfunction and in screening and serial follow-up strategies.

Meta-analyses reiterate this diagnostic role, demonstrating the robust performance of native T1 and ECV in detecting CA.[156,157] Furthermore, these studies show that both parameters have prognostic value, with consistent associations with mortality and cardiovascular events.[156,158] However, ECV consistently demonstrates greater prognostic robustness, with a direct relationship between its increase and the risk of events, characterizing a dose–response relationship.[157,158] ECV represents a direct measure of extracellular space expansion and, therefore, of the amyloid deposition burden. In patients with ATTR, there is a strong correlation between ECV, functional markers, and biomarkers, as well as an independent association with clinical outcomes.[159] Studies have also demonstrated that ECV more specifically reflects amyloid buildup compared to native T1, which incorporates additional components related to the myocyte response.[159,160]

The role of T1M in patient follow-up represents one of the most important recent advances. In LC amyloidosis, reductions in ECV following treatment are consistently associated with hematologic response and improved prognosis.[161] Native T1 has also demonstrated the ability to serve as a marker of treatment response, even performed without contrast, with reduced values associated with improved survival.[162,163] These data expand the utility of native T1 as a tool for serial monitoring. In LC amyloidosis, interpretation must take into account the pathophysiology of the disease. Even after a sustained hematologic response, the ECV may remain elevated, reflecting residual amyloid deposition, while native T1 may exhibit more dynamic behavior, related to changes in myocardial composition and reduced toxicity of the light chains.[162] Thus, integrated longitudinal analysis of these parameters is essential for the correct interpretation of disease progression. In ATTR amyloidosis, the role of T1M in follow-up is even more consistent.

Longitudinal studies demonstrate that the ECV tracks disease progression in untreated patients and stabilizes or progresses more slowly in patients receiving disease-modifying therapies.[164] This point is particularly relevant in the current landscape, where multiple therapies for ATTR are now available, including transthyretin stabilizers and silencers. Furthermore, evidence shows that changes in ECV over time are associated with clinical outcomes, suggesting that CMR can be used as an objective tool to identify treatment response.[164] In some settings, there is even evidence of a reduction in ECV with treatment, suggesting potential regression of amyloid deposits, which reinforces the method's role in longitudinal follow-up. CMR with T1M also plays a growing role in clinical settings such as HF, particularly in HF with preserved ejection fraction (HFpEF), where it aids in the differential diagnosis of infiltrative causes and in the follow-up of these conditions.[165,166] The ability to detect early changes and track subtle changes over time makes these techniques especially valuable.

Taken together, three key concepts emerge. First, native T1 enhances diagnostic sensitivity and allows contrast-free assessment, making it particularly useful for screening and serial follow-up. Second, ECV provides the most specific measure of amyloid burden and offers greater prognostic robustness, as supported by meta-analyses. Third, and most importantly, the longitudinal analysis of these parameters allows for monitoring of progression, stability, or response to treatment in both LC and ATTR amyloidosis.

In short, T1M has established itself as a core quantitative tool in the contemporary management of cardiac amyloidosis, with a growing role in support of clinical decision-making and assessment of treatment response

5.3.2.1. Key Takeaways

- Native T1: enables early diagnosis of cardiac amyloidosis with high accuracy, even without contrast, and is useful for screening and follow-up;
- ECV: is the most specific marker of amyloid burden and the parameter with the greatest prognostic value, correlating with mortality and cardiovascular events;
- Follow-up: serial analysis of native T1 and ECV enables monitoring of disease progression and response to treatment, making CMR a core tool in the management of cardiac amyloidosis.

5.3.3. Fabry Disease

Fabry disease is a rare X-linked lysosomal storage disorder resulting from mutations in the *GLA* gene, leading to a deficiency of the enzyme α-galactosidase A.[167,168] This enzyme deficiency results in the progressive accumulation of glycosphingolipids, particularly globotriaosylceramide (Gb3) and its deacetylated form, lyso-Gb3, in multiple tissues, including the myocardium, vascular endothelium, central nervous system, kidneys, and skin.[169,170] The phenotypic variability of Fabry disease is wide, with clinical manifestations ranging from classic forms with early onset, predominantly in men, to variant forms with late onset and predominantly cardiac involvement, which are often indistinguishable from other hypertrophic cardiomyopathies.

Cardiac involvement, characterized by LVH, myocardial fibrosis, diastolic dysfunction, arrhythmias, and progressive HF, is one of the leading causes of morbidity and mortality in Fabry disease. Early diagnosis is critical for the initiation of specific therapies, such as enzyme replacement therapy (ERT) and enzyme stabilizers (pharmacological chaperones), which have been shown benefit in modifying the natural history of the disease, especially when started early.

CMR has established itself as the primary noninvasive imaging tool for myocardial characterization in Fabry disease. The ability of CMR to integrate anatomic, functional, and tissue-level information through techniques such as T1M and T2M, calculation of ECV, and LGE allows not only early detection of cardiac involvement but also disease staging and monitoring of treatment response.[171,172]

5.3.3.1. Morphofunctional Characterization by Cardiac Magnetic Resonance Imaging

LVH is the most common CMR finding in patients with Fabry disease. Approximately 50%–60% of patients present with LVH, typically with a symmetric concentric pattern; however, in up to 10% of cases, there may be an asymmetric septal or apical distribution, which complicates the differential diagnosis with sarcomeric cardiomyopathies.[170] Disproportionate papillary muscle hypertrophy is observed in many patients and may precede the onset of overt LVH.[169]

Papillary muscle volume and mass can be quantified by CMR and represent early, specific markers of cardiac involvement. In addition, left atrial enlargement and mitral or aortic valve thickening with mild regurgitation are common findings. LV systolic function generally remains preserved until the advanced stages of the disease, with a normal ejection fraction. However, CMR analysis of myocardial strain by GLS via feature tracking has demonstrated early reductions, especially in the basal myocardial segments, as shown in recent SCMR studies and a systematic review.[172] Loss of the base-apex strain gradient is an early and sensitive marker of subclinical dysfunction.

5.3.3.2. T1 and T2 Mapping

Native T1M is one of the most valuable biomarkers for the early diagnosis of Fabry disease; it is characteristically reduced due to the intracellular accumulation of Gb3, which is considered a classic finding of the disease in its early stages, especially in the absence of significant fibrosis.

However, at more advanced stages, when interstitial myocardial fibrosis develops, T1 values may normalize or even increase, a phenomenon known as pseudonormalization. Therefore, the interpretation of T1 must always be contextualized with the other multiparametric variables. T2M, in turn, provides supplemental information. Elevated T2 values suggest the presence of edema and inflammation, a phenomenon well known to occur in the intermediate stages of the disease. Some studies correlating CMR findings with myocardial biopsy suggest that subclinical inflammation may play a role in the onset of fibrosis (which may precede LGE, especially inferolateral), reinforcing the role of T2 as a marker of disease activity.[168,169,171] Figure 13 illustrates a case of Fabry disease.

5.3.3.3. Extracellular Volume

ECV is an indirect measure of the fraction of interstitial space relative to the total volume of myocardium. In Fabry disease, ECV tends to be normal in the early stages, reflecting a predominance of intracellular accumulation. However, in more advanced stages, as interstitial fibrosis sets in, ECV increases. Values < 25% are considered normal, while values > 28% suggest significant fibrosis. It may also be useful in distinguishing Fabry disease from cardiac amyloidosis (ECV > 40%).[5]

Longitudinal studies indicate that a progressive increase in ECV correlates with clinical deterioration, poorer functional capacity, and a higher risk of arrhythmic events, making it a robust prognostic marker.[168,169,171,172]

5.3.3.4. Late Enhancement

LGE is a marker of fibrotic replacement and is present in up to 50% of patients with Fabry disease. The typical pattern is mesocardial or subepicardial in the basal inferolateral wall, generally sparing the subendocardium. This pattern is highly suggestive of the disease and often precedes functional or clinical changes, particularly in women. The extent of LGE is directly associated with electrical abnormalities and the risk of ventricular tachyarrhythmias.[168,169,171,172]

The presence of LGE also has prognostic value, being associated with lower survival and a poorer response to ERT. Therefore, patients with LGA should be carefully stratified regarding the need for intensive electrophysiologic monitoring.

5.3.3.5. Diagnostic Strategy Based on Multiparametric Maps

A systematic approach based on multiparametric CMR allows for robust stratification of myocardial involvement in Fabry disease, as outlined below.[168,169,171,172]

- Phase 1 – Deposition (low T1, normal ECV, no LGE): early marker, optimal to prompt treatment initiation;
- Phase 2 – Inflammation (low or normal T1, high T2, borderline ECV, absent or early LGE): disease activity with potential for reversibility;

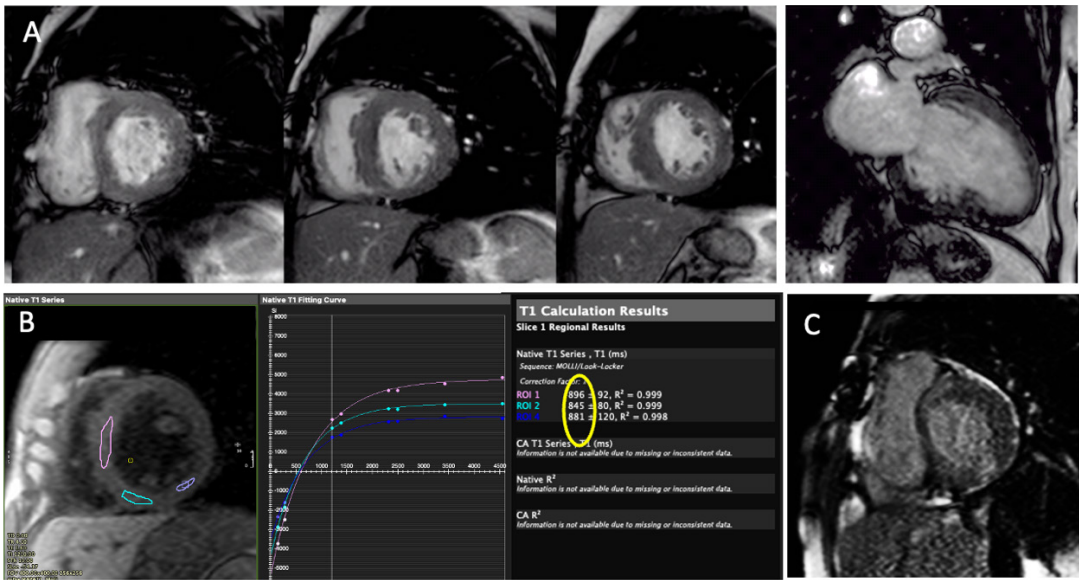


Figure 13 – *Hypertrophic phenotypes: Fabry disease. Top panel (A): SSFP cine imaging sequences showing short-axis and two-chamber ventricular hypertrophy. B: T1 map showing low native T1 values in the mid-short-axis segments. C: late enhancement consistent with myocardial fibrosis in the basal inferolateral segment. SSFP: steady-state free precession.*

• Phase 3 – Fibrosis (pseudonormal or elevated T1, increased ECV, LGE present): late phase, with established structural impairment.

Integrating these phases into a clinical model allows for more precise and individualized therapeutic decision-making.[5]

5.3.3.6. Diagnostic Flowchart

Unexplained LVH → Multiparametric CMR
↓
T1 < 930 ms with ECV < 25%? → Yes → High suspicion of Fabry disease → Confirm with genetic testing/α-GalA
↓
Normal T1 with LGE or ECV > 28%? → Evaluate other etiologies or late fibrotic stage of Fabry disease

CMR: cardiac magnetic resonance imaging; ECV: extracellular volume; LGE: late gadolinium enhancement; LVH: left ventricular hypertrophy; α-GalA: alpha-galactosidase A.

5.3.3.7. Clinical Applications and Treatment Monitoring

In addition to diagnosis, multiparametric CMR is essential for monitoring the clinical course of patients with Fabry disease and may be recommended annually for this purpose.[5,172] Several prospective studies have shown that changes in T1, ECV, and the extent of LGE are directly associated with the response to ERT. Stabilization or regression of imaging findings is associated with improved clinical outcomes, reduced wall thickness, and improved ventricular function. Furthermore, in the context of chaperone therapy, which depends on specific genetic variants, CMR helps identify the compatible phenotype and assess the early response to enzyme stabilization.[5,172]

• LGE + increased ECV: poorer response to enzyme therapy;

• RT > 5% of LV mass: increased arrhythmic events.

5.3.3.8. Limitations and Challenges

Despite its diagnostic robustness, the use of CMR faces some limitations:

• Lack of interinstitutional standardization in T1 and ECV reference values;

• Technical interference (magnetic field, sequence, gadolinium type);

• Overlap with other causes of LVH (eg, amyloidosis, HCM);

• High cost and limited availability at some centers;

• LGE may be absent in early-stage forms, even with reduced T1.

International standardization of acquisition protocols and the creation of normal reference curves for each scanner and population are essential to increasing clinical applicability.

5.3.3.9. Conclusion

• CMR with multiparametric mapping is an essential tool for early diagnosis, risk stratification, and assessment of treatment response in Fabry disease;

• The integrated use of T1, T2, ECV, and LGE assessment allows for precise characterization of the myocardial substrate and should be routinely incorporated into the evaluation of patients with hypertrophic phenotypes of uncertain etiology;

• Routine incorporation into clinical practice should be encouraged, especially in centers specializing in rare diseases, and represents one of the greatest contributions of modern cardiovascular imaging to precision medicine.

5.3.3.9. Key Takeaways

• Abnormal native T1 with normal ECV is the most sensitive early marker;

• ECV and LGE are essential for identifying fibrosis and stratifying prognosis;

• Mesocardial inferolateral LGE is the most specific pattern;

• The integration of clinical, laboratory, and imaging data is essential for diagnosis and follow-up;

• Multiparametric CMR should be considered in all cases of LVH of unknown etiology.

5.3.4. Others (Danon, Pompe, Glycogen Storage Diseases)

Glycogen storage cardiomyopathies constitute a heterogeneous group of rare genetic disorders characterized by the intracellular accumulation of glycogen in cardiac myocytes.[173] This buildup leads to progressive structural and functional abnormalities, including myocardial hypertrophy, ventricular dysfunction, and arrhythmias.[174] CMR, especially using T1M and T2M techniques and perfusion assessment, has proven to be a valuable tool for the early detection, tissue characterization, and monitoring of these conditions.[175]

5.3.4.1. Danon Disease

Danon disease is an X-linked myopathy caused by mutations in the *LAMP2* gene, which encodes lysosome-associated membrane protein 2.[176] Despite its severe nature, it remains infrequently diagnosed, even at specialized centers, and its exact prevalence remains unknown.[176] Clinically, it is characterized by a classic triad consisting of cardiomyopathy, skeletal myopathy, and neuropsychiatric abnormalities.[177] Electrocardiographic findings such as Wolff-Parkinson-White syndrome and atrioventricular blocks are also common, as are elevated liver enzymes and ocular involvement.[178] Affected individuals are at significantly increased risk of arrhythmias, early HF, and sudden death.[176]

The clinical phenotype is typically more aggressive in males, who generally present with the full typical picture. In contrast, in women, the clinical presentation tends to be milder, with a later onset – usually in adulthood – and a predominance of isolated cardiac involvement.[178] The disease may initially – or exclusively – manifest as cardiac involvement, making CMR an important tool in detecting findings suggestive of the diagnosis.[174]

The predominant phenotype of cardiomyopathy in Danon disease is hypertrophic, present in approximately 88% of cases. Among these, about two-thirds present a symmetric pattern of ventricular thickening, followed by an asymmetric pattern.[173] The dilated form of cardiomyopathy is rare, occurring in only 5% of patients. In addition, a small proportion of patients have cardiac morphology within normal limits, highlighting the phenotypic variability of the disease.[173,175]

Regarding LGE patterns, patients frequently present with extensive areas of late enhancement, which account, on average, for approximately 35% of LV mass. The enhancement pattern observed in patients with the disease has characteristics distinct from those found in sarcomeric HCM and idiopathic dilated cardiomyopathy.[173] The basal and mid regions of the interventricular septum are spared in 88% of cases, while 100% of patients exhibit LGE at the ventricular apex and 94% in the lateral segment. The subendocardial enhancement pattern is common and may occur in isolation or extend to the middle layers and even become transmural.[173,175,179]

This pattern contrasts with that of sarcomeric HCM, in which the hypertrophic interventricular septum is generally the region most affected by LGE, with a predominantly punctate pattern in the mid-wall region and rare involvement of the subendocardial layer. In dilated cardiomyopathy, however, LGE tends to present a linear mid-mural pattern, frequently involving the interventricular septum.[173]

Regarding parametric maps, in the largest retrospective series published to date, which included 16 patients diagnosed with Danon disease, four patients who underwent T1M had elevated native T1 and global ECV values.[173]

When regions with and without late enhancement in the mid-LV segments were evaluated separately, areas showing enhancement had increased native T1 and ECV values. In distal regions without enhancement, native T1 values remained elevated, while ECV was within normal limits.[173]

Another case series, which included histological analysis and reported the same findings, demonstrated elevated native T1 values affecting the interventricular septum in areas free of late enhancement. Electron microscopy of these regions revealed the presence of intracellular autophagic vacuoles, confirming underlying structural changes correlated with the increased signal on T1M.[180] Based on these data, T1M may offer advantages in the early detection of myocardial dysfunction and abnormalities in patients with Danon disease, even in the absence of late enhancement.

Regarding T2-weighted images (not including T2M), approximately half of the patients included in the largest available case series exhibited T2 signal abnormalities, with four showing isolated hyperintensity and three presenting with a combination of hyper- and hypointensity.[173]

Specifically regarding T2M, a case report including three generations of a family demonstrated that T2 values were increased in the free wall of the LV, reflecting myocardial inflammation or edema, while they remained within normal limits in the interventricular septum. In all three patients evaluated, values in the lateral wall exceeded 55 ms, while values in the interventricular septum were less than 50 ms.[181]

The description of abnormalities on T2-weighted cardiac images, including myocardial hyperintensity and increased T2 map values, is relevant and emerges as a possible characteristic imaging signature of Danon disease.[176]

T1M:

- Elevated native T1 values and increased ECV in regions with LGE;
- Regions free of enhancement also show increased native T1, but normal ECV;
- Histological analysis confirms intracytoplasmic autophagic vacuoles in interventricular areas with increased T1, even in the absence of late enhancement, indicating microstructural changes;
- T1M can detect early myocardial dysfunction and changes before late enhancement becomes visible.

T2M:

- Increased T2 values (> 55 ms) observed in the free wall of the LV, suggesting myocardial edema or inflammation;
- Normal T2 values (< 50 ms) in the interventricular septum;
- T2 abnormalities, in both conventional signal and parametric mapping, constitute a possible imaging signature of Danon disease.

5.3.4.2. Pompe Disease

Pompe disease is a rare metabolic myopathy caused by a deficiency of the lysosomal enzyme acid alpha-glucosidase, which is responsible for the breakdown of glycogen in lysosomes.[182] This enzyme deficiency leads to a progressive buildup of glycogen in skeletal muscle, cardiac muscle, and other organs, resulting in systemic muscle dysfunction.[182] The disease manifests across a wide age range, with classic childhood forms and late-onset forms, varying in clinical severity and organ involvement.[183] Early diagnosis is essential to allow timely initiation of ERT, which improves survival and muscle function.[184]

In the classic infantile-onset form, the cardiac phenotype is characterized by myocardial hypertrophy, with symmetric biventricular thickening and systolic dysfunction of varying degrees, often associated with early congestive HF and generalized muscle weakness. Case series have reported diffuse and prominent myocardial hypertrophy of both ventricles and the papillary muscles, especially in the LV and interventricular septum.[185,186]

LGE is generally absent in this specific pediatric presentation. This relative absence may be attributed to the younger age of the patients and the short follow-up period, since myocardial fibrosis tends to be a cumulative process, potentially mitigated by ERT when initiated early.[187] However, when not initiated in a timely manner, as reported in a recent case report involving a 3-month-old infant with the infantile-onset form of the disease, LGE revealed a pattern of focal mesocardial and scattered enhancement in the septum. Meanwhile, the values for native T1M (1265 ms), T2 (40 ms), and the ECV fraction (34%) were all increased in the corresponding regions.[186]

In another report, T1M images obtained before and after gene therapy in a 1-year-old child with the infantile-onset form showed elevated T1 values at baseline. After 4 months of treatment, a slight reduction in native T1 values was observed in the abnormal regions of the middle anteroseptal wall and in the junctional regions, when comparing pre- and post-treatment values (1351.69 ms to 1294.22 ms and 1273.31 ms to 1218.17 ms, respectively).[188]

In late-onset Pompe disease, a series of 17 cases evaluated by CMR showed normal ventricular volumes and preserved ejection fractions in all patients. When compared to healthy controls, neither conventional cine images nor myocardial strain analysis by feature tracking identified systolic dysfunction, not even subclinical.[189] Three patients (18%) had non-ischemic LGE localized to the basal inferolateral wall, and 21% had increased global ECV values, suggesting interstitial myocardial fibrosis. Two of these three patients with positive LGE also had hypertension and a global ECV > 30%. In contrast to the early-onset form, only a small proportion of patients with the late-onset form of Pompe disease have cardiac abnormalities detectable by CMR, and these are generally mild and nonspecific.[189]

There is no consistent evidence regarding the use of myocardial T2M in Pompe disease. The initiation of ERT has been associated with a decrease and even normalization of T2M values.[190]

T1M:

- Infantile-onset form:
  - Increased native T1 in regions with late enhancement;
  - Partial reduction in values after gene therapy, suggesting a response to treatment;
- Late-onset form:
  - Normal native T1 signal in most cases.

T2M:

- Limited data; studies of skeletal muscle reveal increased T2 values in this population, with a reduction in values following ERT.

5.3.4.3. Type III and IV Glycogen Storage Diseases

Cardiac involvement in glycogen storage diseases type III (Cori or Forbes disease) and type IV (Andersen disease) is a significant, often underestimated clinical manifestation that can progress to significant cardiomyopathy. In glycogen storage disease type III, especially subtype IIIa, which affects both the liver and the muscles (including the heart), studies show that LVH is a common finding.[191,192] In type IV glycogen storage disease, deficiency of the glycogen branching enzyme leads to the accumulation of polyglucosans, affecting multiple systems, including the heart. Case reports demonstrate varied clinical presentations, ranging from dilated cardiomyopathy to asymptomatic cardiac hypertrophy.[192]

CMR findings in these forms of glycogen storage disease are heterogeneous, with reports ranging from ventricular hypertrophy and systolic dysfunction to extensive patterns of transmural enhancement, although absence of LGE has also been reported in some cases. Regarding T1M, there is evidence of diffuse increase in native T1 in areas of myocardium free of LGE, without, however, an increase in ECV. This finding suggests that the increase in T1 reflects intracellular glycogen accumulation, without expansion of the extracellular space during this process.[193-195]

Despite these findings, the available data on the use of parametric maps in these populations remain limited, highlighting the need for additional studies to better characterize and understand myocardial involvement in glycogen storage diseases.

5.3.4.4. PRKAG2

PRKAG2 syndrome is a rare autosomal dominant glycogen storage disease caused by mutations in the γ2 regulatory subunit of AMP-activated protein kinase.[196] Clinically, it typically manifests in late adolescence, with characteristic structural and electrophysiological cardiac findings. Among morphological abnormalities, non-sarcomeric ventricular hypertrophy stands out, with varying degrees of phenotypic expression, which may progress to systolic dysfunction and dilated cardiomyopathy. The main complications include HF, complex arrhythmias, and a significantly increased risk of sudden cardiac death.[197]

From a morphological standpoint, CMR often shows LVH, which may be symmetric or asymmetric, varying according to the stage of disease progression. In the early stages, hypertrophy is usually more localized, predominantly affecting the mid-lateral wall, whereas in more advanced stages it becomes diffuse, with more pronounced thickening of the interventricular septum.[198]

Native T1M has proven useful for detecting changes related to glycogen buildup. In individuals with a mutation in the *PRKAG2* gene, reduced native T1 values were observed compared to controls. Mean (SD) T1 values were around 918 (11) ms, while non-carriers had mean values of approximately 963 ms. This reduction may be attributed to the presence of intracellular glycogen, which alters the longitudinal relaxation properties of the myocardium. As the disease progresses, particularly when interstitial fibrosis develops, native T1 values may increase. LGE analysis corroborates this process, as it is generally absent in the early stages but present in more advanced stages.[198,199]

T2 relaxation times remained within normal limits in all patients evaluated, with no evidence of elevation suggestive of myocardial edema. Furthermore, no significant associations were observed between segments with hypertrophy and T2 values, suggesting an absence of inflammation in the PRKAG2 syndrome cases analyzed.[198]

T1M:

- Reduced values in patients with the *PRKAG2* mutation, consistent with intracellular glycogen accumulation;
- T1 may increase in more advanced stages due to the presence of fibrosis;
- A pattern distinct from sarcomeric HCM, which features early T1 increase.

T2M:

• T2 relaxation times are within normal limits in all patients;

• No significant association between hypertrophied segments and T2 values;

• This indicates absence of myocardial edema or active inflammation.

5.3.4.5. Limitations

• Data on parametric maps in glycogen storage cardiomyopathies remain limited, with few series and small studies, making it difficult to generalize findings;

• Considerable phenotypic heterogeneity and variation exist among disease subtypes, which affects the interpretation of T1, T2, and ECV values;

• The clinical role of parametric maps in treatment monitoring and prognosis still needs to be better defined.

5.3.4.6. Conclusion

Glycogen storage cardiomyopathies pose a diagnostic and clinical challenge, particularly due to their phenotypic heterogeneity and rarity. The use of parametric maps in CMR, particularly T1M and T2M, has shown potential for detecting early myocardial changes even in areas without late enhancement, reflecting microstructural changes that are not visible with conventional techniques. However, the clinical application of these parameters is still limited by the scarcity of robust data and variability among patients. Thus, future studies are essential to consolidate the role of parametric maps in the diagnosis, monitoring, and prognosis of these rare conditions.

5.3.4.7. Key Takeaways

• Parametric CMR mapping, particularly native T1 and ECV assessment, is critical for detecting early myocardial changes in glycogen storage cardiomyopathies, even before the onset of LGE;

• In Danon disease, elevated native T1 and ECV values indicate structural changes and fibrosis, while regions without LGE may also show increased T1, suggesting subclinical involvement;

• In Pompe disease, especially in the infantile-onset form, T1M may show elevations related to glycogen buildup and respond to gene therapy with a reduction in these values;

• In glycogen storage diseases types III and IV, T1M demonstrates diffuse increases in native T1 without expansion of ECV, reflecting intracellular glycogen accumulation without associated fibrosis; however, data are still limited;

• T2M shows promise for identifying myocardial inflammation or edema, but there are still few studies confirming its utility and standardization in these diseases;

• In summary, parametric maps expand our understanding of the disease beyond conventional imaging, aiding in early detection and monitoring; nevertheless, larger, standardized studies are needed to consolidate their clinical role.

5.4. Restrictive Phenotype

5.4.1. Endomyocardial Fibrosis

Endomyocardial fibrosis (EMF) is a rare restrictive cardiomyopathy characterized by subendocardial myocardial fibrosis, with a predilection for the apical portions of the ventricles. The disease is often associated with diastolic dysfunction, atrial enlargement and, in some cases, valvular regurgitation. It is most prevalent in tropical regions of Africa, South America, and Asia, likely due to environmental, infectious, and immune-mediated factors. Clinically, it may present as HF, conduction disturbances, and thromboembolic events, and diagnosis is often challenging.[200]

CMR plays a key role in the assessment of EMF and is considered the primary noninvasive method for tissue characterization.[200] LGE in EMF exhibits a typical pattern, with linear "V"-shaped enhancement, predominantly at the ventricular apexes. This finding allows the examiner to distinguish three distinct layers: the preserved myocardium, the thickened endocardium with intense fibrosis, and an adjacent layer, often corresponding to organized thrombus or endocardial calcification. Fibrosis may also extend to the ventricular inflow tract, while the outflow tracts are generally spared.[201]

In addition to LGE, quantitative techniques such as native T1M and ECV estimation provide a complementary and more comprehensive assessment of myocardial fibrosis, allowing its detection even in areas without visible enhancement. These methods are summarized in Table 8, which outlines the main findings and their relevance to tissue characterization in EMF.[202]

Native T1M quantifies the T1 relaxation time at each pixel in the myocardium, providing information about the intrinsic properties of the tissue. In the presence of fibrosis, the buildup of collagen in the extracellular space leads to a prolongation of the T1 relaxation time. For this reason, increased T1 values generally correspond to areas of LGE.[202]

Furthermore, T1 can reveal early or diffuse fibrosis not identified by gadolinium, contributing to a more detailed quantitative assessment of the extent of myocardial involvement.[70] Gonzalez-Bartol et al. corroborated this applicability, demonstrating the utility of T1M in the early detection of fibrosis in patients with EMF.[203]

CMR-based ECV, estimated from pre- and post-gadolinium T1 values, is a quantitative biomarker of myocardial interstitial fibrosis, validated across multiple clinical settings. In populations with diffuse fibrosis, increased ECV correlates with diastolic dysfunction. In EMF, CMR reveals extensive areas of subendocardial fibrosis, and reports describe the use of T1/ECV in fibrotic regions to reinforce histopathological findings, although dedicated studies demonstrating a direct correlation between ECV and diastole in EMF are still lacking.[204]

The ability to objectively quantify the burden of myocardial fibrosis using T1M and ECV contributes to monitoring the progression of EMF and supports clinical management, including the assessment of response to pharmacological interventions and procedures aimed at reversing fibrosis or controlling diastolic function. Although fibrosis in EMF is largely irreversible, there are reports of partial improvement in T1 and ECV values following

Table 8 – Tissue characterization of endomyocardial fibrosis by cardiac magnetic resonance imaging

CMR assessment	Description	Relevance
Late enhancement	Subendocardial enhancement in an inverted "V" shape, predominantly at the ventricular apices, which may extend to the ventricular inflow tract.	Qualitative marker of fibrosis.
Native T1	Elevated native T1 values, particularly at the apices and in areas of ventricular tapering.	Quantitative marker of fibrosis.
ECV	ECV is directly correlated with the extent of myocardial fibrosis and is elevated in affected regions.	Quantifies the extent of fibrosis. Correlates with the severity of diastolic dysfunction.

CMR: cardiac magnetic resonance imaging; ECV: extracellular volume.

specific interventions. Endomyocardial resection surgery with valve repair, for instance, can promote ventricular remodeling and reduce diastolic overload, resulting in stabilization or slight improvement of these markers in viable segments. Furthermore, in selected cases with an active inflammatory component, the use of immunosuppressants may slow the progression of fibrosis and modestly improve native T1 values. Despite this, the prognostic value of improvement in these parameters following intervention is not yet well established in EMF. Studies show that elevated T1 and ECV reflect a higher fibrosis burden and greater functional severity, but there is no consistent evidence that their reduction, in isolation, is associated with better clinical outcomes.[203,205]

The incorporation of these quantitative techniques into CMR represents an advance in the evaluation of EMF. T1M and ECV quantification supplement echocardiography, allowing for a more precise and detailed tissue characterization.

5.4.1.1. Conclusion

The incorporation of quantitative techniques (T1 and ECV) into CMR represents an advance in the assessment of EMF, allowing for more precise tissue characterization, with the potential to monitor fibrosis and guide therapeutic decision-making.

5.4.1.2. Key Takeaways

- EMF is a rare restrictive cardiomyopathy characterized by subendocardial fibrosis, predominantly in the ventricular apices;
- It is associated with diastolic dysfunction, atrial enlargement, and valvular regurgitation, and is predominant in tropical regions (Africa, South America, Asia);
- Clinically, it manifests as HF, conduction disturbances, and thromboembolic events;
- CMR is the gold-standard noninvasive method for tissue characterization in EMF;
- Late enhancement shows a typical apical "V"-shaped pattern;
- Native T1 and ECV further enhance tissue characterization, detecting diffuse fibrosis even in areas without late enhancement;
- Elevated T1 indicates collagen accumulation and can identify early fibrosis;
- ECV is a quantitative biomarker of interstitial fibrosis, correlating with diastolic dysfunction in fibrotic diseases;
- Quantification of T1/ECV aids in monitoring the progression of EMF and in assessing treatment response;
- Endomyocardial surgery and immunosuppressive therapy may partially reduce T1/ECV in viable segments.

5.5. Non-Dilated Phenotype

5.5.1. Genetic Cardiomyopathy

Recent ESC guidelines have based the classification of cardiomyopathies primarily on their phenotypic characteristics. Accordingly, they define non-dilated LV cardiomyopathy (NDLVC) as a myocardial disorder not explained by overload conditions (hypertension or valvular heart disease) or coronary artery disease, and which is characterized by the presence of non-ischemic scarring/fibrosis or fatty infiltration in the absence of LV enlargement, regardless of the presence of global or regional ventricular wall motion abnormalities. This classification also includes cases of isolated LV dysfunction without enlargement.[1]

This new definition includes heart diseases previously defined as early-stage dilated cardiomyopathy (without enlargement), arrhythmogenic LV cardiomyopathy, left-dominant arrhythmogenic RV cardiomyopathy, and arrhythmogenic dilated cardiomyopathy.[130] As a result, specific information regarding its actual prevalence and other epidemiological characteristics is not very precise. Furthermore, the genetic mechanisms that are likely the primary cause of this condition have not yet been fully established.[1,206] Much of this information and the associated genes derive from and, therefore, overlap with those of dilated cardiomyopathy and arrhythmogenic RV cardiomyopathy. Eda et al. observed a 22% prevalence of NDLVC among 363 patients diagnosed with non-ischemic cardiomyopathy and reduced ejection fraction.[207] This study demonstrated that the risk of cardiac events was similar between this group and the group with dilated cardiomyopathy, even though the former group had a higher prevalence of atrial fibrillation

and less late enhancement identified by CMR (34% *vs.* 53%). However, patients with NDLVC who developed ventricular enlargement during the follow-up period had a worse prognosis.

Mutations can affect the severity, progression, and risk of sudden death in NDLVC. Mutations in desmoplakin (DSP), filamin C (FLNC), desmin, lamin A/C (LMNA), and phospholamban (PLN) are most closely associated with this cardiomyopathy. Therefore, genetic screening is important for diagnosis, family counseling, prognostic assessment, and treatment planning – such as the indication for ICD implantation.[148]

Cardiomyopathies associated with LMNA and FLNC have a sudden cardiac death rate of approximately 5% to 10% per year, while those associated with PLN and DSP have a mortality rate of about 3% to 5% per year.[206,208]

Since the classification of cardiomyopathies is based on phenotypic definition, CMR is essential for the diagnosis, classification, and prognostic assessment of these diseases. Furthermore, not only the precise assessment of ventricular function, chamber diameters, and volumes but also tissue characterization is of the utmost importance for optimal evaluation of these conditions. To this end, the method relies on the relaxation properties of hydrogen protons following excitation with radiofrequency waves. In addition to the late enhancement technique, which plays a key role in identifying the presence and distribution pattern of myocardial fibrosis/scarring, cine CMR (SSFP) images and T1- and T2-weighted "black-blood" images are very useful for assessing the presence of edema, hyperemia, and fatty infiltration of the myocardium. More recently, native T1 parametric maps, post-contrast T1 maps with ECV calculation, and T2 maps have been gaining particular interest and relevance in tissue characterization.[11]

T1 parametric maps have been studied for their potential to aid in the early diagnosis of cardiomyopathies, particularly in individuals with a family history of such conditions and/or sudden death. Some studies have demonstrated a worse prognosis in patients with increased native myocardial T1 values and ECV even in the absence of LGE, enabling the early detection of myocardial abnormalities in the subclinical stage.[209] Other studies have demonstrated abnormalities in the T2 map, ECV,[210] and in the dispersion of native myocardial T1 map values in asymptomatic mutation carriers.[132] However, these findings still require clinical validation and further studies to assess their actual clinical utility.

The use of T2 maps has attracted particular interest due to the increasingly clear correlation between cardiomyopathies of genetic etiology and acute episodes of myocardial inflammation.[211] This relationship is of particular importance in cases of recurrent myocarditis and in cases recurring within the same family. The pathogenesis of this phenomenon is not yet fully understood; however, increasingly robust scientific evidence suggests that myocardial inflammation – whether resulting from purely endogenous factors or triggered by exogenous factors – is a key determinant in cardiomyopathies, particularly in desmosomal forms.[212,213] Bariani et al. reported that the main genes identified in these acute episodes ("hot phases") are DSP in approximately 69% of cases, followed by placophilin-2 (9%) and desmoglein-2 (6%).[214]

CMR has become increasingly important for the diagnosis and prognosis of myocarditis, allowing for the identification of both inflammatory myocardial lesions in the acute and subacute phases and the fibrotic scarring frequently present in the chronic phase of the disease.[21] Recently, T1 and T2 parametric maps have been incorporated into the updated Lake Louise criteria to enhance the sensitivity and specificity of the diagnosis.[21,85] Consequently, use of these maps has also gained importance in the evaluation of cardiomyopathies during "hot phases" (Figure 14).

5.5.1.1. Conclusion

The use of multiparametric maps is essential for the comprehensive evaluation of genetic cardiomyopathies, allowing early identification of fibrosis, inflammation, and fatty infiltration; risk stratification; guiding selection of strategies for preventing sudden death; and informing therapeutic decision-making.

5.5.1.2. Key Takeaways

- NDLVC is defined as non-ischemic fibrosis/scarring or fatty infiltration without LV enlargement, in the absence of overload or CAD;
- Its genetic basis has not yet been fully established; mutations in *DSP, FLNC, DES, LMNA,* and *PLN* are most commonly associated;
- Genetic testing is essential for diagnosis, family counseling, and risk stratification;
- *LMNA* and *FLNC* mutations → risk of sudden death 5%–10% per year; *PLN* and *DSP* → 3%–5% per year;
- Progressive ventricular enlargement during follow-up predicts a worse prognosis;
- CMR is the primary method for diagnosis and prognosis in genetic cardiomyopathies;
- It allows comprehensive assessment of function, volumes, edema, fibrosis, and fatty infiltration;
- Late enhancement identifies patterns of myocardial fibrosis, while T1/T2 black-blood and SSFP cine images assess inflammation and fat;
- Elevated T1 and ECV indicate diffuse fibrosis and have prognostic value even in the absence of LGE;
- Increased T2 signal reflects myocardial inflammation – common during the "hot phases" of genetic cardiomyopathies;
- These changes can be detected early in asymptomatic carriers of mutations;
- Recurrent inflammation episodes ("hot phases") are common in desmosomal mutations, particularly in *DSP*, *PKP2*, and *DSG2;*
- Hot phases can mimic viral myocarditis, justifying use of the updated Lake Louise criteria with T1/T2 maps.

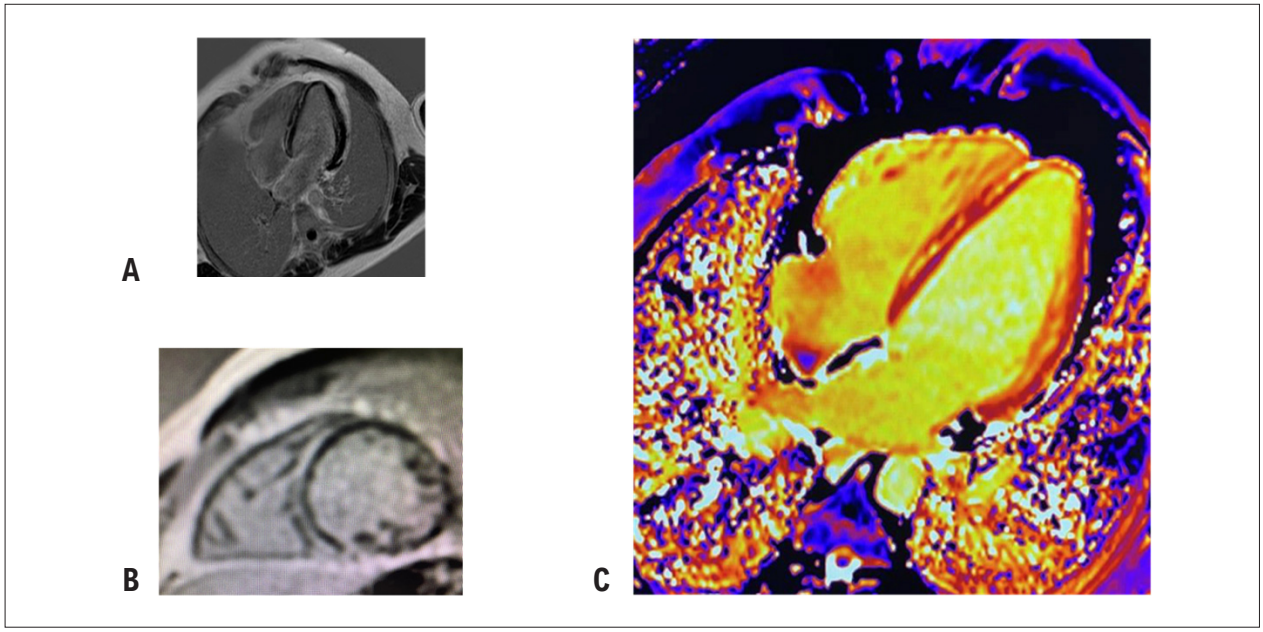


Figure 14 – *Late enhancement (A and B) and extracellular volume (C) images of a patient with non-dilated left ventricular cardiomyopathy.*

5.6. Other

5.6.1. Athlete's Heart

Few studies have evaluated multiparametric mapping in athletes, and most have focused on T1M. This technique has received increasing attention due to the clinical challenge of differentiating physiological adaptations of the so-called "athlete's heart" from pathological conditions in the context of hypertrophic phenotypes.[215,216] Studies demonstrate that intense, chronic exercise can modulate T1M parameters. In elite athletes, significantly lower native T1 values were observed compared to the general population, suggesting that physiological myocardial remodeling influences this parameter.[216,217] These findings highlight the need for caution when interpreting T1 values in isolation in athletes, since reductions in these values do not necessarily reflect myocardial disease.

On the other hand, there is evidence that T1M, when combined with ECV quantification, may be useful for distinguishing the athlete's heart from HCM. In HCM, there may be a consistent increase in ECV, reflecting interstitial fibrosis, which contrasts with findings in athletes, in whom there is generally no significant increase in ECV.[148,215] Thus, the integration of native T1 with ECV and other imaging parameters is recommended to increase diagnostic accuracy.

The impact of sex, sport, and training intensity should also be considered, as different athletic modalities may exhibit variations in T1 and T2 values, as well as in cardiac structural and functional adaptations.[218] Furthermore, longitudinal studies suggest that the combined assessment of T1M and cardiac function may provide greater precision in characterizing cardiac remodeling in athletes.[219]

In summary, T1M is a promising tool with great potential in the context of evaluating the athlete's heart. However, it is recommended that its interpretation be performed in an integrated manner, taking into account clinical context, sport or exercise modality, sex, ventricular function, additional CMR parameters (T2, ECV, and LGE), and, when necessary, serial scans. The use of native T1 alone should not be considered sufficient to distinguish physiological adaptations from cardiomyopathies.

5.6.2. Hypertensive Cardiomyopathy

Hypertensive cardiomyopathy is a common condition in clinical practice and presents a variable spectrum of cardiac remodeling. In the early stages, CMR typically demonstrates concentric LVH related to chronic afterload increase. In more advanced stages, there may be a transition to ventricular enlargement and systolic dysfunction, characterizing a continuum that progresses from compensatory hypertrophy to adverse remodeling.[143,146]

T1M and T2M have emerged as essential tools for better characterizing these phenotypes. Studies have shown that native T1 and ECV are capable of distinguishing hypertensive cardiomyopathy from HCM, since the increase in T1 and ECV in hypertensive patients reflects the presence of diffuse interstitial fibrosis, albeit to a lesser extent compared to HCM.[143,146] These parameters are particularly useful in patients with preserved or mildly reduced ejection fraction, in whom isolated hypertrophy could hinder diagnostic differentiation.[220]

In addition, multiparametric CMR analysis, including T2M, can provide additional information regarding inflammation or transient edema, especially in the early stages of remodeling. Although T2 values are not classically altered significantly in chronic hypertension, their association with T1 and ECV can aid in the early detection of subtle myocardial changes.[221]

Thus, in the evaluation of hypertensive cardiomyopathy, T1M should be considered a complementary tool for the

structural and functional characterization of the LV, contributing to the differential diagnosis from other causes of myocardial hypertrophy, particularly HCM. The integrated use of T1, ECV, and T2, correlated with clinical and echocardiographic context, can provide greater precision in the management of these patients.

6. Valvular Heart Disease

Valvular heart disease encompasses a spectrum of conditions that affect the heart valves, leading to hemodynamic disturbances and consequent myocardial remodeling. Although traditional imaging modalities are effective in assessing valve morphology and function, they often fail to adequately characterize myocardial tissue. In this context, multiparametric CMR mapping techniques have emerged as valuable tools, providing quantitative information on myocardial composition and enabling the early detection of pathological changes.

6.1. Aortic Stenosis

Aortic stenosis (AoS) causes pressure overload, resulting in concentric LVH and interstitial fibrosis. Native T1 and ECV values are elevated in patients with AoS, correlating with histologically confirmed fibrosis and adverse outcomes.[222,223] Studies have shown that higher native T1 values predict increased mortality and hospitalizations for HF.[222,223] Following aortic valve replacement, reductions in native T1 and ECV values are associated with improved LV function, highlighting the potential of these parameters for monitoring treatment response.[222-224]

Lee et al. demonstrated that native T1M correlates with diffuse myocardial fibrosis in asymptomatic patients with moderate to severe aortic stenosis and preserved ejection fraction. Elevated native T1 values were associated with structural and functional changes, including increased LV mass, diastolic dysfunction, and reduced strain.[225]

In a histological study, Milano et al. analyzed myocardial biopsies from patients with severe AoS who underwent surgical valve replacement and found that the degree of interstitial fibrosis independently predicted postoperative survival. Patients with a higher degree of fibrosis had worse long-term outcomes.[226]

A multicenter study by Everett et al. evaluated the role of quantifying ECV by CMR in patients with AoS. Increased myocardial ECV, indicative of diffuse fibrosis, was independently associated with a worse prognosis, including higher rates of mortality and adverse cardiovascular events. These findings reinforce the clinical utility of ECV as a noninvasive biomarker for risk stratification and to aid in determining the optimal timing for valve intervention.[227]

Subsequently, Kwak et al. investigated the prognostic value of myocardial injury markers derived from CMR – specifically LGE and ECV – in patients with aortic stenosis. Both types of fibrosis, focal and diffuse, predicted all-cause mortality, regardless of symptomatic status or the severity of stenosis.[228]

Another study, by Hwang et al., demonstrated that a reduction in native T1 values following aortic valve replacement was associated with improved LV function and reverse remodeling. Patients with a greater reduction in T1 showed better clinical and functional recovery, supporting the use of native T1 as a marker of myocardial recovery and postoperative prognosis in severe aortic stenosis.[223]

6.2. Aortic Regurgitation

Chronic aortic regurgitation (AR) leads to volume overload, resulting in eccentric hypertrophy and the development of myocardial fibrosis. Compared to AoS, data on fibrosis in AR are more limited and often include mixed populations with both AoS and AR, with LGE being the most commonly used technique. Regarding T1M, a study by Senapati et al. evaluated the prognostic value of replacement fibrosis (assessed via LGE) and interstitial fibrosis (via ECV) in patients with chronic AR. Both types of fibrosis were independently associated with all-cause mortality and adverse cardiovascular outcomes, even in patients with preserved ejection fraction. These findings highlight the value of combining LGE and ECV techniques for comprehensive risk stratification in chronic AR.[229]

6.3. Mitral Regurgitation

In mitral regurgitation (MR), chronic volume overload leads to LV enlargement and myocardial remodeling. Previous studies have shown that elevated levels of myocardial fibrosis, both focal and diffuse, are associated with increased mortality and hospitalization for HF.[230,231]

Edwards et al. evaluated asymptomatic patients with chronic primary degenerative MR using T1M and ECV quantification. Even in the absence of symptoms or systolic dysfunction, the patients had elevated ECV values, suggesting early diffuse myocardial remodeling. These findings indicate that T1-based tissue characterization can detect subclinical changes and help determine the optimal timing for surgery.[232]

Kitkungvan et al. demonstrated that, in primary MR, elevated ECV was associated with greater severity of regurgitation, a higher symptom burden, and worse clinical outcomes. Both diffuse interstitial fibrosis (by ECV) and focal replacement fibrosis (by LGE) independently predicted adverse events.[233]

In a related study, the same group evaluated ECV in 144 asymptomatic patients with preserved ventricular function. Elevated ECV was associated with a higher probability of progression to symptom-driven surgery or cardiovascular death, suggesting that fibrosis acts as an independent prognostic marker in addition to the severity of regurgitation.[234]

Guglielmo et al. investigated the role of T1M and feature tracking using CMR in patients with mitral valve prolapse (MVP). Patients with MVP had elevated native T1 values and impaired myocardial strain, even with preserved ventricular function. These findings suggest that multiparametric CMR can identify early myocardial involvement and improve risk stratification in MVP beyond conventional imaging.[235]

Similarly, Pavon et al. showed that, in patients with MVP and mitral annular disjunction, elevated synthetic end-diastolic volume (ECVsyn) measured by T1M was significantly associated with complex ventricular arrhythmias, even in the absence of LGE. Both ECVsyn and LGE identified individuals

at high risk for out-of-hospital cardiac arrest, supporting diffuse fibrosis as a marker of arrhythmic risk in this population.[236]

6.3.1. Conclusion

In summary, CMR multiparametric mapping techniques – especially native T1 and ECV quantification – have provided valuable insights into myocardial remodeling in various forms of valvular heart disease. These techniques have shown potential for risk stratification, early detection of subclinical myocardial involvement, and guidance on the optimal timing for intervention. However, despite growing evidence, the routine use of T1M and T2M techniques in clinical practice has not yet been established. Additional prospective studies and standardized protocols are needed to define how these tissue characterization tools can be effectively integrated into diagnostic algorithms and management strategies for patients with valvular heart disease.

6.3.2. Key Takeaways

- Valvular heart disease causes hemodynamic overload and myocardial remodeling;
- Multiparametric mapping (T1, T2, ECV) using CMR allows for the quantification of fibrosis and inflammation, detecting subclinical changes before ventricular dysfunction occurs;
- Native T1 and ECV are elevated and correlate with histological fibrosis and worse clinical outcomes;
- Elevated T1/ECV values predict mortality and HF, even in asymptomatic patients;
- After valve replacement, a reduction in T1/ECV indicates myocardial recovery and a better prognosis;
- ECV is a useful noninvasive biomarker for risk stratification and determining the timing of surgery;
- Both LGE (replacement fibrosis) and ECV (interstitial fibrosis) predict **mortality** and **cardiovascular events;**
- The combination of LGE and ECV improves risk stratification, even with a preserved ejection fraction;
- Elevated ECV indicates early diffuse remodeling, even in asymptomatic patients with normal ejection fraction;
- Focal fibrosis (LGE) and diffuse fibrosis (ECV) predict adverse events and future need for surgery;
- In MVP, elevated T1/ECV ratios and reduced strain indicate early myocardial involvement;
- Elevated synthetic ECV is associated with ventricular arrhythmias and a risk of sudden death, even in the absence of LGE.

7. Takotsubo Syndrome

Takotsubo syndrome, originally described in 1990 by Sato et al.,[237] is an acute, generally transient cardiomyopathy characterized by ventricular systolic dysfunction with ballooning of the apical portion of the ventricle in the absence of obstructive coronary artery disease and accounts for approximately 1%–2% of cases of acute coronary syndrome.[238]

The etiology of takotsubo syndrome remains unknown, but in most cases it is triggered by emotional or physical stress, including surgical stress, which results in excess release of catecholamines. Most patients experience remission of symptoms within a few weeks, but some may develop HF, mitral regurgitation, arrhythmias, and cardiogenic shock.[239]

Initially, the diagnosis of takotsubo syndrome by CMR was based on regional LV wall motion abnormalities (Figures 15A, 15B; Figures 16A–D), the identification of myocardial edema on T2-weighted anatomical sequences (Figures 16E, 16F), and the absence (in most patients) of LGE indicative of myocardial fibrosis (Figures 15E, 16G, 16H). However, the development of parametric maps has provided additional information for the evaluation of these patients using CMR.

In 2012, Ferreira et al.[88] showed that native T1 was significantly increased in myocardial segments of patients with takotsubo syndrome compared to healthy volunteers (Figures 15C, 15D). Furthermore, the native T1 map demonstrated greater accuracy (area under the curve = 0.94) than the assessment of myocardial edema on T2-weighted images (area under the curve = 0.58; $p < 0.03$).

Dabir et al.[22] identified elevated native T2 values (Figures 17A–C) and ECV in patients with takotsubo syndrome compared to healthy volunteers, in addition to elevated native T1 values. Interestingly, native T1 and T2 values, as well as ECV, were increased even in remote myocardial segments without abnormal contractility in patients with takotsubo syndrome, indicating a greater extent of disease than imaging methods had previously identified.

Vermes et al.,[240] in a study of 30 patients with takotsubo syndrome and 34 control subjects using a 1.5-T scanner, established high accuracies for increased native T2 (0.89; threshold > 56 ms), increased native T1 (0.89; threshold > 1011 ms), and increased ECV (0.91; threshold > 27%). The combination of native T1 and T2 provided a sensitivity of 91.7% and a specificity of 88.2% in the diagnosis of takotsubo syndrome, leading the authors to propose the use of non-contrast CMR in this population.

In this context, Gil et al.[241] evaluated the utility of CMR in assessing patients who survived a near-fatal cardiac event in 2023. The imaging method was able to establish the cause of the event in 66% of cases, and the use of parametric maps was essential for diagnosing myocarditis or takotsubo syndrome in 48% of these cases.

Beyond purely diagnostic aspects, Aikawa et al.[242] evaluated 23 patients with takotsubo syndrome and reported that the area under the curve for native T1 values (0.96) and ECV (0.92) was significantly greater ($p = 0.005$) than the area under the curve for native T2 values (0.86) in detecting segments with altered contractility. Notably, the LVEF was lower in patients with increased native T1 and T2 values in the basal region, an area typically spared from systolic dysfunction. Furthermore, the greater the number of segments with increased native T1 (> 1339 ms, 3 T), the worse the baseline LVEF and the longer the time required for recovery from dysfunction.

Finally, in 2023, Arcari et al.[243] investigated the association between changes in parametric maps and ECG in patients with takotsubo syndrome and identified an inverse relationship

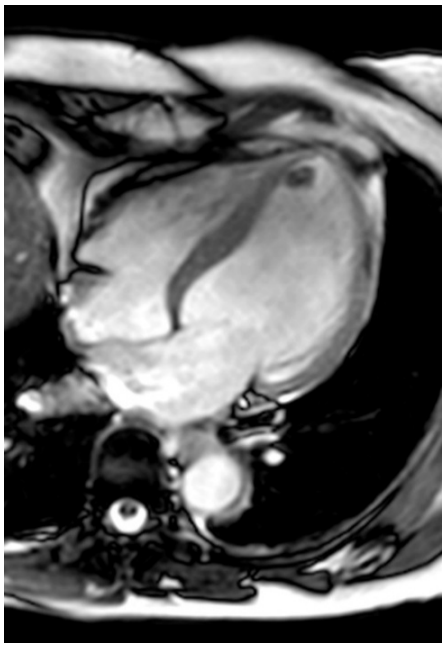


Figure 15A – *SSFP cine imaging, four-chamber view in diastole. SSFP: steady-state free precession.*

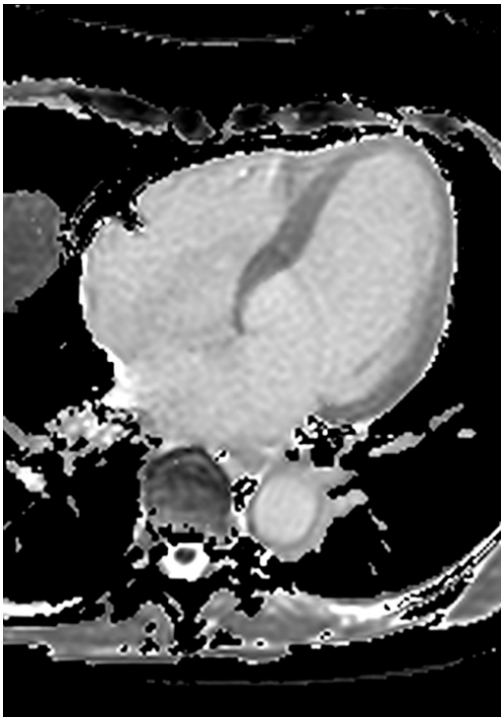


Figure 15C – *Native T1 map, four-chamber view (3 T).*

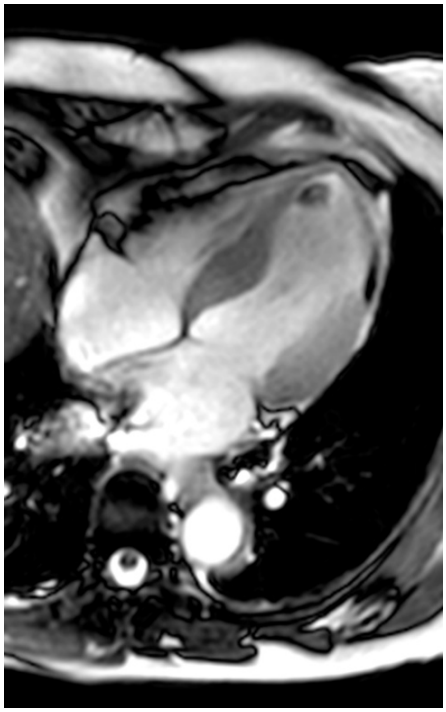


Figure 15B – *SSFP cine imaging, four-chamber view in systole, showing ballooning of the apical portion of the left ventricle. SSFP: steady-state free precession.*

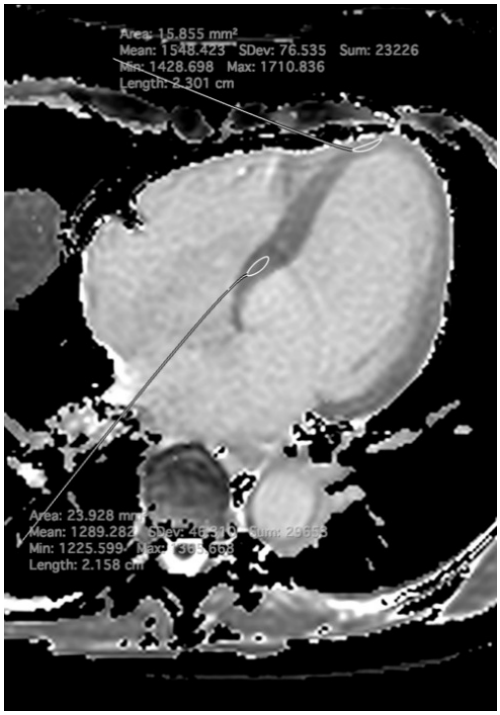


Figure 15D – *Native T1 map, four-chamber view, showing increased values in the apical septum (1548 ms, with contractile abnormality) and basal septum (1289 ms, without regional wall motion abnormalities) (3 T).*

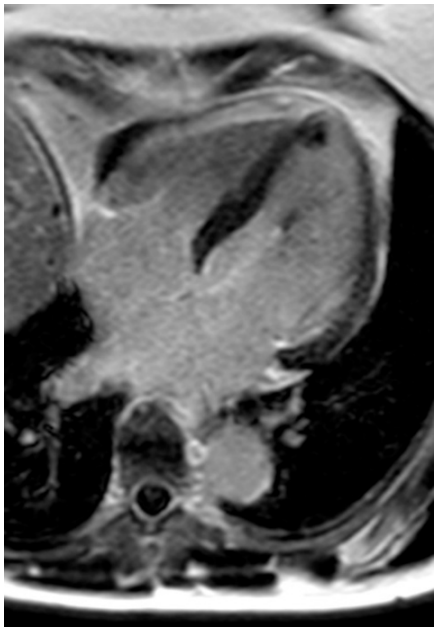


Figure 15E – *Late enhancement, four-chamber view, showing a thrombus near the apex of the left ventricle and absence of late myocardial enhancement.*

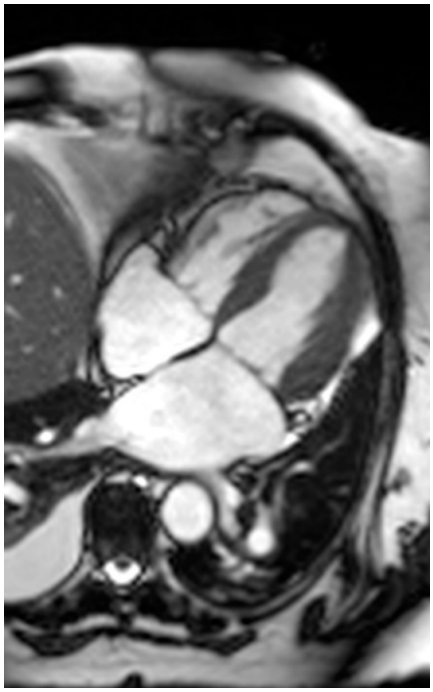


Figure 16B – *SSFP cine imaging, four-chamber view in systole, showing ballooning of the apical portion of both ventricles. SSFP: steady-state free precession.*

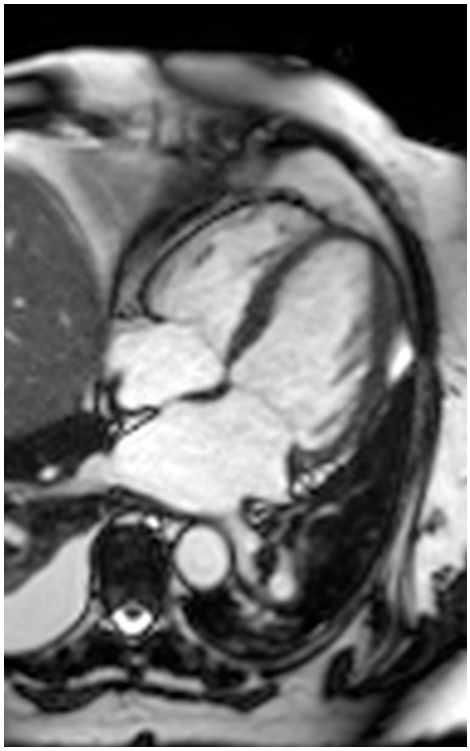


Figure 16A – *SSFP cine imaging, four-chamber view in diastole. SSFP: steady-state free precession.*

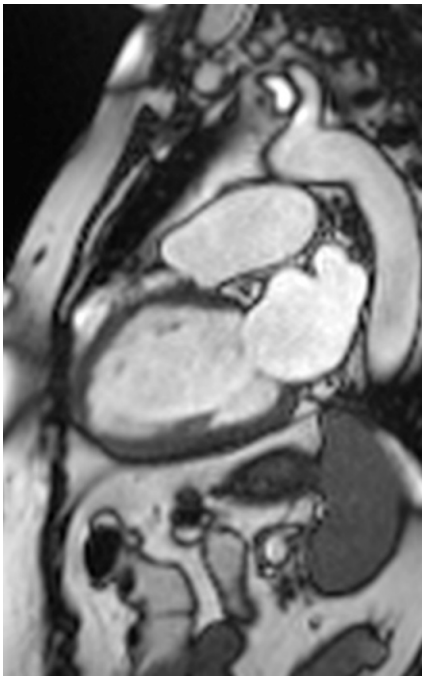


Figure 16C – *SSFP cine imaging, two-chamber view in diastole. SSFP: steady-state free precession.*

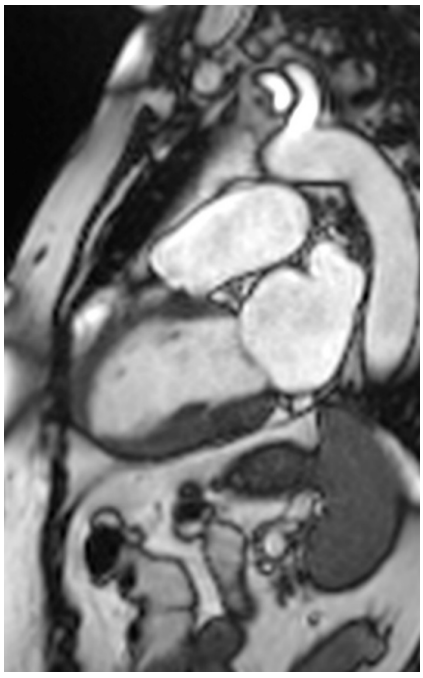


Figure 16D – *SSFP cine imaging, two-chamber view in systole, showing ballooning of the apical portion of the left ventricle. SSFP: steady-state free precession.*



Figure 16F – *T2-weighted triple inversion-recovery pulse black-blood sequence, 2-chamber view, showing hyperintensity in the anteromedial-apical segment, apex, and inferior-apical segment of the left ventricle suggestive of myocardial edema.*

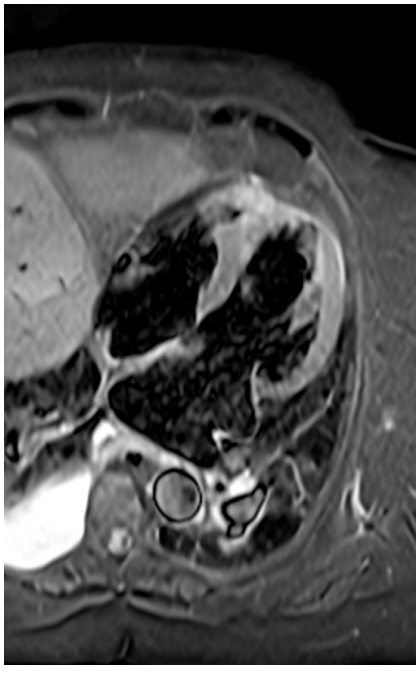


Figure 16E – *T2-weighted triple inversion-recovery pulse black-blood sequence, for-chamber view, showing hyperintensity in the apical portion of both ventricles suggestive of myocardial edema.*

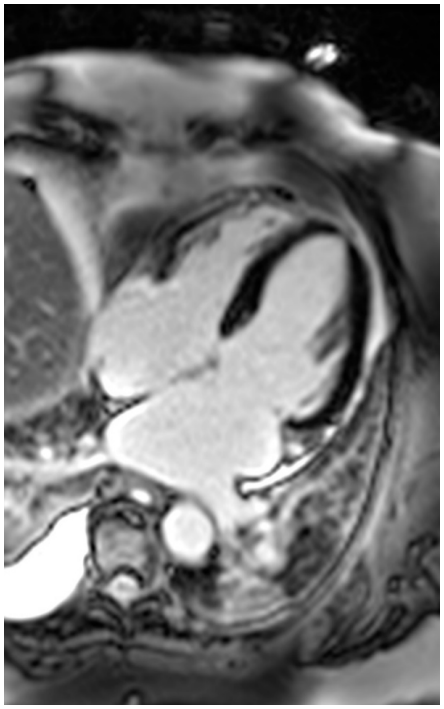


Figure 16G – *Late enhancement, four-chamber view, showing absence of late myocardial enhancement.*

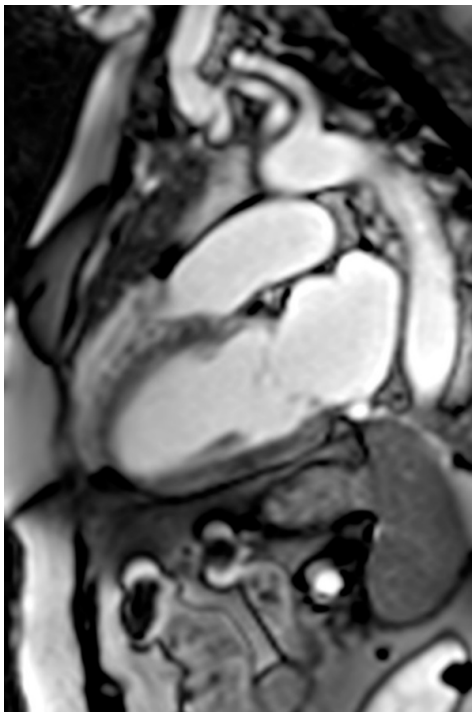


Figure 16H – *Late enhancement, two-chamber view, showing absence of late myocardial enhancement.*

between interventricular septal ECV and QRS complex voltage in lead aVR, as well as a positive relationship between the apicobasal gradient of native T2 and the sum of the voltages of the negative T waves. These findings may explain some of the ECG changes observed in patients with acute takotsubo syndrome.

7.1. Limitations

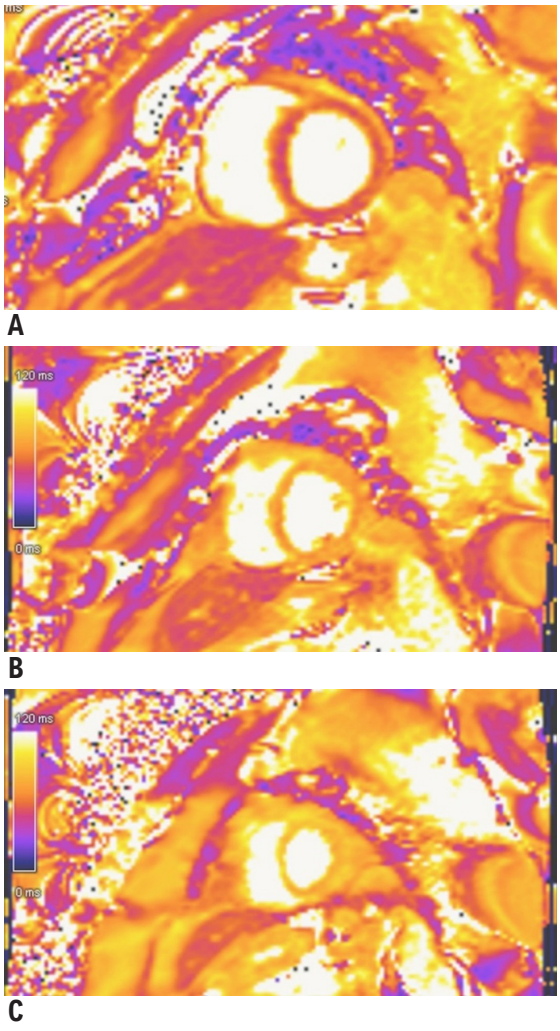
As in other conditions, parametric maps lack standardization regarding normal values. The number of CMR studies in the specific clinical context of this condition remains small, partly due to its low incidence. Furthermore, the studies published to date have small sample sizes.

7.2. Key Takeaways

- Patients with a clinical presentation and initial findings suggestive of takotsubo syndrome should be referred for CMR with parametric mapping, which improves the accuracy of the method in diagnosing the condition beyond that of standard sequences;
- Some parametric map variables may have prognostic value.

8. Congenital Heart Disease

Ejection fraction and ventricular volumes, taken in isolation, may not fully reflect the complexity of structural and functional changes in the heart in congenital heart disease. The LGE technique has provided valuable insights into the



Figures 17A, B and C – *Native T2 map of the short-axis basal (A), mid (B), and apical (C) sections showing an increased value in the apical portion (98 ms) compared to the basal portion (59 ms) (1.5 T).*

understanding of heart disease in general. However, the search for new tools that could not only identify focal fibrosis but also broaden our understanding of interstitial changes has driven interest in more precise tissue characterization.[244,245]

In this context, multiparametric maps have come to be used as complementary tools in the assessment of myocardial tissue characteristics, which – when altered by clinical or pathological conditions – can be analyzed by measuring myocardial relaxation time and calculating the ECV. Changes in parametric maps and ECV may indicate the presence of interstitial fibrosis, edema, inflammation, or the accumulation of intracellular or extracellular material. These tools serve as sensitive, early markers with diagnostic, prognostic, and treatment-monitoring value.

The application of parametric maps in the study of congenital heart diseases has expanded to include both the LV and the RV.[246] LV assessment using T1M and ECV is more well-established, given favorable anatomical characteristics such

as greater myocardial thickness and less trabeculation, while the RV poses additional technical challenges. Its thinner, more trabeculated wall increases the risk of partial-volume artifacts, which can compromise the accuracy of measurements. These challenges are even more pronounced in pediatric patients, who have smaller hearts, higher heart rates, and frequently contain metallic artifacts resulting from previous sternotomies, such as wires located near the RV, which are situated anteriorly in the chest. Strategies to minimize these limitations include acquiring images during systole – when the ventricular wall is thickest – and using sequences with higher spatial resolution and better motion tolerance.[247]

It is also worth noting that, even in congenital heart diseases affecting the right side of the heart, the LV may be compromised, a fact that is often overlooked. Recent studies have expanded our understanding of the impact of the LV in congenital heart diseases affecting the right heart.

8.1. Tetralogy of Fallot

Myocardial fibrosis in patients with tetralogy of Fallot can be attributed to a combination of factors, including chronic preoperative hypoxemia, genetic predisposition, a pro-inflammatory response to cardiopulmonary bypass, ventriculostomy, and conditions of volume or pressure overload following surgical correction. Chronic hemodynamic sequelae following initial repair may trigger the development of fibrosis, which in turn may contribute to the onset of electrical and/or mechanical complications.

In the postoperative course of tetralogy of Fallot, residual lesions may occur, with pulmonary insufficiency being the most commonly found defect. This residual defect can directly impact myocardial structure and function, triggering a complex pathophysiological cascade that may culminate in ventricular dysfunction, arrhythmias, exercise intolerance, and, potentially, sudden death. The presence of volume overload promoting adverse myocardial remodeling may be associated with an increase in ECV, which in turn is associated with a higher incidence of arrhythmias.[5] The combination of a reduced RV mass-to-volume ratio and increased ECV may be related to a process of maladaptation characterized by cardiomyocyte atrophy and diffuse fibrosis.

In patients with residual stenosis and significant hypertrophy, an association with diffuse fibrosis appears to be present, as evidenced by an increase in ECV, particularly in cases where systolic function is impaired.

Although the focus of the evaluation is the RV – since this is a congenital heart disease affecting the right chambers and requiring surgical interventions on them – involvement of the LV is also recognized and is associated with adverse outcomes. The LV ECV may also be increased in these patients, possibly as a consequence of myocardial injury induced by cardiopulmonary bypass, despite the use of cardioprotective strategies during the procedures.[248] Furthermore, the phenomenon of ventricular interdependence in the postoperative period following tetralogy of Fallot has also been well documented, as evidenced by abnormal septal motion, ventricular dyssynchrony, and reduced diastolic filling of the LV cavity, which may contribute to inadequate LV remodeling.[249]

Chen et al. demonstrated that an increase in LV ECV was an independent factor associated with the occurrence of arrhythmias in patients who underwent correction of tetralogy of Fallot.[250] Elevated ECV – and especially RV ECV – was more strongly associated with volume overload than with pressure overload or mixed overload in young adult patients. In the pediatric population, Yim et al. observed an increase in native T1 of the RV, but not of the LV, compared to controls. This increase was present, above all, in cases with predominant volume overload, consistent with the findings of Chen et al.[250,251]

An increase in native T1 and ECV in the interventricular septum, compared to the free wall of the LV, could suggest greater involvement of the myocardium directly adjacent to the RV – with which it shares muscle fibers – and which may be more susceptible to ventriculo-ventricular interactions. Further studies are needed to better understand regional variations in fibrotic remodeling.

More accurate myocardial assessment in this group of patients is of great importance for a better understanding of the causes of complications, since adverse events such as VT, HF, and sudden death may occur during follow-up. The use of noninvasive imaging markers can help elucidate the mechanisms involved and aid in deciding the optimal timing for intervention to address residual defects, thereby removing the hemodynamic stimulus responsible for the progression of myocardial fibrosis.

8.2. Systemic Right Ventricle

The systemic RV scenario includes patients with congenitally corrected transposition of the great arteries (CCTGA) and those who have undergone atrial-level correction (Senning/Mustard) of transposition of the great arteries. Several studies have already demonstrated that patients with a systemic RV are at significant risk of developing ventricular dysfunction over time. In both conditions, the RV remains connected to the aorta, leading to significant pressure overload and consequent marked enlargement and hypertrophy – factors that may contribute to adverse myocardial remodeling.[252]

Although assessment of the RV is often challenging due to its thin wall, in this specific scenario the RV is hypertrophied, which allows for more reliable measurements of the native T1 map and calculation of ECV. The underlying myocardial structural changes reflect compensatory processes, and characterizing the myocardium proves useful in attempting to stratify the risk associated with RV systemic physiology and to guide therapeutic decisions more precisely before ventricular dysfunction progresses. In addition to changes in the RV, the LV also undergoes remodeling, with atrophy and fibrosis, as it is not subjected to systemic afterload. Shehu et al. demonstrated elevated native T1 in the subpulmonary LV, correlating with the presence of diffuse fibrosis in this chamber.[253]

Some studies have shown evidence of diffuse fibrosis in the systemic RV in patients with transposition of the great arteries following atrial redirection surgery, with a higher RV ECV compared to controls. In patients with a systemic RV, the increased RV ECV correlates directly with end-diastolic volume and inversely with ejection fraction.[254]

8.3. Univentricular Heart

A wide anatomical spectrum of congenital malformations is observed in this subgroup of patients. In univentricular configurations, either the LV or the RV may serve as the main chamber. These patients generally undergo total cavopulmonary shunt surgery, in which the superior and inferior systemic venous returns are diverted to the pulmonary parenchyma, while the main ventricle takes on the exclusive role of managing the systemic circulation. This physiology can result in systemic venous congestion, reduced cardiac output, and chronic hypoxia, with both cardiac and hepatic repercussions.

Changes in preload resulting from different palliative approaches, repeated exposure to cardiopulmonary bypass, volume overload, and afterload are among the main factors involved in the pathogenesis of diffuse myocardial fibrosis.

Patients with a right-sided main ventricle may be at higher risk of developing ventricular dysfunction. Additionally, the right main ventricle may exhibit higher native T1 and ECV.[255] An increased ECV appears to correlate with a higher end-diastolic pressure of the single ventricle in this population.

Hepatic abnormalities are often found in this group of patients, ranging from hepatomegaly to chronic liver disease with advanced fibrosis. In these cases, increased native T1 and hepatic ECV have been described.[256,257]

8.4. Other Congenital Heart Diseases

Despite advances in the use of T1M in congenital heart diseases, evidence for many conditions remains scarce or inconclusive, highlighting the need for further studies focused on these specific populations.

Apical displacement of the tricuspid valve to varying degrees, along with consequent tricuspid regurgitation and RV atrialization, are responsible for the right-sided HF that occurs at some stage in the course of Ebstein's anomaly, depending on the severity of the structural abnormalities. Although involvement of the right chambers is predominant, the left heart also appears to be involved in the pathogenesis of HF.

Yang et al. demonstrated that elevated ECV, indicative of interstitial fibrosis, was present in more than 45% of patients with unrepaired Ebstein's anomaly, exceeding the prevalence of focal fibrosis. There was also a correlation between increased ECV and the presence of biventricular dysfunction. This expands the understanding that LV dysfunction is secondary not only to compression by the dilated RV and abnormal movement of the interventricular septum but also to diffuse interstitial fibrosis of the LV.[258]

The pathogenesis of interstitial fibrosis remains unclear; however, Aly et al. hypothesized that fibrotic remodeling of the LV correlates with the severity of tissue hypoxia, supported by the strong association between increased ECV and native T1 and reductions in oxygen saturation.[259]

In the context of aortic coarctation, adverse ventricular remodeling has been the subject of investigation using parameters such as ECV, native T1M, intracellular water lifetime, and global LV measures. This study, which evaluated 46 patients using a 3-T scanner, reinforced the clinical relevance of the T1 map and ECV calculation in risk stratification and follow-up of these patients. Patients with severe aortic coarctation and/or bicuspid aortic valve had significantly increased ECV, native T1, and intracellular water lifetime compared to healthy controls. Interestingly, the presence of a bicuspid aortic valve in patients with aortic coarctation – even when mild – proved to be an aggravating factor in cardiac remodeling, being associated with higher values of ECV and native T1. Furthermore, the use of antihypertensive medications appears to exert a protective effect against remodeling, resulting in lower ECV and native T1 values.[260]

8.5. Conclusion

Multiparametric CMR mapping (T1, T2, and ECV) allows for the early identification of fibrosis and myocardial remodeling in congenital heart disease, serving as a noninvasive biomarker for diagnosis, prognosis, and therapeutic monitoring, with the potential to guide the optimal timing of intervention and improve the clinical management of these patients.

8.6. Key Takeaways

- Multiparametric tissue mapping serves as an adjunct to conventional morphofunctional assessment, enabling the early detection of fibrosis, inflammation, and myocardial edema;
- ECV and native T1 serve as early quantitative and prognostic biomarkers, useful for diagnosis and therapeutic monitoring;
- Tetralogy of Fallot: diffuse myocardial fibrosis associated with postoperative hemodynamic overload; increased ECV and native T1 correlate with arrhythmias and RV and LV dysfunction;
- Systemic RV (CCTGA, Senning/Mustard procedure): fibrotic remodeling and progressive RV dysfunction; elevated ECV is associated with dilation and a lower ejection fraction. The subpulmonary LV also exhibits diffuse fibrosis;
- Univentricular heart (Fontan circulation): diffuse myocardial fibrosis and ventricular dysfunction – more pronounced in the RV – correlate with higher T1 and ECV; hepatic fibrosis is also common;
- Other congenital heart diseases (Ebstein's anomaly, aortic coarctation): increased ECV and native T1 indicate diffuse fibrosis and adverse remodeling; correlation with biventricular dysfunction and chronic hypoxia;
- Technical aspects: RV mapping is more challenging (thin, trabeculated wall), requiring acquisition during systole and high spatial resolution;
- Clinical value: the combined use of multiparametric CMR and quantitative biomarkers aids in risk stratification, prediction of adverse events, and determining the optimal timing for interventions.

9. Cardio-Oncology

Cardiotoxicity related to cancer treatment represents a growing challenge in clinical practice.[261] Among classic chemotherapeutic agents, anthracyclines remain the primary cause of dose-dependent LV systolic dysfunction, associated with cumulative and potentially irreversible myocardial damage.[262] Trastuzumab, an anti-HER2 monoclonal antibody, is also associated with ventricular dysfunction, but with a reversible profile and no clear relationship to cumulative dose; it is frequently used in combination with anthracyclines in patients with breast cancer.[263]

With advances in immunotherapy, ICIs, such as anti-PD-1, PD-L1, and CTLA-4 agents, have emerged as effective drugs, but they can trigger inflammatory adverse events; immune-mediated myocarditis is a serious, albeit rare, manifestation that often has an early onset and is associated with high mortality. In addition, thoracic radiation therapy, used in the treatment of lymphomas and breast or lung cancers, can induce late-onset cardiovascular damage, including coronary artery disease, myocardial fibrosis, valvular heart disease, and constrictive pericarditis, even decades after initial exposure.[261] In this context, early identification of subclinical myocardial injury and continuous cardiovascular monitoring are essential to mitigating risks and optimizing comprehensive care of patients with cancer. Thus, CMR emerges as an important tool in the early diagnosis of cardiotoxicity, aiding in the management of these patients.[264]

9.1. Anthracycline- and Trastuzumab-Induced Cardiotoxicity

Traditionally, patients who develop cardiotoxicity due to anthracyclines or trastuzumab present with a decreased LVEF in the absence of late myocardial enhancement.[264] A study using multiparametric CMR mapping in these patients aimed at the early diagnosis of myocardial involvement.[265] The use of T1M by CMR for the early detection of anthracycline-induced cardiotoxicity was initially demonstrated in animal models. In an experimental study, mice treated with doxorubicin showed a significant increase in native T1 values before the onset of detectable functional changes in ejection fraction, indicating that T1M could reflect subclinical interstitial changes, such as edema and early fibrosis, related to myocardial toxicity.[266,267]

Subsequent studies evaluated the accuracy of multiparametric CMR parameters, in combination with biochemical markers, in the early detection and prediction of cardiotoxicity in cancer patients undergoing chemotherapy.[265] Evaluation of these methods during chemotherapy (before chemotherapy, at 6 months, and at 24 months of follow-up) revealed a significant increase in native T1 and T2 values as early as 6 months in patients who developed cardiotoxicity during follow-up.[265]

It is important to note that variations in T1 map findings during chemotherapy should be interpreted with caution. Although multiparametric techniques show promise in identifying subclinical changes, intra- and inter-observer variability may exist. In addition, minor physiological fluctuations or variations related to the imaging protocol could impact clinical interpretation of the findings. This highlights the importance of technical standardization, specific training, and longitudinal analysis with rigorous quality control methods so that CMR can be fully incorporated as a reliable tool for monitoring chemotherapy-induced cardiotoxicity.[268]

Compared with healthy controls, childhood cancer survivors have significantly higher native T1 values, even in the absence of systolic ventricular dysfunction. Furthermore, increased T1 values correlated with a higher cumulative dose of anthracyclines and with changes in longitudinal strain, suggesting a persistent, subclinical process of myocardial remodeling. Thus, the use of T1M as a sensitive biomarker is valuable not only for the early detection of myocardial injury during chemotherapy but also for the long-term monitoring of structural sequelae in long-term survivors.[269]

A recent meta-analysis evaluated the role of native T1M by CMR in the early detection of anthracycline-induced cardiotoxicity. The results showed that patients exposed to anthracyclines had significantly higher native T1 values compared to healthy controls. Furthermore, among patients treated with anthracyclines, those who developed cardiotoxicity exhibited even higher native T1 values. These findings indicate that the increase in myocardial T1 occurs before overt systolic dysfunction, reinforcing the value of T1M as a sensitive and noninvasive biomarker for the early identification of subclinical myocardial injury in cancer patients.[270]

Another recent meta-analysis evaluated the utility of parametric CMR techniques – including native T1M, T2M, and ECV fraction – in the early detection of anthracycline-induced myocardial changes in adult patients with preserved LVEF. The analysis demonstrated that, even in individuals with normal systolic function, there is a significant elevation in native T1, T2, and ECV values compared to healthy controls. These findings suggest the presence of subclinical myocardial injury associated with edema and interstitial fibrosis, even in the absence of apparent ventricular dysfunction.[271]

Trastuzumab-induced cardiotoxicity, especially when this agent is used in combination with anthracyclines in the treatment of HER2-positive breast cancer, has been the subject of growing attention in cardio-oncology, given its potential reversibility and functional impact on the LV. Recent studies have demonstrated the value of CMR tissue mapping techniques, particularly T1M and T2M, in the early detection of subclinical myocardial changes associated with trastuzumab exposure. Patients with breast cancer treated with anthracyclines, with or without trastuzumab, were followed longitudinally; those who developed ventricular dysfunction exhibited a significant increase in native T1 and T2 values as early as the initial phases of treatment, suggesting the occurrence of edema and the onset of interstitial fibrosis prior to a decline in ejection fraction.[272]

9.2. Cardiotoxicity from Immune Checkpoint Inhibitors

ICI immunotherapy has been associated with the development of acute myocarditis. The diagnosis is classically made using the Lake Louise criteria, which are well established in the literature.[87] The utility of multiparametric CMR maps in the detection and stratification of immunotherapy-associated cardiotoxicity was demonstrated by an international

multicenter study. Among 136 patients with suspected ICI-induced myocarditis who underwent CMR, T1 maps were available for 86 (63%) and T2 maps for 79 (58%). The mean native values were significantly elevated compared to reference ranges, with abnormal T1 and T2 values observed in 78% and 43% of patients, respectively.

Applying the modified Lake Louise criteria, 95% met the criterion for non-ischemic myocardial injury and 53% met the criterion for edema. Native T1 demonstrated remarkable prognostic value: each one-unit increase in the z-score was associated with a 44% increase in the risk of major cardiovascular events and showed excellent discriminatory ability for these events. These findings indicate that the simultaneous incorporation of T1, T2, and late enhancement into CMR protocols allows not only for the early diagnosis of ICI-related myocarditis but also for the identification of patients at higher risk of adverse outcomes.[93]

Although CMR is the gold standard for myocardial tissue characterization, contrast-enhanced CT has been studied for estimating ECV (CT-ECV). In patients treated with ICIs, increases in CT-ECV have been associated with elevated troponin levels, reduced myocardial strain, and a higher incidence of cardiovascular events, suggesting the detection of subclinical myocardial inflammation or early fibrosis. These results indicate that CT-ECV may serve as a complementary tool when CMR is unavailable or contraindicated.[273]

9.3. Radiotherapy-Induced Cardiotoxicity

Radiation therapy can lead to late-onset cardiotoxicity. Few studies have evaluated the role of multiparametric imaging in this setting. One such study assessed patients previously treated with thoracic radiation therapy, primarily for breast cancer or Hodgkin lymphoma, with an average exposure time of 11.5 years prior to cardiac MRI. Native T1 values were significantly elevated in patients with negative LGE, suggesting the presence of diffuse fibrosis even in the absence of visible enhancement.[274] Further studies are needed to evaluate the role of these maps in radiation-induced cardiotoxicity.

9.4. Key Takeaways

- Multiparametric mapping should be performed in patients with suspected anthracycline- and trastuzumab-induced cardiotoxicity, both during chemotherapy and after treatment has ended;
- In patients with cardiotoxicity, elevated T1 and ECV values are expected;
- In patients with suspected immunotherapy-induced myocarditis, the use of T1 and T2 maps aids in early diagnosis and can provide important prognostic information.

10. Systemic Conditions

CMR, with its advanced parametric mapping techniques, has established itself as an important diagnostic and prognostic tool in the detection and management of cardiac involvement in patients with autoimmune rheumatic diseases (ARDs).[4,77,275-277] Parametric maps provide a detailed view of myocardial tissue composition, revealing inflammation and fibrosis at stages that are often subclinical, before they manifest as overt symptoms or ventricular dysfunction detectable by conventional methods.

10.1. The Need for Advanced Diagnostic Tools in the Context of Autoimmune Rheumatic Diseases

Cardiac involvement is a common and serious complication of autoimmune diseases that can lead to a spectrum of adverse outcomes, including HF, complex arrhythmias, and, ultimately, premature mortality. The silent or subclinical nature of these cardiac manifestations, particularly in the early stages, makes early detection a significant challenge with conventional tests, such as echocardiography, which may fail to identify the arrhythmic substrate or diffuse tissue changes. This difficulty in early identification underscores the urgent need for more sensitive screening tools. Endomyocardial biopsy, although the gold standard for histopathological diagnosis, is an invasive procedure with inherent risks and the potential for sampling error.[4,77,275-277] In this context, CMR emerges as a robust noninvasive alternative, capable of providing a comprehensive and quantitative tissue characterization of the myocardium (Table 9).

10.2. The Value of Parametric Maps in Myocardial Tissue Characterization

Multiparametric maps are indicated for tissue characterization in systemic diseases, due to their previously discussed ability to detect fibrosis and edema.[4,77,275-277]

10.3. Systemic Lupus Erythematosus

Systemic lupus erythematosus (SLE) is a multisystem autoimmune disease which features significant cardiac involvement. CMR with multiparametric mapping has demonstrated the ability to detect silent cardiac involvement even in treatment-naïve patients with newly diagnosed SLE, or in those with inactive disease.[278]

Both native T1 map and ECV are significantly increased in patients with SLE compared with healthy controls. For example, the mean (SD) native T1 was 1369 (79) ms in patients with SLE vs. 1092 (57) ms in controls, and the ECV was 32% (5%) vs. 24% (3%) ($p < 0.001$ for both), respectively, on a 3.0-T scanner. These increases, indicative of diffuse changes in the extracellular matrix, were observed even in subgroups with inactive SLE and were independent of clinical disease activity. This suggests that diffuse myocardial changes may occur early and plateau, showing no significant further increase in patients with long-standing SLE compared with those with recent-onset SLE.[277]

Increased T2 map values show a strong correlation with SLE disease activity and changes in ultra-high-sensitivity troponin. Mean T2 values of 58 (5.6) ms in SLE correlated with disease activity on 1.5-T scanners.[276] Patients with newly diagnosed SLE exhibited significantly higher T2 values (55.3 ms vs. 52.8 ms, $p < 0.05$) compared with the long-standing SLE group, suggesting more pronounced myocardial edema in newly diagnosed patients (3.0-T scans).

Tabela 9 – Papel da ressonância magnética cardíaca nas doenças reumáticas sistêmicas

Aspect	Description
Importance of CMR	Should be considered essential in the evaluation of ARDs with unexplained arrhythmias and normal LVEF.
Diagnostic value	T1/T2 mapping and ECV provide incremental diagnostic value, even in the absence of obvious functional abnormalities.
Therapeutic application	CMR can guide interventions such as device implantation in patients with arrhythmias.
Limitations of echocardiography	Conventional echocardiography may not identify the arrhythmogenic substrate in ARDs.
Presence of LGE	LGE was present in only half of the patients with abnormal maps in ARDs.
Parametric maps	T1, T2, and ECV were abnormal in most cases, even with normal systolic function (4)

ARDs: autoimmune rheumatic diseases; CMR: cardiac magnetic resonance imaging; ECV: extracellular volume; LGE: late gadolinium enhancement; LVEF: left ventricular ejection fraction.

In contrast to the high sensitivity of parametric maps, LGE was positive in only 12% of patients with newly diagnosed SLE, with no significant difference compared to controls. This finding reinforces that T1 and ECV are more sensitive for detecting diffuse changes that late enhancement may fail to capture.

Disease progression and functional impact: myocardial structural and functional changes progress with the stage of the disease. In patients with long-standing SLE, cardiac involvement is more pronounced, manifesting as elevated atrial natriuretic peptide, pulmonary hypertension, RV remodeling (increased volume and reduced RV ejection fraction), and a higher prevalence (40%) and extent of LGE. The study also observed a more significant impact on the RV in both SLE groups, which may be related to the involvement of small and medium-sized arteries in SLE rather than merely to pulmonary hypertension. Notably, changes in GLS were observed only in more advanced stages (long-standing SLE), correlating with the presence of LGE, while myocardial function and strain in the recent-onset group were still within normal limits.[277]

Thus, native T1 and ECV values can serve as markers for the early detection of myocardial injury, preceding the presence of fibrosis visible by LGE and functional decompensation detected by other clinical and cardiac indices. This early detection provides a solid basis for the timely initiation of cardioprotective medications.[278]

10.4. Systemic Sclerosis

The heart is an organ frequently involved in systemic sclerosis (SSc), but cardiovascular disease often remains subclinical.[6] Patients with overt clinical features of cardiovascular disease in SSc are at increased risk of deterioration and premature cardiovascular death.[280]

T2M: consists of a sensitive technique for detecting myocardial inflammation in patients with SSc, even in the absence of striking clinical or laboratory findings. The inclusion of T2M via CMR significantly improves the detection of subclinical myocarditis in SSc.[280]

Native T1 and ECV: patients with SSc have significantly higher native myocardial T1 values (1007 [29] ms vs. 958 [20] ms in controls, $p < 0.001$) and larger areas of myocardial involvement detected by native T1 (> 990 ms) (median of 52% vs. 3% in controls, $p < 0.001$). The ECV was also significantly increased in patients with SSc (35.4% [4.8%] vs. 27.6 [2.5%] in controls, $p < 0.001$).[279] Even in patients with SSc without LGE, native T1 and ECV were significantly elevated compared with controls, indicating that these techniques detect diffuse involvement that LGE is unable to capture. This is particularly relevant because late enhancement (focal fibrosis) is found in 53% of patients with SSc, but native T1 and late enhancement may have limited value for measuring disease activity due to pre-existing diffuse fibrosis, as shown in Figure 18.

10.4.1. Correlations and Prognosis

Elevated T1 has prognostic value and is associated with more severe forms of SSc. Patients with higher T1 levels had an increased risk of cardiac events, regardless of LVEF. Higher T1 values were also associated with the diffuse form of SSc; specific immune patterns such as anti-Scl70, anti-RNA polymerase III, and anti-fibrillarin antibodies; higher skin scores (mRSS); and the presence of interstitial lung disease. The positive correlation between T1 and mRSS indicates that greater cutaneous fibrosis is accompanied by greater microscopic myocardial involvement. Myocardial involvement detected by T1 and ECV correlated significantly with disease activity and the severity of cutaneous fibrosis. Native T1 also correlated with serum C-reactive protein, an inflammatory marker. Although biventricular size and global function (LVEF) may be preserved, mapping can detect incipient changes.[281]

10.5. Rheumatoid Arthritis

Rheumatoid arthritis (RA) is a chronic inflammatory disease that can also affect the heart, even in asymptomatic patients.[282]

T1M, T2M, and ECV: these techniques detect diffuse fibrosis and inflammation in patients with RA. Patients with RA had significantly higher mean (SD) native T1 values (973 [27] ms vs. 961 [18] ms; $p = 0.03$) and an increase in ECV (30.3% [3.4%]

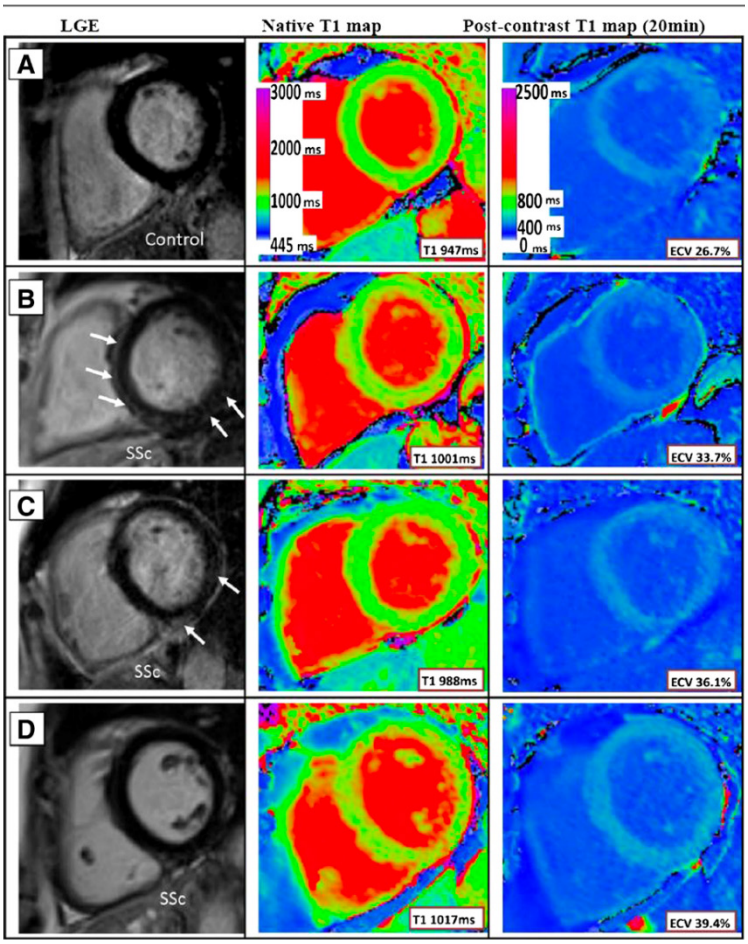


Figure 18 – *Representative examples of native T1 and post-contrast maps with corresponding LGE images in patients with SSc and controls. Upper panel (A): normal control, without LGE; native T1 of 947 ms, post-contrast T1 of 514 ms, ECV of 26.7%. Second panel (B): patient with SSc, showing linear septal LGE and focal areas of LGE in the inferolateral basal wall; native T1 of 1001 ms, post-contrast T1 of 453 ms, ECV of 33.7%. Third panel (C): patient with SSc showing small areas of mesocardial LGE in the inferior and lateral regions; native T1 of 988 ms, post-contrast T1 of 439 ms, ECV of 36.1%. Fourth panel (D): patient with SSc without detectable LGE; native T1 of 1017 ms, post-contrast T1 of 421 ms, ECV of 39.4%.[279] ECV: extracellular volume; LGE: late gadolinium enhancement; SSc: systemic sclerosis.*

vs. 27.9% [2.0%]; $p < 0.001$) compared with controls. Larger areas of myocardial involvement were detected by native T1 > 990 ms (median of 35% vs. 2% in controls). These findings of diffuse fibrosis and inflammation were present regardless of the presence of LGE on 1.5-T scanners.[275]

Correlation with disease activity and prognosis: elevated T1 and ECV values are associated with a worse prognosis and greater disease activity. Myocardial T1 and ECV values were correlated with RA disease activity and myocardial deformation. Interestingly, diffuse myocardial fibrosis was not related to the duration of RA or to positivity for rheumatoid factor or anti-cyclic citrullinated peptide antibodies.[275]

In one study, LGE showed focal fibrosis/myocardial scarring in 46% of patients with RA, compared with none of the controls; most cases were of a non-ischemic nature, with mid-parietal enhancement patterns. Overall, late enhancement was observed in 55% of RA cases, with high values for native T1M, T2M, and ECV, showing a strong correlation with disease activity and severity.[3,275]

10.6. Idiopathic Inflammatory Myopathies

Cardiac involvement secondary to inflammatory myopathies, such as dermatomyositis (DM) and polymyositis (PM), is more severe and is associated with adverse events and even death, requiring immunotherapy for treatment, unlike viral myocarditis, which generally responds to more conservative treatment.[283]

T1 and T2 maps are more accurate than late enhancement for evaluating these conditions. Studies have shown that up

to 90% of patients with idiopathic inflammatory myopathies (IIM) without LGE had elevated T1 and T2 values. Patients with IIM had a higher mean native T1 value of skeletal muscle (963 [127] ms) and a higher ECV (19% [7%]) compared to patients with acute viral myocarditis and controls. Patients with PM/DM had significantly higher native myocardial T1 values (1263.7 [84.0] ms) and significantly higher ECV (32.6% [3.7%]) compared with controls (native T1: 1200.6 [43.0] ms; ECV: 26.7% [2.3%]). This suggests the presence of diffuse myocardial fibrosis (elevated T1) and edema/expansion of the extracellular space (expanded ECV) even in the absence of symptoms,[284] as shown in Figure 19.

As a first step, the visible skeletal muscles were delineated in the first image with TI after appropriate adjustment of grayscale levels. Next, each muscle ROI was propagated to all subsequent images with different TIs. Third, each propagated ROI was zoomed in on, and the grayscale levels were adjusted to allow for redrawing and repositioning of the ROIs in order to avoid fat and vessels, as well as to accommodate muscle deformation when necessary. Finally, for each ROI, the grayscale levels were calculated as the average across successive images with different TIs, and the resulting signal was fitted to an exponential model to calculate the native T1 in the example above. It is worth noting that this process is first performed on the native T1 dataset, and the resulting ROIs are copied to the post-contrast T1 and T2 datasets, with the correction process repeated.

In subclinical disease, routine LV functional parameters (such as end-diastolic volume, end-systolic volume, and LVEF) showed no significant differences between patients with PM/DM and controls. Early detection may be crucial for timely treatment and to prevent adverse remodeling and cardiac mortality. No significant correlations were found between the mapping parameters and levels of creatine kinase, troponin T, or disease duration.[284]

In this specific study (conducted using a 3-T scanner), the diagnostic thresholds for cardiac involvement in IIM were T1 > 1275 ms or T2 > 42.3 ms. The area under the ROC curve for the diagnosis of cardiac involvement was 0.78. Late enhancement occurred in only 35% of patients with IIM-associated myocarditis.[9]

10.7. Antineutrophil Cytoplasmic Antibody-Associated Vasculitis

These forms of vasculitis, such as granulomatous polyangiitis, microscopic polyangiitis (MPA), and eosinophilic granulomatosis with polyangiitis, can lead to myocarditis, fibrosis, or myocardial infarction coexisting with vasculopathy.[281]

The use of parametric maps in antineutrophil cytoplasmic antibodies (ANCA)-positive vasculitis has proven to be an important prognostic predictor, independent of the presence of late enhancement (8). Patients with ANCA-associated vasculitis had significantly higher mean native T1 values (988 ms vs. 952 ms; $p < 0.001$), significantly lower post-contrast T1 values (488 ms vs. 524 ms; $p = 0.03$), increased ECV (27.5% vs. 24.5%; $p < 0.001$), and significantly higher mean myocardial T2 values (53 ms vs. 49 ms; $p < 0.001$) compared with controls. These findings of elevated native T1, ECV, and T2 did not correlate with the presence of LGE, suggesting that mapping techniques provide additional information regarding diffuse myocardial involvement.[282]

10.8. Detection of Arrhythmogenic Substrates

CMR with parametric mapping is particularly valuable in identifying arrhythmogenic substrates, such as subclinical inflammation and fibrosis, even in patients with ARDs who have preserved LV systolic function (LVEF), and which are not detected by conventional echocardiography.[278]

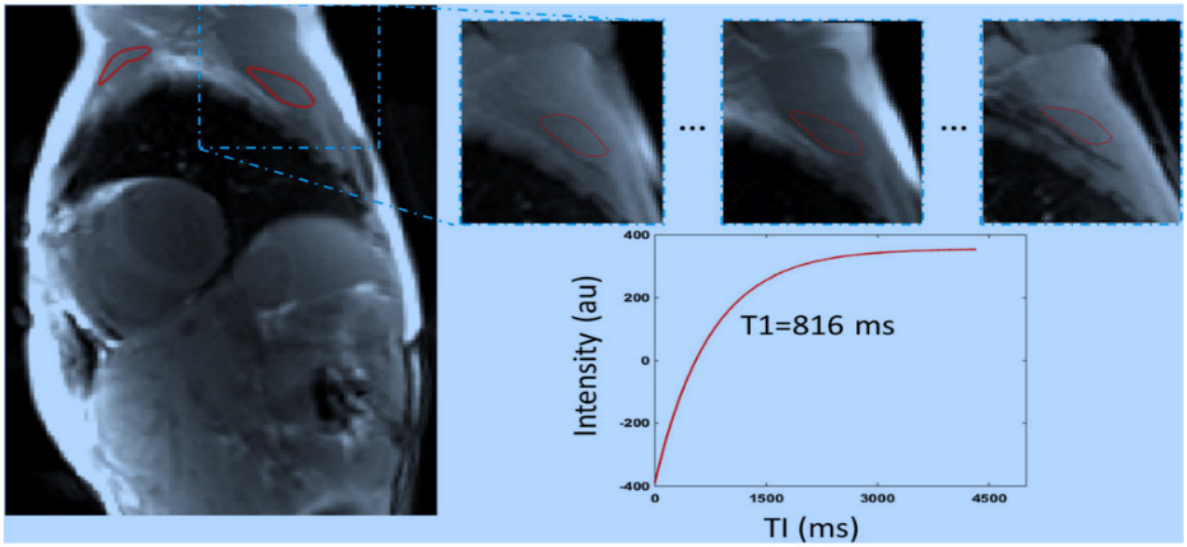


Figure 19 – *Estimation of mapping parameters in skeletal muscle.*[283]

In patients with ARDs (SLE, SSc, DM, etc.) who had documented VT and LVEF > 50%, changes in CMR were observed at the following rates:

- LGE was positive in 55.8% of cases;
- Native T1 was increased in 93%;
- T2 map was increased in 86%;
- ECV was increased in 81.4%.

Therefore, T1, T2, and ECV values were independent predictors of the presence of VT in ARDs, even after adjusting for age, sex, and LVEF. This means that diffuse inflammation and fibrosis (detected by T1, T2, and ECV) were abnormal in most patients, even in the absence of LGE.[3] Conventional echocardiography may fail to identify this arrhythmic substrate in ARDs.

CMR with parametric mapping offers significant incremental diagnostic value and can guide crucial therapeutic decisions, such as the need for an ICD.[148] Specifically in the left endocardium, both native T1 and ECV were significantly higher in patients with VT ($p < 0.05$). Although in SSc there was a trend toward increased T1 and ECV in patients with TV, this was not statistically significant, and the T2 map was numerically higher in the groups with TV, but without a statistically significant difference in either the SLE or SSc subgroups.[3]

10.9. Implications for Monitoring and Therapy

The ability of CMR with parametric mapping to detect subclinical myocardial lesions early, especially through native T1 measurement and ECV calculation, provides a solid basis for the timely introduction of cardioprotective medications at an early stage of the disease. This detection may precede the presence of LGE-visible fibrosis and functional decompensation. The authors of a study on SLE suggest that T1 and ECV values can be used as noninvasive indices for screening subclinical disease and as monitoring tools to guide targeted treatments before LGE and functional decompensation actually manifest.[277]

Another crucial aspect is that T1 and T2 maps can be used to monitor response to treatment, and a reduction in their values correlates well with response to immunosuppressants. This allows physicians to adjust therapies based on objective, quantitative data regarding the reduction of inflammation and fibrosis.[276]

10.10. Conclusions

In summary, CMR is an essential tool with high incremental diagnostic value in the evaluation of cardiac involvement in patients with ARDs (Chart 3).

Given the prevalence and severity of cardiac involvement in RA, as well as the often-asymptomatic nature of these conditions, multiparametric CMR should be considered a complementary tool for screening, diagnosis, and follow-up of these patients, optimizing clinical management and, ultimately, improving long-term outcomes.

10.11. Key Takeaways

CMR with parametric mapping is essential for:

- Providing valuable prognostic information related to disease activity and severity;
- Identifying arrhythmogenic substrates even in patients with preserved ventricular function;
- Guiding earlier and more targeted therapeutic decisions, including the initiation of cardioprotective therapy or consideration of placement of devices such as an ICD;
- Monitoring the response to immunosuppressive treatment.

11. Masses

Cardiac masses remain a diagnostic challenge in clinical practice. MRI has established itself as an important tool in this regard.

Among primary cardiac tumors, 90% are benign, originating in the pericardium or myocardium, with an estimated incidence of 1380 per 100 million individuals (Tables 10 and 11). Secondary tumors, on the other hand, have an incidence 22 to 132 times higher and are, by definition, malignant. Unlike in most organs, in the heart even a benign tumor can produce adverse effects such as arrhythmias and hemodynamic compromise, depending on its location and size.[285,286]

Through its excellent spatial resolution and tissue contrast, CMR allows analysis of the function, mass, morphology, and dimensions of the cardiac chambers and pericardium. LGE plays an important role in differentiating tissue composition, revealing areas of fibrosis, and serves as a powerful diagnostic tool for cardiomyopathies and cardiac masses.[287,288]

T1M was most recently introduced to fill a gap in the assessment of interstitial fibrosis (still early stages of disease) and in the estimation of ECV. In the diagnosis of cardiac masses, CMR plays a fundamental and well-established role, with good correlation to myocardial biopsy. The combination of morphological and functional assessment, the presence or absence of late enhancement and perfusion, and, more recently, the T1 map provide important diagnostic and prognostic information, and are also helpful in post-chemotherapy and radiotherapy follow-up.[270]

11.1. Cardiac Tumors

Cardiac tumors can be classified as primary, secondary (metastases), benign, or malignant. The most common primary tumors are benign, with myxoma being most frequent (50%). Among malignant tumors, angiosarcoma ranks first, accounting for 30–40% of diagnoses. Rhabdomyoma is prevalent in children and is strongly associated with tuberous sclerosis. Among secondary/metastatic types, the relative incidence is approximately 20 to 40 times higher than that of primary tumors. The most common sites of origin are the lung, breast, melanoma, kidney, and lymphoma, with the most frequent site of involvement being the pericardium, followed by the myocardium and endocardium.[5,270]

For a more detailed assessment, a CMR malignancy score was created that includes morphological characteristics of the mass (non-left-sided location, sessile, multilobular, heterogeneity, infiltration, pericardial effusion) and characterization of the mass tissue (first-pass perfusion and heterogeneous enhancement); a score ≥ 5 was independently predictive of malignancy with excellent accuracy.[289]

Chart 3 – Summary of parametric changes in autoimmune diseases

Autoimmune rheumatic disease	Characteristics of cardiac involvement	Findings and diagnostic/prognostic implications
Systemic lupus erythematosus	Cardiac involvement is often subclinical, with a risk of arrhythmias and HF.	Elevated T1 and ECV even in inactive disease. T2 correlates with disease activity. LGE is not very sensitive. Important for early detection and monitoring of response to immunosuppression.
Systemic sclerosis	Higher morbidity and mortality when cardiac involvement is due to fibrosis or inflammation. Often subclinical.	Elevated T1 and ECV even in the absence of LGE. T2 is sensitive to inflammation. T1 has prognostic value and is associated with the diffuse form
Rheumatoid arthritis	Subclinical involvement is common, with increased cardiovascular risk.	Elevated T1 and ECV indicate diffuse fibrosis. Associated with disease activity. LGE in 46%, mostly non-ischemic.
Idiopathic inflammatory myopathies	Subclinical cardiac involvement. Severe HF requiring immunosuppression.	Elevated T1 and ECV even in the absence of symptoms. Absent LGE in 90% of cases with mapping abnormalities. Adjust T1 to account for skeletal muscle.
ANCA-associated vasculitis	Myocarditis, fibrosis, and myocardial infarction coexisting with vasculopathy.	Elevated T1, ECV, and T2, even in the absence of LGE. Correlates with ECG abnormalities. Mapping has independent prognostic value.
Sjögren syndrome	Myocarditis is extremely rare.	No relevant data for CMR.
Autoimmune thyroid diseases	Cardiac involvement is rare.	Overall T1 and T2 values show no significant differences. Radiomics detects subtle changes.

ANCA: antineutrophil cytoplasmic antibodies; CMR: cardiac magnetic resonance imaging; ECG: electrocardiogram; ECV: extracellular volume; HF: heart failure; LGE: late gadolinium enhancement.

Table 10 – Primary cardiac tumors – benign

Tumor	Relative incidence	Age/Notes	Location
Myxoma	50% (of primary tumors)	Adults (ages 30–60)	Left atrium
Lipoma	10–15%	Any age	Myocardium and epicardium
Fibroelastic papilloma	5–10%	Adults	Valves (aortic > mitral)
Fibroma	5–10%	Children	Left ventricle
Rhabdomyoma	5–10%	Children, associated with tuberous sclerosis	Ventricles
Other benign lesions	< 5%	Variable	Variable

Table 11 – Primary cardiac tumors – malignant

Tumor	Relative incidence	Age	Location
Angiosarcoma	30–40% of primary malignancies	Adults	Right atrium
Leiomyosarcoma	20–25%	Adults	Left atrium
Rhabdomyosarcoma	15–20%	Children	Ventricles
Other sarcomas	15–30%	Rare	Variable

The three most common clinical presentations of cardiac tumors are:

a) Systemic: constitutional symptoms (fever, arthralgia, fatigue, weight loss) and paraneoplastic syndromes;

b) Cardiac: symptoms of dyspnea, chest pain, presyncope, and syncope, which may be associated with mass effects altering cardiac hemodynamics or causing arrhythmias;

c) Embolic: episodes of systemic or pulmonary embolism.

Assessment of cardiac masses can be performed in multiple ways, taking into account the characteristics of each CMR sequence. Protocols generally include:[290]

a) Cine: provides an initial assessment of the mass – presence and location, relationship to surrounding structures, potential hemodynamic consequences, and associated abnormalities;

b) Tagging: reveals the absence of contractility and delineates the borders of the mass to assess invasive growth;

c) T1- and T2-weighted images: identify whether the mass has a high fat or fluid content;

d) First-pass perfusion: provides an assessment of whether the mass is vascularized;

e) LGE: detects focal areas of fibrotic tissue or myocyte necrosis and is also related to mass vascularization;

f) Parametric maps: direct assessment of the magnetic resonance properties of the tissue of interest, such as T1, T2, and T2*. These methods are still undergoing validation and are rarely used in daily practice.

The major advantage over conventional tissue characterization (which is based on relative variations in signal intensity) is that parametric maps provide a direct assessment of the T1, T2, and T2* relaxation times.

11.2. Cardiac Magnetic Resonance Imaging and Parametric Maps

Tissue characterization using MRI allows for a detailed assessment of the intrinsic composition of lesions. Lesions that exhibit reduced native T1 relaxation times, accompanied by intense signal hyperintensity on T1-weighted sequences, include lipid-rich neoplasms, such as lipomas and liposarcomas; recent hemorrhages, in which methemoglobin predominates; and melanomas, due to their high concentration of melanin. In contrast, prolonged native T1 relaxation times are indicative of a higher content of free water, fibrosis, or amyloid infiltration. Thus, elevated T1 values are characteristic of cysts (particularly those containing low-protein fluid), vascular malformations, and most malignant masses.[5,290]

Prolonged T2 relaxation times reflect the presence of edema. Cystic structures and highly vascularized neoplasms, such as hemangiomas, exhibit prolonged T2 times and, consequently, hyperintensity on T2-weighted images. Finally, a shortened T2* time is associated with iron buildup, a condition observed in thrombi and in hemorrhages of cardiac origin.

Evaluation using parametric maps has not yet proven effective on its own in distinguishing benign from malignant tumors, largely due to the heterogeneity of these masses. One interesting finding was the increase in T1 map values in areas adjacent to primary tumors when compared to values in remote healthy areas of the same heart – a finding not observed in patients with benign tumors.[291,292]

In a published case series of myxomas, increased T1 and T2 map values as well as ECV were reported. These findings are consistent with an increase in interstitial space and fluid.[292]

For rarer tumors, the number of patients is insufficient for a case series to establish reference values. In these cases, mapping studies provide a more detailed tissue analysis, incorporating data for a more accurate diagnosis. In a case of atrial melanoma published by Caspar et al.,[293] the mass exhibited reduced T1-weighted map values compared to the myocardium and a slight elevation in T2-weighted map values – characteristics consistent with the presence of melanin[294] (Tables 12 and 13).

In tumors affecting the pediatric population, good interobserver reproducibility was observed, with distinct values among subtypes when considering ECV and native T1 map values. ECV values proved to be more accurate in differentiating the subtypes of these tumors: lipoma (close to zero), rhabdomyoma (similar to myocardium), hemangioma (similar to blood), and fibroma (approximately 100%).[294]

11.3. Challenges and Future Prospects

The use of T1M in cardiac tumors represents a significant advance in noninvasive tissue characterization. This technique is gaining ground in distinguishing benign from malignant masses. Potential advances include greater diagnostic accuracy, integration with AI tools, and better monitoring of treatment response. Nevertheless, limitations remain, such as variability among scanners, the need for standardized protocols, and interference from arrhythmias or motion artifacts. Furthermore, the overlap of T1 values among different types of lesions can still make definitive interpretation difficult.

11.4. Conclusion

T1M is a valuable tool for evaluating cardiac masses, providing quantitative data that enhance tissue characterization. However, its use should be understood as adjunctive rather than in isolation, since definitive diagnosis requires integration with clinical findings, other MRI sequences, and additional imaging modalities, such as echocardiography and CT scans. This multimodal approach ensures greater accuracy in differentiating between tumors and pseudotumors, in addition to guiding safer therapeutic approaches.

11.5. Key Takeaways

- Cardiac masses pose a diagnostic challenge, and CMR is the most comprehensive method for their characterization;
- Most primary cardiac tumors are benign (≈90), with myxoma being the most common;
- Secondary/metastatic tumors are much more common than primary tumors (22–132 times more frequent);
- Even benign tumors can cause significant clinical impact (arrhythmias, obstruction, hemodynamic symptoms);

Table 12 – Tumor types and T1 map, T2 map, and extracellular volume findings

Author (year)	Mass type	N	Native T1	Native T2	ECV	Notes
Yue et al. (2023)[292]	Various (benign and malignant)	42	Variable; malignant > benign	High heterogeneity (malignant ↑)	Malignant tumors generally ↑; fibroma very high; lipoma ~0	Malignant tumors generally ↑; fibroma very high; lipoma ~0
Nasser et al. (2020)[291]	Myxoma	17	Elevated (vs. myocardium)	Elevated	Elevated (~40–45%)	Myxomas show a consistent increase in T1/T2/ECV
Haider et al. (2023)[295]	Benign (myxoma, fibroma, lipoma, hemangioma, rhabdomyoma)	N/A (narrative review)	Myxoma ↑; fibroma unchanged/↑; lipoma ↓	Myxoma ↑; fibroma low; lipoma ↑ (fatty)	Fibroma ↑↑; lipoma ~0	Review of parametric behavior in benign tumors
Saba et al. (2015)[296]	Various tumors (melanoma, myxoma, thrombus)	46	Melanoma ↑ (melanin); myxoma ↑; thrombus variable	Low for melanoma; high for myxoma; variable for thrombus	Not reported	Initial study demonstrating the applicability of the T1 map

ECV: extracellular volume, N/A: not applicable.

Table 13 – Typical T1/T2/extracellular volume values for cardiac masses – general

Mass type	Native T1 (ms)	Native T2 (ms)	ECV (%)	Characteristic pattern
Myxoma	~1500–1600 (↑)	~200 (↑)	~45 (↑)	Elevated across all maps – heterogeneous
Fibroma	~850–900 (↓/-)	reduced	~90 (↑↑)	ECV nearly 100%
Lipoma	~200–250 (↓↓)	High (fat)	zero	Predominance of fat; ECV zero
Rhabdomyoma	~1000 (~myocardium)	~myocardium	~23	No significant enhancement
Hemangioma	~1450 (↑)	slightly (↑)	~55	ECV close to blood
Paraganglioma	~1700 (↑)	~80 (↑)	Variable	High T1 and T2 – vascularity
Malignant tumors	~1,600 (↑)	~60–65 (↑)	~35 (↑)	Heterogeneous
Thrombus	reduced in chronic cases / elevated in acute cases	variable	~zero	No enhancement

ECV: extracellular volume.

- CMR allows integrated morphological, functional, and tissue-based assessment (T1/T2 maps, perfusion, and LGE);
- LGE helps assess composition (fibrosis/necrosis) and contributes to tumor differentiation;
- Native T1 map and ECV add value, especially in initial assessment and as a prognostic/follow-up tool (e.g., post-chemotherapy/radiotherapy);
- A CMR malignancy score ≥ 5 performs well in predicting malignancy;
- Parametric maps are becoming increasingly valuable, but they do not yet replace the multimodal approach – complementarity is essential.

12. Final Considerations

As discussed in this document, multiparametric CMR maps have established themselves as fundamental tools for myocardial tissue characterization, with sustained growth in practice and consistent support in the international scientific literature. Recent ESC guidelines and SCMR consensus

statements recognize the central role of T1, T2, and T2* mapping, as well as ECV, in the evaluation of various heart diseases, highlighting their ability to detect diffuse myocardial changes, act as adjuncts to LGE, and add diagnostic and prognostic value. Table 14 summarizes the main findings of this position statement.

Currently available mapping sequences have been technically and clinically validated, with good reproducibility and applicability across different platforms, which supports their progressive incorporation into clinical CMR protocols. In this context, the use of multiparametric maps should be encouraged in a rational and standardized manner, in accordance with international and national recommendations, and integrated with morphological, functional, and myocardial perfusion analysis, always guided by the clinical question.

`In the Brazilian context, the adoption of these methods must take into account the specific characteristics of the Unified Health System (SUS) and private health insurance. Multiparametric maps offer significant potential to refine diagnosis, reduce clinical uncertainties, and optimize risk stratification, contributing to a more efficient use of resources and more assertive therapeutic decision-making. This document aims to promote the use of these technologies in our country.

The limitations historically associated with multiparametric maps – including variability among manufacturers, differences in reference values, and greater technical complexity – have been progressively overcome through harmonization across platforms, the development of specific recommendations by scientific societies, and the expansion of expertise at national centers. This process has reduced barriers to implementation and increased the reliability of results.

The future outlook is made particularly promising by the incorporation of AI and machine learning techniques. These tools are expected to facilitate the automation of image acquisition and postprocessing, reduce inter-observer variability, enable integrated analysis of multiple parameters, and support the development of more accurate predictive models. Additionally, a positive impact is expected in reducing scan time and expanding access – aspects that are especially relevant to the Brazilian context.

Thus, multiparametric maps represent a cornerstone of contemporary CMR, with a growing and sustainable role in clinical practice. This position statement reinforces the importance of their structured use, aligned with international guidelines and adapted to the specific characteristics of the Brazilian health care system, with a focus on quality of care, patient safety, and enhanced clinical impact in different cardiovascular care settings.

Table 14 – Summary of the main findings of multiparametric maps in different pathological conditions

	T2*	T2	Native T1	ECV	Notes
Average normal values from international references (MOLLI sequence)	> 20 ms (1.5 T)	45–55 ms (1.5 T); 40–50 ms (3 T)	950–1050 ms (1.5 T); 1100–1250 ms (3 T)	> 30% (1.5 T); > 30% (3 T)	–
Acute ischemic heart disease	N/A	Increased in infarcted segments	Increased in infarcted segments	May be increased in advanced cases	In ACS, it may help identify the culprit artery
Chronic ischemic heart disease	N/A	Normal	Increased in infarcted segments. May be reduced in old infarcts (lipomatous metaplasia)	May be increased in advanced cases	Native T1 may be useful in patients who cannot receive gadolinium
Acute myocarditis	N/A	Increased	Generally increased in the acute phase	Often normal. May be increased in advanced cases	T2, T1, and ECV are associated with a higher risk of cardiovascular events (death, heart failure, transplantation, recurrence)
Sarcoidosis	N/A	Increased	Significantly increased (> 1150 at 1.5 T)	Often increased	Native T1 and T2 can be used for therapeutic monitoring
Chagas disease	N/A	Frequently increased	Increased	May be increased in advanced stages	T1 and ECV are associated with an increased risk of cardiovascular events

Iron overload	Reduced	N/A	Reduced	N/A	T2* can be used for therapeutic monitoring
Arrhythmogenic cardiomyopathy	N/A	Often normal. May be increased during "hot phases"	Increased	Often normal. May be increased in advanced cases	Increased ECV predicts sustained VT
Hypertrophic cardiomyopathy	N/A	May be increased	Regional enlargement	May be increased in advanced cases	Very useful in the differential diagnosis of phenocopies (amyloidosis, Fabry disease)
Cardiac amyloidosis	N/A	May be increased (mainly in AL)	Generally increased	Increased	ECV may be used for therapeutic monitoring
Fabry disease	N/A	May be increased in phase 2	Decreased in phases 1 and 2, mainly in the septum	Normal. May be increased in stage 3	A combination of the maps may indicate disease stages
Endomyocardial fibrosis	N/A	Often normal. May be increased in the intermediate stage (Löffler)	Regional apical elevation	Often normal	ECV may be a biomarker of diastolic dysfunction
Hypertensive heart disease	N/A	Normal	Often normal. May be increased in advanced stages	Often normal. May be increased in advanced stages	In advanced stages, there may be minor elevations in T1 and ECV compared to amyloidosis and HCM
Athlete's heart	N/A	Normal	Often normal. May be reduced in elite athletes	Normal	Very useful in the differential diagnosis of phenocopies (amyloidosis, HCM)

ACS: acute coronary syndrome; LC: light chain; ECV: extracellular volume; HCM: hypertrophic cardiomyopathy; N/A: not applicable; T: Tesla; VT: ventricular tachycardia.

References

1. Arbelo E, Protonotarios A, Gimeno JR, Arbustini E, Barriales-Villa R, Basso C, et al. 2023 ESC Guidelines for the Management of Cardiomyopathies. Eur Heart J. 2023;44(37):3503-626. doi: 10.1093/eurheartj/ehad194.
2. Magalhães TA, Carneiro ACC, Moreira VM, Trad HS, Lopes MMU, Cerci RJ, et al. Cardiovascular Computed Tomography and Magnetic Resonance Imaging Guideline of the Brazilian Society of Cardiology and the Brazilian College of Radiology - 2024. Arq Bras Cardiol. 2024;121(9):e20240608. doi: 10.36660/abc.20240608.
3. Mavrogeni S, Schwitter J, van Rossum A, Nijveldt R, Aletras A, Kolovou G, et al. Cardiac Magnetic Resonance Imaging in Myocardial Inflammation in Autoimmune Rheumatic Diseases: An Appraisal of the Diagnostic Strengths and Limitations of the Lake Louise Criteria. Int J Cardiol. 2018;252:216-9. doi: 10.1016/j.ijcard.2017.11.032.
4. Mavrogeni SI, Sfikakis PP, Markousis-Mavrogenis G, Bournia VK, Poulos G, Koutsogeorgopoulou L, et al. Cardiovascular Magnetic Resonance Imaging Pattern in Patients with Autoimmune Rheumatic Diseases and Ventricular Tachycardia with Preserved Ejection Fraction. Int J Cardiol. 2019;284:105-9. doi: 10.1016/j.ijcard.2018.10.067.
5. Messroghli DR, Moon JC, Ferreira VM, Grosse-Wortmann L, He T, Kellman P, et al. Clinical Recommendations for Cardiovascular Magnetic Resonance Mapping of T1, T2, T2* and Extracellular Volume: A Consensus Statement by the Society for Cardiovascular Magnetic Resonance (SCMR) Endorsed by the European Association for Cardiovascular Imaging (EACVI). J Cardiovasc Magn Reson. 2017;19(1):75. doi: 10.1186/s12968-017-0389-8.
6. Moon JC, Messroghli DR, Kellman P, Piechnik SK, Robson MD, Ugander M, et al. Myocardial T1 Mapping and Extracellular Volume Quantification: A Society for Cardiovascular Magnetic Resonance (SCMR) and CMR Working Group of the European Society of Cardiology consensus statement. J Cardiovasc Magn Reson. 2013;15(1):92. doi: 10.1186/1532-429X-15-92.
7. Ascione R, Giorgi M, Dell'Aversana S, Di Costanzo G, Nappi C, Imbriaco M, et al. The Additional Value of T1 Mapping in Cardiac Disease: State of the Art. Curr Cardiovasc Imaging Rep. 2024;17:1-19. doi: 10.1007/s12410-023-09588-y.
8. Messroghli DR, Radjenovic A, Kozerke S, Higgins DM, Sivananthan MU, Ridgway JP. Modified Look-Locker Inversion Recovery (MOLLI) for High-Resolution T1 Mapping of the Heart. Magn Reson Med. 2004;52(1):141-6. doi: 10.1002/mrm.20110.

9. Higgins DM, Moon JC. Review of T1 Mapping Methods: Comparative Effectiveness Including Reproducibility Issues. Curr Cardiovasc Imaging Rep. 2014;7(3):9252. doi: 10.1007/s12410-013-9252-y.

10. Kellman P, Hansen MS. T1-Mapping in the Heart: Accuracy and Precision. J Cardiovasc Magn Reson. 2014;16(1):2. doi: 10.1186/1532-429X-16-2.

11. Haaf P, Garg P, Messroghli DR, Broadbent DA, Greenwood JP, Plein S. Cardiac T1 Mapping and Extracellular Volume (ECV) in Clinical Practice: A Comprehensive Review. J Cardiovasc Magn Reson. 2016;18(1):89. doi: 10.1186/s12968-016-0308-4.

12. Puntmann VO, Peker E, Chandrashekhar Y, Nagel E. T1 Mapping in Characterizing Myocardial Disease: A Comprehensive Review. Circ Res. 2016;119(2):277-99. doi: 10.1161/CIRCRESAHA.116.307974.

13. Taylor AJ, Salerno M, Dharmakumar R, Jerosch-Herold M. T1 Mapping: Basic Techniques and Clinical Applications. JACC Cardiovasc Imaging. 2016;9(1):67-81. doi: 10.1016/j.jcmg.2015.11.005.

14. Robinson AA, Chow K, Salerno M. Myocardial T1 and ECV Measurement: Underlying Concepts and Technical Considerations. JACC Cardiovasc Imaging. 2019;12(11 Pt 2):2332-44. doi: 10.1016/j.jcmg.2019.06.031.

15. Roujol S, Weingärtner S, Foppa M, Chow K, Kawaji K, Ngo LH, et al. Accuracy, Precision, and Reproducibility of Four T1 Mapping Sequences: A Head-to-Head Comparison of MOLLI, ShMOLLI, SASHA, and SAPPHIRE. Radiology. 2014;272(3):683-9. doi: 10.1148/radiol.14140296.

16. Treibel TA, Fontana M, Maestrini V, Castelletti S, Rosmini S, Simpson J, et al. Automatic Measurement of the Myocardial Interstitium: Synthetic Extracellular Volume Quantification without Hematocrit Sampling. JACC Cardiovasc Imaging. 2016;9(1):54-63. doi: 10.1016/j.jcmg.2015.11.008.

17. Xue H, Shah S, Greiser A, Guetter C, Littmann A, Jolly MP, et al. Motion Correction for Myocardial T1 Mapping using Image Registration with Synthetic Image Estimation. Magn Reson Med. 2012;67(6):1644-55. doi: 10.1002/mrm.23153.

18. Roujol S, Foppa M, Weingärtner S, Manning WJ, Nezafat R. Adaptive Registration of Varying Contrast-Weighted Images for Improved Tissue Characterization (ARCTIC): Application to T1 Mapping. Magn Reson Med. 2015;73(4):1469-82. doi: 10.1002/mrm.25270.

19. Kranzusch R, Siepen FA, Wiesemann S, Zange L, Jeuthe S, Silva TF, et al. Z-Score Mapping for Standardized Analysis and Reporting of Cardiovascular Magnetic Resonance Modified Look-Locker Inversion Recovery (MOLLI) T1 Data: Normal Behavior and Validation in Patients with Amyloidosis. J Cardiovasc Magn Reson. 2020;22(1):6. doi: 10.1186/s12968-019-0595-7.

20. Naßenstein K, Nensa F, Schlosser T, Bruder O, Umutlu L, Lauenstein T, et al. Cardiac MRI: T2-Mapping versus T2-Weighted Dark-Blood TSE Imaging for Myocardial Edema Visualization in Acute Myocardial Infarction. Rofo. 2014;186(2):166-72. doi: 10.1055/s-0033-1350516.

21. Eichhorn C, Greulich S, Bucciarelli-Ducci C, Sznitman R, Kwong RY, Gräni C. Multiparametric Cardiovascular Magnetic Resonance Approach in Diagnosing, Monitoring, and Prognostication of Myocarditis. JACC Cardiovasc Imaging. 2022;15(7):1325-38. doi: 10.1016/j.jcmg.2021.11.017.

22. Dabir D, Luetkens J, Kuetting DLR, Feisst A, Isaak A, Schild HH, et al. Cardiac Magnetic Resonance Including Parametric Mapping in Acute Takotsubo Syndrome: Preliminary Findings. Eur J Radiol. 2019;113:217-24. doi: 10.1016/j.ejrad.2019.02.026.

23. Ojha V, Khurana R, Ganga KP, Kumar S. Advanced Cardiac Magnetic Resonance Imaging in Takotsubo Cardiomyopathy. Br J Radiol. 2020;93(1115):20200514. doi: 10.1259/bjr.20200514.

24. Haslbauer JD, Lindner S, Valbuena-Lopez S, Zainal H, Zhou H, D'Angelo T, et al. CMR Imaging Biosignature of Cardiac Involvement due to Cancer-Related Treatment by T1 and T2 Mapping. Int J Cardiol. 2019;275:179-86. doi: 10.1016/j.ijcard.2018.10.023.

25. Usman AA, Taimen K, Wasielewski M, McDonald J, Shah S, Giri S, et al. Cardiac Magnetic Resonance T2 Mapping in the Monitoring and Follow-Up of Acute Cardiac Transplant Rejection: A Pilot Study. Circ Cardiovasc Imaging. 2012;5(6):782-90. doi: 10.1161/CIRCIMAGING.111.971101.

26. Vermes E, Pantaléon C, Auvet A, Cazeneuve N, Machet MC, Delhommais A, et al. Cardiovascular Magnetic Resonance in Heart Transplant Patients: Diagnostic Value of Quantitative Tissue Markers: T2 Mapping and Extracellular Volume Fraction, for Acute Rejection Diagnosis. J Cardiovasc Magn Reson. 2018;20(1):59. doi: 10.1186/s12968-018-0480-9.

27. Giri S, Chung YC, Merchant A, Mihai G, Rajagopalan S, Raman SV, et al. T2 Quantification for Improved Detection of Myocardial Edema. J Cardiovasc Magn Reson. 2009;11(1):56. doi: 10.1186/1532-429X-11-56.

28. Thavendiranathan P, Walls M, Giri S, Verhaert D, Rajagopalan S, Moore S, et al. Improved Detection of Myocardial Involvement in Acute Inflammatory Cardiomyopathies using T2 Mapping. Circ Cardiovasc Imaging. 2012;5(1):102-10. doi: 10.1161/CIRCIMAGING.111.967836.

29. Kramer CM, Barkhausen J, Bucciarelli-Ducci C, Flamm SD, Kim RJ, Nagel E. Standardized Cardiovascular Magnetic Resonance Imaging (CMR) Protocols: 2020 Update. J Cardiovasc Magn Reson. 2020;22(1):17. doi: 10.1186/s12968-020-00607-1.

30. O'Brien AT, Gil KE, Varghese J, Simonetti OP, Zareba KM. T2 Mapping in Myocardial Disease: A Comprehensive Review. J Cardiovasc Magn Reson. 2022;24(1):33. doi: 10.1186/s12968-022-00866-0.

31. Huang TY, Liu YJ, Stemmer A, Poncelet BP. T2 Measurement of the Human Myocardium using a T2-Prepared Transient-State TrueFISP Sequence. Magn Reson Med. 2007;57(5):960-6. doi: 10.1002/mrm.21208.

32. Giri S, Shah S, Xue H, Chung YC, Pennell ML, Guehring J, et al. Myocardial T□ Mapping with Respiratory Navigator and Automatic Nonrigid Motion Correction. Magn Reson Med. 2012;68(5):1570-8. doi: 10.1002/mrm.24139.

33. Baeßler B, Schaarschmidt F, Stehning C, Schnackenburg B, Maintz D, Bunck AC. Cardiac T2-Mapping Using a Fast Gradient Echo Spin Echo Sequence - First in Vitro and in Vivo Experience. J Cardiovasc Magn Reson. 2015;17(1):67. doi: 10.1186/s12968-015-0177-2.

34. Schulz-Menger J, Bluemke DA, Bremerich J, Flamm SD, Fogel MA, Friedrich MG, et al. Standardized Image Interpretation and Post-Processing in Cardiovascular Magnetic Resonance - 2020 Update: Society for Cardiovascular Magnetic Resonance (SCMR): Board of Trustees Task Force on Standardized Post-Processing. J Cardiovasc Magn Reson. 2020;22(1):19. doi: 10.1186/s12968-020-00610-6.

35. Sprinkart AM, Luetkens JA, Träber F, Doerner J, Gieseke J, Schnackenburg B, et al. Gradient Spin Echo (GraSE) Imaging for Fast Myocardial T2 Mapping. J Cardiovasc Magn Reson. 2015;17(1):12. doi: 10.1186/s12968-015-0127-z.

36. Wiesmueller M, Wuest W, Heiss R, Treutlein C, Uder M, May MS. Cardiac T2 Mapping: Robustness and Homogeneity of Standardized in-Line Analysis. J Cardiovasc Magn Reson. 2020;22(1):39. doi: 10.1186/s12968-020-00619-x.

37. Wassmuth R, Prothmann M, Utz W, Dieringer M, von Knobelsdorff-Brenkenhoff F, Greiser A, et al. Variability and Homogeneity of Cardiovascular Magnetic Resonance Myocardial T2-Mapping in Volunteers Compared to Patients with Edema. J Cardiovasc Magn Reson. 2013;15(1):27. doi: 10.1186/1532-429X-15-27.

38. Carpenter JP, He T, Kirk P, Roughton M, Anderson LJ, Noronha SV, et al. On T2* Magnetic Resonance and Cardiac Iron. Circulation. 2011;123(14):1519-28. doi: 10.1161/CIRCULATIONAHA.110.007641.

39. Anderson LJ, Holden S, Davis B, Prescott E, Charrier CC, Bunce NH, et al. Cardiovascular T2-Star (T2*) Magnetic Resonance for the Early Diagnosis of Myocardial Iron Overload. Eur Heart J. 2001;22(23):2171-9. doi: 10.1053/euhj.2001.2822.

40. Marsella M, Borgna-Pignatti C, Meloni A, Caldarelli V, Dell'Amico MC, Spasiano A, et al. Cardiac Iron and Cardiac Disease in Males and Females with Transfusion-Dependent Thalassemia Major: A T2* Magnetic Resonance Imaging Study. Haematologica. 2011;96(4):515-20. doi: 10.3324/haematol.2010.025510.

41. Triadyaksa P, Oudkerk M, Sijens PE. Cardiac T2 * Mapping: Techniques and Clinical Applications. J Magn Reson Imaging. 2020;52(5):1340-51. doi: 10.1002/jmri.27023.

42. Pepe A, Meloni A, Rossi G, Midiri M, Missere M, Valeri G, et al. Prediction of Cardiac Complications for Thalassemia Major in the Widespread Cardiac Magnetic Resonance Era: A Prospective Multicentre Study By a Multi-Parametric Approach. Eur Heart J Cardiovasc Imaging. 2018;19(3):299-309. doi: 10.1093/ehjci/jex012.

43. Topriceanu CC, Pierce I, Moon JC, Captur G. T2 and T2′ Mapping and Weighted Imaging in Cardiac MRI. Magn Reson Imaging. 2022;93:15-32. doi: 10.1016/j.mri.2022.07.012.

44. Nazarova EE, Tereshchenko GV, Kupriyanov DA, Smetanina NS, Novichkova GA. Free-Breathing T2* Mapping for MR Myocardial Iron Assessment at 3 T. Eur Radiol Exp. 2020;4(1):25. doi: 10.1186/s41747-020-00156-3.

45. Ridgway JP. Cardiovascular Magnetic Resonance Physics for Clinicians: Part I. J Cardiovasc Magn Reson. 2010;12(1):71. doi: 10.1186/1532-429X-12-71.

46. He T. Cardiovascular Magnetic Resonance T2* for Tissue Iron Assessment in the Heart. Quant Imaging Med Surg. 2014;4(5):407-12. doi: 10.3978/j.issn.2223-4292.2014.10.05.

47. Zhang J, Nguyen TD, Solomon E, Li C, Zhang Q, Li J, et al. mcLARO: Multi-Contrast Learned Acquisition and Reconstruction Optimization for Simultaneous Quantitative Multi-Parametric Mapping. Magn Reson Med. 2024;91(1):344-56. doi: 10.1002/mrm.29854.

48. Atalay MK, Poncelet BP, Kantor HL, Brady TJ, Weisskoff RM. Cardiac Susceptibility Artifacts Arising from the Heart-Lung Interface. Magn Reson Med. 2001;45(2):341-5. doi: 10.1002/1522-2594(200102)45:2<341::aid-mrm1043>3.0.co;2-q.

49. Pereira TB, Balk M, Pereira GB, Ramos VS, Giordani L, Schvartzman PR, et al. Myocarditis: Whole Heart Involvement Revealed by Cardiac Magnetic Resonance Mapping. A Case-Control Study. ABC Heart Fail Cardiomyop. 2022;2(3):250-8. doi: 10.36660/abchf.20220075.

50. Hundley WG, Bluemke DA, Bogaert J, Flamm SD, Fontana M, Friedrich MG, et al. Society for Cardiovascular Magnetic Resonance (SCMR) Guidelines for Reporting Cardiovascular Magnetic Resonance Examinations. J Cardiovasc Magn Reson. 2022;24(1):29. doi: 10.1186/s12968-021-00827-z.

51. Kawel-Boehm N, Hetzel SJ, Ambale-Venkatesh B, Captur G, Chin CWL, François CJ, et al. Society for Cardiovascular Magnetic Resonance reference values ("Normal Values") in Cardiovascular Magnetic Resonance: 2025 Update. J Cardiovasc Magn Reson. 2025;27(1):101853. doi: 10.1016/j.jocmr.2025.101853.

52. Brown JJ, Peterson TM, Slutsky RA. Regional Myocardial Blood Flow, Edema Formation, and Magnetic Relaxation Times during Acute Myocardial Ischemia in the Canine. Invest Radiol. 1985;20(5):465-71. doi: 10.1097/00004424-198508000-00005.

53. O h-Ici D, Ridgway JP, Kuehne T, Berger F, Plein S, Sivananthan M, et al. Cardiovascular Magnetic Resonance of Myocardial Edema using a Short Inversion Time Inversion Recovery (STIR) Black-Blood Technique: Diagnostic Accuracy of Visual and Semi-Quantitative Assessment. J Cardiovasc Magn Reson. 2012;14(1):22. doi: 10.1186/1532-429X-14-22.

54. Tahir E, Sinn M, Bohnen S, Avanesov M, Säring D, Stehning C, et al. Acute versus Chronic Myocardial Infarction: Diagnostic Accuracy of Quantitative Native T1 and T2 Mapping versus Assessment of Edema on Standard T2-weighted Cardiovascular MR Images for Differentiation. Radiology. 2017;285(1):83-91. doi: 10.1148/radiol.2017162338.

55. Layland J, Rauhalammi S, Lee MM, Ahmed N, Carberry J, May VTY, et al. Diagnostic Accuracy of 3.0-T Magnetic Resonance T1 and T2 Mapping and T2-Weighted Dark-Blood Imaging for the Infarct-Related Coronary Artery in Non-ST-Segment Elevation Myocardial Infarction. J Am Heart Assoc. 2017;6(4):e004759. doi: 10.1161/JAHA.116.004759.

56. Berry C, Kellman P, Mancini C, Chen MY, Bandettini WP, Lowrey T, et al. Magnetic Resonance Imaging Delineates the Ischemic Area at Risk and Myocardial Salvage in Patients with Acute Myocardial Infarction. Circ Cardiovasc Imaging. 2010;3(5):527-35. doi: 10.1161/CIRCIMAGING.109.900761.

57. Bulluck H, White SK, Rosmini S, Bhuva A, Treibel TA, Fontana M, et al. T1 Mapping and T2 Mapping at 3T for Quantifying the Area-at-Risk in Reperfused STEMI Patients. J Cardiovasc Magn Reson. 2015;17(1):73. doi: 10.1186/s12968-015-0173-6.

58. Liu D, Borlotti A, Viliani D, Jerosch-Herold M, Alkhalil M, De Maria GL, et al. CMR Native T1 Mapping Allows Differentiation of Reversible versus Irreversible Myocardial Damage in ST-Segment-Elevation Myocardial Infarction: An OxAMI Study (Oxford Acute Myocardial Infarction). Circ Cardiovasc Imaging. 2017;10(8):e005986. doi: 10.1161/CIRCIMAGING.116.005986.

59. Dall'Armellina E, Piechnik SK, Ferreira VM, Si QL, Robson MD, Francis JM, et al. Cardiovascular Magnetic Resonance by Non Contrast T1-Mapping Allows Assessment of Severity of Injury in Acute Myocardial Infarction. J Cardiovasc Magn Reson. 2012;14(1):15. doi: 10.1186/1532-429X-14-15.

60. Hamirani YS, Wong A, Kramer CM, Salerno M. Effect of Microvascular Obstruction and Intramyocardial Hemorrhage by CMR on LV Remodeling and Outcomes after Myocardial Infarction: A Systematic Review and Meta-Analysis. JACC Cardiovasc Imaging. 2014;7(9):940-52. doi: 10.1016/j.jcmg.2014.06.012.

61. Bulluck H, Rosmini S, Abdel-Gadir A, Bhuva AN, Treibel TA, Fontana M, et al. Diagnostic Performance of T1 and T2 Mapping to Detect Intramyocardial Hemorrhage in Reperfused ST-Segment Elevation Myocardial Infarction (STEMI) Patients. J Magn Reson Imaging. 2017;46(3):877-86. doi: 10.1002/jmri.25638.

62. Chen Y, Ren D, Guan X, Yang HJ, Liu T, Tang R, et al. Quantification of Myocardial Hemorrhage using T2* Cardiovascular Magnetic Resonance at 1.5T with Ex-Vivo Validation. J Cardiovasc Magn Reson. 2021;23(1):104. doi: 10.1186/s12968-021-00779-4.

63. Virani SS, Newby LK, Arnold SV, Bittner V, Brewer LC, Demeter SH, et al. 2023 AHA/ACC/ACCP/ASPC/NLA/PCNA Guideline for the Management of Patients with Chronic Coronary Disease: A Report of the American Heart Association/American College of Cardiology Joint Committee on Clinical Practice Guidelines. Circulation. 2023;148(9):e9-e119. doi: 10.1161/CIR.0000000000001168.

64. Ricci F, Khanji MY, Bisaccia G, Cipriani A, Di Cesare A, Ceriello L, et al. Diagnostic and Prognostic Value of Stress Cardiovascular Magnetic Resonance Imaging in Patients with Known or Suspected Coronary Artery Disease: A Systematic Review and Meta-Analysis. JAMA Cardiol. 2023;8(7):662-73. doi: 10.1001/jamacardio.2023.1290.

65. Messroghli DR, Walters K, Plein S, Sparrow P, Friedrich MG, Ridgway JP, et al. Myocardial T1 Mapping: Application to Patients with Acute and Chronic Myocardial Infarction. Magn Reson Med. 2007;58(1):34-40. doi: 10.1002/mrm.21272.

66. Kaolawanich Y, Azevedo CF, Kim HW, Jenista ER, Wendell DC, Chen EL, et al. Native T1 Mapping for the Diagnosis of Myocardial Fibrosis in Patients with Chronic Myocardial Infarction. JACC Cardiovasc Imaging. 2022;15(12):2069-79. doi: 10.1016/j.jcmg.2022.09.011.

67. Bauner KU, Biffar A, Theisen D, Greiser A, Zech CJ, Nguyen ET, et al. Extracellular Volume Fractions in Chronic Myocardial Infarction. Invest Radiol. 2012;47(9):538-45. doi: 10.1097/RLI.0b013e3182631c37.

68. Kim RJ, Shah DJ, Judd RM. How we Perform Delayed Enhancement Imaging. J Cardiovasc Magn Reson. 2003;5(3):505-14. doi: 10.1081/jcmr-120022267.

69. Zhang Q, Burrage MK, Shanmuganathan M, Gonzales RA, Lukaschuk E, Thomas KE, et al. Artificial Intelligence for Contrast-Free MRI: Scar Assessment in Myocardial Infarction using Deep Learning-Based Virtual Native Enhancement. Circulation. 2022;146(20):1492-503. doi: 10.1161/CIRCULATIONAHA.122.060137.

70. Puntmann VO, Carr-White G, Jabbour A, Yu CY, Gebker R, Kelle S, et al. Native T1 and ECV of Noninfarcted Myocardium and Outcome in Patients with Coronary Artery Disease. J Am Coll Cardiol. 2018;71(7):766-78. doi: 10.1016/j.jacc.2017.12.020.

71. Yang EY, Ghosn MG, Khan MA, Gramze NL, Brunner G, Nabi F, et al. Myocardial Extracellular Volume Fraction Adds Prognostic Information Beyond Myocardial Replacement Fibrosis. Circ Cardiovasc Imaging. 2019;12(12):e009535. doi: 10.1161/CIRCIMAGING.119.009535.

72. McCommis KS, Goldstein TA, Abendschein DR, Misselwitz B, Pilgram T, Gropler RJ, et al. Roles of Myocardial Blood Volume and Flow in Coronary Artery Disease: An Experimental MRI Study at Rest and during Hyperemia. Eur Radiol. 2010;20(8):2005-12. doi: 10.1007/s00330-010-1740-8.

73. Mahmod M, Piechnik SK, Levelt E, Ferreira VM, Francis JM, Lewis A, et al. Adenosine Stress Native T1 Mapping in Severe Aortic Stenosis: Evidence for a Role of the Intravascular Compartment on Myocardial T1 Values. J Cardiovasc Magn Reson. 2014;16(1):92. doi: 10.1186/s12968-014-0092-y.

74. Liu A, Wijesurendra RS, Francis JM, Robson MD, Neubauer S, Piechnik SK, et al. Adenosine Stress and Rest T1 Mapping Can Differentiate Between Ischemic, Infarcted, Remote, and Normal Myocardium without the Need for Gadolinium Contrast Agents. JACC Cardiovasc Imaging. 2016;9(1):27-36. doi: 10.1016/j.jcmg.2015.08.018.

75. Nakamori S, Fahmy A, Jang J, El-Rewaidy H, Neisius U, Berg S, et al. Changes in Myocardial Native T1 and T2 after Exercise Stress: A Noncontrast CMR Pilot Study. JACC Cardiovasc Imaging. 2020;13(3):667-80. doi: 10.1016/j.jcmg.2019.05.019.

76. Levelt E, Piechnik SK, Liu A, Wijesurendra RS, Mahmod M, Ariga R, et al. Adenosine Stress CMR T1-Mapping Detects Early Microvascular Dysfunction in Patients with Type 2 Diabetes Mellitus without Obstructive Coronary Artery Disease. J Cardiovasc Magn Reson. 2017;19(1):81. doi: 10.1186/s12968-017-0397-8.

77. Piechnik SK, Neubauer S, Ferreira VM. State-Of-The-Art Review: Stress T1 Mapping-Technical Considerations, Pitfalls and Emerging Clinical Applications. MAGMA. 2018;31(1):131-41. doi: 10.1007/s10334-017-0649-5.

78. Melo RJL, Assunção AN Jr, Morais TC, Nomura CH, Scanavacca MI, Martinelli-Filho M, et al. Detection of Early Diffuse Myocardial Fibrosis and Inflammation in Chagas Cardiomyopathy with T1 Mapping and Extracellular Volume. Radiol Cardiothorac Imaging. 2023;5(3):e220112. doi: 10.1148/ryct.220112.

79. Torreão JA, Ianni BM, Mady C, Naia E, Rassi CH, Nomura C, et al. Myocardial Tissue Characterization in Chagas' Heart Disease by Cardiovascular Magnetic Resonance. J Cardiovasc Magn Reson. 2015;17:97. doi: 10.1186/s12968-015-0200-7.

80. Sousa AS, Derenne ME, Hasslocher-Moreno AM, Xavier SS, Gottlieb I. Myocardial Edema without Fibrosis by Magnetic Resonance T2 Mapping in Acute Chagas' Myocarditis. Arq Bras Cardiol. 2017;109(4):378-9. doi: 10.5935/abc.20170113.

81. Marin-Neto JA, Rassi A Jr, Oliveira GMM, Correia LCL, Ramos AN Jr, Luquetti AO, et al. SBC Guideline on the Diagnosis and Treatment of Patients with Cardiomyopathy of Chagas Disease - 2023. Arq Bras Cardiol. 2023;120(6):e20230269. doi: 10.36660/abc.20230269.

82. Silva S, Barros MV, Nunes MD, Silva L, Edvardsen T, Araujo F, et al. Abstract 11768: Regression of Inflammation by Cardiac Magnetic Resonance in Chronic Chagasic Patients Treated with Benznidazole. Circulation. 2023;148(Suppl 1):A11768-A. doi: 10.1161/circ.148.suppl_1.11768.

83. Lima PE, Silva RC, Fernandes AMS, Menezes MS, Camara EJN. Myocardial Deformation (Strain) and Myocardial Fibrosis in Mild Cardiac Chagas Disease. Arq Bras Cardiol: Imagem Cardiovasc. 2021;34(3):eabc173. doi: 10.47593/2675-312X/20213403eabc173.

84. Pinheiro MVT, Moll-Bernardes RJ, Camargo GC, Siqueira FP, Azevedo CF, Holanda MT, et al. Associations between Cardiac Magnetic Resonance T1 Mapping Parameters and Ventricular Arrhythmia in Patients with Chagas Disease. Am J Trop Med Hyg. 2020;103(2):745-51. doi: 10.4269/ajtmh.20-0122.

85. Montera MW, Marcondes-Braga FG, Simões MV, Moura LAZ, Fernandes F, Mangine S, et al. Brazilian Society of Cardiology Guideline on Myocarditis - 2022. Arq Bras Cardiol. 2022;119(1):143-211. doi: 10.36660/abc.20220412.

86. Friedrich MG, Sechtem U, Schulz-Menger J, Holmvang G, Alakija P, Cooper LT, et al. Cardiovascular Magnetic Resonance in Myocarditis: A JACC White Paper. J Am Coll Cardiol. 2009;53(17):1475-87. doi: 10.1016/j.jacc.2009.02.007.

87. Ferreira VM, Schulz-Menger J, Holmvang G, Kramer CM, Carbone I, Sechtem U, et al. Cardiovascular Magnetic Resonance in Nonischemic Myocardial Inflammation: Expert Recommendations. J Am Coll Cardiol. 2018;72(24):3158-76. doi: 10.1016/j.jacc.2018.09.072.

88. Ferreira VM, Piechnik SK, Dall'Armellina E, Karamitsos TD, Francis JM, Choudhury RP, et al. Non-Contrast T1-Mapping Detects Acute Myocardial Edema with High Diagnostic Accuracy: A Comparison to T2-Weighted Cardiovascular Magnetic Resonance. J Cardiovasc Magn Reson. 2012;14(1):42. doi: 10.1186/1532-429X-14-42.

89. Bohnen S, Radunski UK, Lund GK, Kandolf R, Stehning C, Schnackenburg B, et al. Performance of T1 and T2 Mapping Cardiovascular Magnetic Resonance to Detect Active Myocarditis in Patients with Recent-Onset Heart Failure. Circ Cardiovasc Imaging. 2015;8(6):e003073. doi: 10.1161/CIRCIMAGING.114.003073.

90. Kotanidis CP, Bazmpani MA, Haidich AB, Karvounis C, Antoniades C, Karamitsos TD. Diagnostic Accuracy of Cardiovascular Magnetic Resonance in Acute Myocarditis: A Systematic Review and Meta-Analysis. JACC Cardiovasc Imaging. 2018;11(11):1583-90. doi: 10.1016/j.jcmg.2017.12.008.

91. Lurz P, Luecke C, Eitel I, Föhrenbach F, Frank C, Grothoff M, et al. Comprehensive Cardiac Magnetic Resonance Imaging in Patients with Suspected Myocarditis: The MyoRacer-Trial. J Am Coll Cardiol. 2016;67(15):1800-11. doi: 10.1016/j.jacc.2016.02.013.

92. Zhang L, Awadalla M, Mahmood SS, Nohria A, Hassan MZO, Thuny F, et al. Cardiovascular Magnetic Resonance in Immune Checkpoint Inhibitor-Associated Myocarditis. Eur Heart J. 2020;41(18):1733-43. doi: 10.1093/eurheartj/ehaa051.

93. Thavendiranathan P, Zhang L, Zafar A, Drobni ZD, Mahmood SS, Cabral M, et al. Myocardial T1 and T2 Mapping by Magnetic Resonance in Patients with Immune Checkpoint Inhibitor-Associated Myocarditis. J Am Coll Cardiol. 2021;77(12):1503-16. doi: 10.1016/j.jacc.2021.01.050.

94. Gräni C, Bière L, Eichhorn C, Kaneko K, Agarwal V, Aghayev A, et al. Incremental Value of Extracellular Volume Assessment by Cardiovascular Magnetic Resonance Imaging in Risk Stratifying Patients with Suspected Myocarditis. Int J Cardiovasc Imaging. 2019;35(6):1067-78. doi: 10.1007/s10554-019-01552-6.

95. Wang Y, Duan X, Zhu L, Xu J, Zhou D, Yang W, et al. Prognostic Value of Myocardial Parametric Mapping in Patients with Acute Myocarditis: A Retrospective Study. Radiol Cardiothorac Imaging. 2025;7(1):e240125. doi: 10.1148/ryct.240125.

96. Chavhan GB, Babyn PS, Thomas B, Shroff MM, Haacke EM. Principles, Techniques, and Applications of T2*-Based MR Imaging and its Special Applications. Radiographics. 2009;29(5):1433-49. doi: 10.1148/rg.295095034.

97. Anderson LJ, Wonke B, Prescott E, Holden S, Walker JM, Pennell DJ. Comparison of Effects of Oral Deferiprone and Subcutaneous Desferrioxamine on Myocardial Iron Concentrations and Ventricular Function in Beta-Thalassaemia. Lancet. 2002;360(9332):516-20. doi: 10.1016/s0140-6736(02)09740-4.

98. Kirk P, Roughton M, Porter JB, Walker JM, Tanner MA, Patel J, et al. Cardiac T2* Magnetic Resonance for Prediction of Cardiac Complications in Thalassemia Major. Circulation. 2009;120(20):1961-8. doi: 10.1161/CIRCULATIONAHA.109.874487.

99. Tanner MA, Galanello R, Dessi C, Smith GC, Westwood MA, Agus A, et al. A Randomized, Placebo-Controlled, Double-Blind Trial of the Effect of Combined Therapy with Deferoxamine and Deferiprone on Myocardial Iron in Thalassemia Major using Cardiovascular Magnetic Resonance. Circulation. 2007;115(14):1876-84. doi: 10.1161/CIRCULATIONAHA.106.648790.

100. Alam MH, Auger D, McGill LA, Smith GC, He T, Izgi C, et al. Comparison of 3 T and 1.5 T for T2* Magnetic Resonance of Tissue Iron. J Cardiovasc Magn Reson. 2016;18(1):40. doi: 10.1186/s12968-016-0259-9.

101. Sado DM, White SK, Piechnik SK, Banypersad SM, Treibel T, Captur G, et al. Identification and Assessment of Anderson-Fabry Disease by Cardiovascular Magnetic Resonance Noncontrast Myocardial T1 Mapping. Circ Cardiovasc Imaging. 2013;6(3):392-8. doi: 10.1161/CIRCIMAGING.112.000070.

102. Sado DM, Maestrini V, Piechnik SK, Banypersad SM, White SK, Flett AS, et al. Noncontrast Myocardial T1 Mapping using Cardiovascular Magnetic Resonance for Iron Overload. J Magn Reson Imaging. 2015;41(6):1505-11. doi: 10.1002/jmri.24727.

103. Hunninghake GW, Costabel U, Ando M, Baughman R, Cordier JF, du Bois R, et al. ATS/ERS/WASOG Statement on Sarcoidosis. American Thoracic Society/European Respiratory Society/World Association of Sarcoidosis and other Granulomatous Disorders. Sarcoidosis Vasc Diffuse Lung Dis. 1999;16(2):149-73.

104. Kouranos V, Sharma R. Cardiac Sarcoidosis: State-Of-The-Art Review. Heart. 2021;107(19):1591-9. doi: 10.1136/heartjnl-2019-316442.

105. Silverman KJ, Hutchins GM, Bulkley BH. Cardiac Sarcoid: A Clinicopathologic Study of 84 Unselected Patients with Systemic Sarcoidosis. Circulation. 1978;58(6):1204-11. doi: 10.1161/01.cir.58.6.1204.

106. Trivieri MG, Spagnolo P, Birnie D, Liu P, Drake W, Kovacic JC, et al. Challenges in Cardiac and Pulmonary Sarcoidosis: JACC State-of-the-Art Review. J Am Coll Cardiol. 2020;76(16):1878-901. doi: 10.1016/j.jacc.2020.08.042.

107. Yeboah J, Lee C, Sharma OP. Cardiac Sarcoidosis: A Review 2011. Curr Opin Pulm Med. 2011;17(5):308-15. doi: 10.1097/MCP.0b013e328349637a.

108. Birnie DH, Kandolin R, Nery PB, Kupari M. Cardiac Manifestations of Sarcoidosis: Diagnosis and Management. Eur Heart J. 2017;38(35):2663-70. doi: 10.1093/eurheartj/ehw328.

109. Drent M, Crouser ED, Grunewald J. Challenges of Sarcoidosis and Its Management. N Engl J Med. 2021;385(11):1018-32. doi: 10.1056/NEJMra2101555.

110. Hutt E, Brizneda MPV, Jellis CL, Ribeiro ML Neto, Jaber WA, Cremer PC. Discordant Cardiac Inflammation between 18F-FDG PET and CMR in Patients with Cardiac Sarcoidosis. EJNMMI Rep. 2024;8(1):31. doi: 10.1186/s41824-024-00218-4.

111. Cheng RK, Kittleson MM, Beavers CJ, Birnie DH, Blankstein R, Bravo PE, et al. Diagnosis and Management of Cardiac Sarcoidosis: A Scientific Statement from the American Heart Association. Circulation. 2024;149(21):e1197-216. doi: 10.1161/CIR.0000000000001240.

112. Nita N, Felbel D, Melnic R, Paukovitsch M, Rottbauer W, Buckert D, et al. Predictors of Poor Long-Term Outcomes in Patients with Newly Diagnosed Asymptomatic Cardiac Sarcoidosis: A Cardiovascular Magnetic Resonance Study. Biomedicines. 2025;13(5):1093. doi: 10.3390/biomedicines13051093.

113. Mushari NA, Soultanidis G, Duff L, Trivieri MG, Fayad ZA, Robson P, et al. An Assessment of PET and CMR Radiomic Features for the Detection of Cardiac Sarcoidosis. Front Nucl Med. 2024;4:1324698. doi: 10.3389/fnume.2024.1324698.

114. Dabir D, Luetkens J, Kuetting D, Nadal J, Schild HH, Thomas D. Myocardial Mapping in Systemic Sarcoidosis: A Comparison of Two Measurement Approaches. Rofo. 2021;193(1):68-76. doi: 10.1055/a-1174-0537.

115. Aitken M, Chan MV, Fresno CU, Farrell A, Islam N, McInnes MDF, et al. Diagnostic Accuracy of Cardiac MRI versus FDG PET for Cardiac Sarcoidosis: A Systematic Review and Meta-Analysis. Radiology. 2022;304(3):566-79. doi: 10.1148/radiol.213170.

116. Snel GJH, van den Boomen M, Hernandez LM, Nguyen CT, Sosnovik DE, Velthuis BK, et al. Cardiovascular Magnetic Resonance Native T2 and T2* Quantitative Values for Cardiomyopathies and Heart Transplantations: A Systematic Review and Meta-Analysis. J Cardiovasc Magn Reson. 2020;22(1):34. doi: 10.1186/s12968-020-00627-x.

117. Greulich S, Kitterer D, Latus J, Aguor E, Steubing H, Kaesemann P, et al. Comprehensive Cardiovascular Magnetic Resonance Assessment in Patients with Sarcoidosis and Preserved Left Ventricular Ejection Fraction. Circ Cardiovasc Imaging. 2016;9(11):e005022. doi: 10.1161/CIRCIMAGING.116.005022.

118. Chamberlin JH, Kocher MR, Aquino G, Fullenkamp A, Dennis DJ, Waltz J, et al. Quantitative Myocardial T2 Mapping Adds Value to Japanese Circulation Society Diagnostic Criteria for Active Cardiac Sarcoidosis. Int J Cardiovasc Imaging. 2023;39(8):1535-46. doi: 10.1007/s10554-023-02863-5.

119. Oyama-Manabe N, Manabe O, Aikawa T, Sobue Y, Asakura R. Updates on Cardiac MRI and PET Imaging for the Diagnosis and Monitoring of Cardiac Sarcoidosis. Korean J Radiol. 2025;26(9):804-16. doi: 10.3348/kjr.2025.0148.

120. Treiber J, Novak D, Fischer-Rasokat U, Wolter JS, Kriechbaum S, Weferling M, et al. Regional Extracellular Volume within Late Gadolinium Enhancement-Positive Myocardium to Differentiate Cardiac Sarcoidosis from Myocarditis of other Etiology: A Cardiovascular Magnetic Resonance Study. J Cardiovasc Magn Reson. 2023;25(1):8. doi: 10.1186/s12968-023-00918-z.

121. Treiber JM, Wolter JS, Backhaus SJ, Siefert EP, Rieth A, Kriechbaum SD, et al. Serial Cardiac Magnetic Resonance Imaging to Assess Myocardial Inflammation in PET-Positive Cardiac Sarcoidosis Under Immunomodulatory Therapy: A Retrospective Observational Study. BMJ Open. 2025;15(8):e098540. doi: 10.1136/bmjopen-2024-098540.

122. Cheung E, Ahmad S, Aitken M, Chan R, Iwanochko RM, Balter M, et al. Combined Simultaneous FDG-PET/MRI with T1 and T2 Mapping as an Imaging Biomarker for the Diagnosis and Prognosis of Suspected Cardiac Sarcoidosis. Eur J Hybrid Imaging. 2021;5(1):24. doi: 10.1186/s41824-021-00119-w.

123. Vanchin B, Ka MM, Arendt CT, Escher F, Nagel E, Puntmann VO. Myocardial Tissue Changes Detected by Cardiac MRI in a Patient with Suspected Systemic Sarcoidosis. BMC Cardiovasc Disord. 2023;23(1):131. doi: 10.1186/s12872-023-03133-x.

124. Le JV, Mendes JK, McKibben N, Wilson BD, Ibrahim M, DiBella EVR, et al. Accelerated Cardiac T1 Mapping with Recurrent Networks and Cyclic, Model-Based Loss. Med Phys. 2022;49(11):6986-7000. doi: 10.1002/mp.15801.

125. Corrado D, Anastasakis A, Basso C, Bauce B, Blomström-Lundqvist C, Bucciarelli-Ducci C, et al. Proposed Diagnostic Criteria for Arrhythmogenic Cardiomyopathy: European Task Force Consensus Report. Int J Cardiol. 2024;395:131447. doi: 10.1016/j.ijcard.2023.131447.

126. McKenna WJ, Thiene G, Nava A, Fontaliran F, Blomstrom-Lundqvist C, Fontaine G, et al. Diagnosis of Arrhythmogenic Right Ventricular Dysplasia/Cardiomyopathy. Task Force of the Working Group Myocardial and Pericardial Disease of the European Society of Cardiology and of the Scientific Council on Cardiomyopathies of the International Society and Federation of Cardiology. Br Heart J. 1994;71(3):215-8. doi: 10.1136/hrt.71.3.215.

127. Marcus FI, McKenna WJ, Sherrill D, Basso C, Bauce B, Bluemke DA, et al. Diagnosis of Arrhythmogenic Right Ventricular Cardiomyopathy/Dysplasia: Proposed Modification of the Task Force Criteria. Circulation. 2010;121(13):1533-41. doi: 10.1161/CIRCULATIONAHA.108.840827.

128. Miles C, Finocchiaro G, Papadakis M, Gray B, Westaby J, Ensam B, et al. Sudden Death and Left Ventricular Involvement in Arrhythmogenic Cardiomyopathy. Circulation. 2019;139(15):1786-97. doi: 10.1161/CIRCULATIONAHA.118.037230.

129. Corrado D, Perazzolo Marra M, Zorzi A, Beffagna G, Cipriani A, et al. Diagnosis of Arrhythmogenic Cardiomyopathy: The Padua Criteria. Int J Cardiol. 2020;319:106-14. doi: 10.1016/j.ijcard.2020.06.005.

130. Paudel B, Pan J, Singulane CC, Wang S, Thomas M, Ayers M, et al. Cardiac Magnetic Resonance Guidance for the Pathogenetic Definition of Cardiomyopathies. Curr Cardiol Rep. 2025;27(1):85. doi: 10.1007/s11886-025-02233-8.

131. Cipriani A, Mattesi G, Bariani R, Cecere A, Martini N, De Michieli L, et al. Cardiac Magnetic Resonance Imaging of Arrhythmogenic Cardiomyopathy: Evolving Diagnostic Perspectives. Eur Radiol. 2023;33(1):270-82. doi: 10.1007/s00330-022-08958-2.

132. Bourfiss M, Prakken NHJ, van der Heijden JF, Kamel I, Zimmerman SL, Asselbergs FW, et al. Diagnostic Value of Native T1 Mapping in Arrhythmogenic Right Ventricular Cardiomyopathy. JACC Cardiovasc Imaging. 2019;12(8 Pt 1):1580-2. doi: 10.1016/j.jcmg.2019.01.023.

133. Georgiopoulos G, Zampieri M, Molaro S, Chaloupka A, Aimo A, Barra B, et al. Cardiac Magnetic Resonance in Patients with ARVC and Family Members: The Potential Role of Native T1 Mapping. Int J Cardiovasc Imaging. 2021;37(6):2037-47. doi: 10.1007/s10554-021-02166-7.

134. Lu G, Cao L, Ye W, Wei X, Xie J, Du Z, et al. Incremental Prognostic Value of Cardiac MRI Feature Tracking and T1 Mapping in Arrhythmogenic Right Ventricular Cardiomyopathy. Radiol Cardiothorac Imaging. 2024;6(5):e230430. doi: 10.1148/ryct.230430.

135. Bariani R, Cipriani A, Rizzo S, Celeghin R, Marinas MB, Giorgi B, et al. 'Hot Phase' Clinical Presentation in Arrhythmogenic Cardiomyopathy. Europace. 2021;23(6):907-17. doi: 10.1093/europace/euaa343.

136. Beltran-Lopez F, Guerra EC, Luna-Alcala S, Garcia-Cardenas M, Espinola-Zavaleta N. Structural Evaluation in Arrhythmogenic Right Ventricular Cardiomyopathy: Should T1 Mapping be a New Criteria? Eur Heart J Cardiovasc Imaging. 2023;24(10):e290. doi: 10.1093/ehjci/jead194.

137. Graziano F, Zorzi A, Cipriani A, Bauce B, Rigato I, Marra MP, et al. Contemporary Diagnostic Approach to Arrhythmogenic Cardiomyopathy: The Three-Step Work-Up. Trends Cardiovasc Med. 2025;35(2):107-13. doi: 10.1016/j.tcm.2024.09.002.

138. Leiner T, Bogaert J, Friedrich MG, Mohiaddin R, Muthurangu V, Myerson S, et al. SCMR Position Paper (2020) on Clinical Indications for Cardiovascular Magnetic Resonance. J Cardiovasc Magn Reson. 2020;22(1):76. doi: 10.1186/s12968-020-00682-4.

139. Corrado D, Thiene G, Bauce B, Calore C, Cipriani A, De Lazzari M, et al. The "Padua Classification" of Cardiomyopathies: Combining Pathobiological Basis and Morpho-Functional Remodeling. Int J Cardiol. 2025;418:132571. doi: 10.1016/j.ijcard.2024.132571.

140. Husereau D, Drummond M, Augustovski F, Briggs AH, Carswell C, Caulley L, et al. Consolidated Health Economic Evaluation Reporting Standards 2022 (CHEERS 2022) Statement: Updated Reporting Guidance for Health Economic Evaluations. BJOG. 2022;129(3):336-44. doi: 10.1111/1471-0528.17012.

141. Xu J, Zhuang B, Sirajuddin A, Li S, Huang J, Yin G, et al. MRI T1 Mapping in Hypertrophic Cardiomyopathy: Evaluation in Patients without Late Gadolinium Enhancement and Hemodynamic Obstruction. Radiology. 2020;294(2):275-86. doi: 10.1148/radiol.2019190651.

142. Chan RH, Maron BJ, Olivotto I, Pencina MJ, Assenza GE, Haas T, et al. Prognostic Value of Quantitative Contrast-Enhanced Cardiovascular Magnetic Resonance for the Evaluation of Sudden Death Risk in Patients with Hypertrophic Cardiomyopathy. Circulation. 2014;130(6):484-95. doi: 10.1161/CIRCULATIONAHA.113.007094.

143. Liang L, Wang X, Yu Y, Zhang Y, Liu J, Chen M, et al. T1 Mapping and Extracellular Volume in Cardiomyopathy Showing Left Ventricular Hypertrophy: Differentiation Between Hypertrophic Cardiomyopathy and Hypertensive Heart Disease. Int J Gen Med. 2022;15:4163-73. doi: 10.2147/IJGM.S350673.

144. Moura B, Aimo A, Al-Mohammad A, Keramida K, Ben Gal T, Dorbala S, et al. Diagnosis and Management of Patients with Left Ventricular Hypertrophy: Role of Multimodality Cardiac Imaging. A Scientific Statement of the Heart Failure Association of the European Society of Cardiology. Eur J Heart Fail. 2023;25(9):1493-506. doi: 10.1002/ejhf.2997.

145. Puntmann VO, Voigt T, Chen Z, Mayr M, Karim R, Rhode K, et al. Native T1 Mapping in Differentiation of Normal Myocardium from Diffuse Disease in Hypertrophic and Dilated Cardiomyopathy. JACC Cardiovasc Imaging. 2013;6(4):475-84. doi: 10.1016/j.jcmg.2012.08.019.

146. Hinojar R, Varma N, Child N, Goodman B, Jabbour A, Yu CY, et al. T1 Mapping in Discrimination of Hypertrophic Phenotypes: Hypertensive Heart Disease and Hypertrophic Cardiomyopathy: Findings from the International T1 Multicenter Cardiovascular Magnetic Resonance Study. Circ Cardiovasc Imaging. 2015;8(12):e003285. doi: 10.1161/CIRCIMAGING.115.003285.

147. Wang J, Zhang J, Liu W, Pu L, Qi W, Xu Y, et al. Prognostic Value of Myocardial T1 Mapping for Predicting Adverse Events in Hypertrophic Cardiomyopathy. Circ Cardiovasc Imaging. 2025;18(3):e017174. doi: 10.1161/CIRCIMAGING.124.017174.

148. Swoboda PP, McDiarmid AK, Erhayiem B, Broadbent DA, Dobson LE, Garg P, et al. Assessing Myocardial Extracellular Volume by T1 Mapping to Distinguish Hypertrophic Cardiomyopathy From Athlete's Heart. J Am Coll Cardiol. 2016;67(18):2189-90. doi: 10.1016/j.jacc.2016.02.054.

149. O'Hara RP, Prakosa A, Binka E, Lacy A, Trayanova NA. Arrhythmia in Hypertrophic Cardiomyopathy: Risk Prediction using Contrast Enhanced MRI, T1 Mapping, and Personalized Virtual Heart Technology. J Electrocardiol. 2022;74:122-7. doi: 10.1016/j.jelectrocard.2022.09.004.

150. Huang L, Ran L, Zhao P, Tang D, Han R, Ai T, et al. MRI Native T1 and T2 Mapping of Myocardial Segments in Hypertrophic Cardiomyopathy: Tissue Remodeling Manifested Prior to Structure Changes. Br J Radiol. 2019;92(1104):20190634. doi: 10.1259/bjr.20190634.

151. Xu Z, Wang J, Cheng W, Wan K, Li W, Pu L, et al. Incremental Significance of Myocardial Oedema for Prognosis in Hypertrophic Cardiomyopathy. Eur Heart J Cardiovasc Imaging. 2023;24(7):876-84. doi: 10.1093/ehjci/jead065.

152. Brodov Y, Kirshenboim Z, Fardman A, Shagraui R, Sabbag A, Konen E, et al. T2 Mapping Cardiovascular Magnetic Resonance Is an Independent Predictor of Adverse Outcome in Hypertrophic Cardiomyopathy. Cardiology. 2025:1-8. doi: 10.1159/000547262.

153. Warnica W, Al-Arnawoot A, Stanimirovic A, Thavendiranathan P, Wald RM, Pakkal M, et al. Clinical Impact of Cardiac MRI T1 and T2 Parametric Mapping in Patients with Suspected Cardiomyopathy. Radiology. 2022;305(2):319-26. doi: 10.1148/radiol.220067.

154. Karamitsos TD, Piechnik SK, Banypersad SM, Fontana M, Ntusi NB, Ferreira VM, et al. Noncontrast T1 Mapping for the Diagnosis of Cardiac Amyloidosis. JACC Cardiovasc Imaging. 2013;6(4):488-97. doi: 10.1016/j.jcmg.2012.11.013.

155. Baggiano A, Boldrini M, Martinez-Naharro A, Kotecha T, Petrie A, Rezk T, et al. Noncontrast Magnetic Resonance for the Diagnosis of Cardiac Amyloidosis. JACC Cardiovasc Imaging. 2020;13(1 Pt 1):69-80. doi: 10.1016/j.jcmg.2019.03.026.

156. Wang TKM, Brizneda MV, Kwon DH, Popovic ZB, Flamm SD, Hanna M, et al. Reference Ranges, Diagnostic and Prognostic Utility of Native T1 Mapping and Extracellular Volume for Cardiac Amyloidosis: A Meta-Analysis. J Magn Reson Imaging. 2021;53(5):1458-68. doi: 10.1002/jmri.27459.

157. Pan JA, Kerwin MJ, Salerno M. Native T1 Mapping, Extracellular Volume Mapping, and Late Gadolinium Enhancement in Cardiac Amyloidosis: A Meta-Analysis. JACC Cardiovasc Imaging. 2020;13(6):1299-310. doi: 10.1016/j.jcmg.2020.03.010.

158. Forouzannia SA, Alavi SRR, Forouzannia SM, Abdulla J, Ioannou A, Francese G, et al. Prognostic Value of CMR Parametric Mapping in Cardiac Amyloidosis: An Updated Systematic Review and Meta-Analysis. Open Heart. 2025;12(2):e003551. doi: 10.1136/openhrt-2025-003551.

159. Martinez-Naharro A, Kotecha T, Norrington K, Boldrini M, Rezk T, Quarta C, et al. Native T1 and Extracellular Volume in Transthyretin Amyloidosis. JACC Cardiovasc Imaging. 2019;12(5):810-9. doi: 10.1016/j.jcmg.2018.02.006.

160. Fontana M, Banypersad SM, Treibel TA, Maestrini V, Sado DM, White SK, et al. Native T1 Mapping in Transthyretin Amyloidosis. JACC Cardiovasc Imaging. 2014;7(2):157-65. doi: 10.1016/j.jcmg.2013.10.008.

161. Martinez-Naharro A, Patel R, Kotecha T, Karia N, Ioannou A, Petrie A, et al. Cardiovascular Magnetic Resonance in Light-Chain Amyloidosis to Guide Treatment. Eur Heart J. 2022;43(45):4722-35. doi: 10.1093/eurheartj/ehac363.

162. Cuddy SAM, Jerosch-Herold M, Falk RH, Kijewski MF, Singh V, Ruberg FL, et al. Myocardial Composition in Light-Chain Cardiac Amyloidosis More Than 1 Year after Successful Therapy. JACC Cardiovasc Imaging. 2022;15(4):594-603. doi: 10.1016/j.jcmg.2021.09.032.

163. Ioannou A, Patel RK, Martinez-Naharro A, Razvi Y, Porcari A, Rauf MU, et al. Tracking Treatment Response in Cardiac Light-Chain Amyloidosis with Native T1 Mapping. JAMA Cardiol. 2023;8(9):848-52. doi: 10.1001/jamacardio.2023.2010.

164. Patel RK, Ioannou A, Sheikh A, Razvi Y, Mansell J, Martinez-Naharro A, et al. Transthyretin Amyloid Cardiomyopathy: Natural History and Treatment Response Assessed by Cardiovascular Magnetic Resonance. Eur Heart J. 2025;46(46):5049-58. doi: 10.1093/eurheartj/ehaf412.

165. Quinaglia T, Bukhari S, Kikuchi DS, Bau AA, Martins CNG, Sharma K, et al. How to Use Imaging: Cardiac Magnetic Resonance Imaging in Heart Failure with Preserved Ejection Fraction: A Stepwise Differential Diagnosis Approach. Circ Cardiovasc Imaging. 2026;19(2):e019000. doi: 10.1161/CIRCIMAGING.125.019000.

166. Kikuchi DS, Quinaglia T, Bukhari S, Sharma K, Coelho-Filho OR, Hays AG. Cardiac Magnetic Resonance Imaging in Heart Failure with Preserved Ejection Fraction. Circ Cardiovasc Imaging. 2025;18(9):e018519. doi: 10.1161/CIRCIMAGING.125.018519.

167. Cameli M, Pieroni M, Pastore MC, Brucato A, Castelletti S, Crotti L, et al. The Role of Cardiovascular Multimodality Imaging in the Evaluation of Anderson-Fabry Disease: from Early Diagnosis to Therapy Monitoring. Eur Heart J Cardiovasc Imaging. 2025;26(5):814-29. doi: 10.1093/ehjci/jeaf038.

168. Aquaro GD, De Gori C, Faggioni L, Parisella ML, Aringhieri G, Cioni D, et al. Cardiac Magnetic Resonance in Fabry Disease: Morphological, Functional, and Tissue Features. Diagnostics. 2022;12(11):2652. doi: 10.3390/diagnostics12112652.

169. Ponsiglione A, De Giorgi M, Ascione R, Nappi C, Sanduzzi L, Pisani A, et al. Advanced CMR Techniques in Anderson-Fabry Disease: State of the Art. Diagnostics. 2023;13(15):2598. doi: 10.3390/diagnostics13152598.

170. Lanzillo C, Fedele E, Martino A, Ferrazza A, Fusco A, Silvetti E, et al. Cardiac Magnetic Resonance in Fabry Disease. Eur Heart J Suppl. 2023;25(Suppl C):C200-C204. doi: 10.1093/eurheartjsupp/suad045.

171. Nordin S, Kozor R, Medina-Menacho K, Abdel-Gadir A, Baig S, Sado DM, et al. Proposed Stages of Myocardial Phenotype Development in Fabry Disease. JACC Cardiovasc Imaging. 2019;12(8 Pt 2):1673-83. doi: 10.1016/j.jcmg.2018.03.020.

172. Vijapurapu R, Baig S, Nordin S, Augusto JB, Price AM, Wheeldon N, et al. Longitudinal Assessment of Cardiac Involvement in Fabry Disease using Cardiovascular Magnetic Resonance Imaging. JACC Cardiovasc Imaging. 2020;13(8):1850-2. doi: 10.1016/j.jcmg.2020.03.004.

173. Wei X, Zhao L, Xie J, Liu Y, Du Z, Zhong X, et al. Cardiac Phenotype Characterization at MRI in Patients with Danon Disease: A Retrospective Multicenter Case Series. Radiology. 2021;299(2):303-10. doi: 10.1148/radiol.2021203996.

174. Lotan D, Salazar-Mendiguchía J, Mogensen J, Rathore F, Anastasakis A, Kaski J, et al. Clinical Profile of Cardiac Involvement in Danon Disease: A Multicenter European Registry. Circ Genom Precis Med. 2020;13(6):e003117. doi: 10.1161/CIRCGEN.120.003117.

175. Rigolli M, Kahn AM, Brambatti M, Contijoch FJ, Adler ED. Cardiac Magnetic Resonance Imaging in Danon Disease Cardiomyopathy. JACC Cardiovasc Imaging. 2021;14(2):514-6. doi: 10.1016/j.jcmg.2020.08.011.

176. Hanneman K. Cardiac MRI in Danon Disease: Sex-specific Differences and Characteristic Imaging Findings. Radiology. 2021;299(2):311-2. doi: 10.1148/radiol.2021210249.

177. D'souza RS, Levandowski C, Slavov D, Graw SL, Allen LA, Adler E, et al. Danon Disease: Clinical Features, Evaluation, and Management. Circ Heart Fail. 2014;7(5):843-9. doi: 10.1161/CIRCHEARTFAILURE.114.001105.

178. Yang Z, McMahon CJ, Smith LR, Bersola J, Adesina AM, Breinholt JP, et al. Danon Disease as an Underrecognized Cause of Hypertrophic Cardiomyopathy in Children. Circulation. 2005;112(11):1612-7. doi: 10.1161/CIRCULATIONAHA.105.546481.

179. Cummings KW, Bhalla S, Javidan-Nejad C, Bierhals AJ, Gutierrez FR, Woodard PK. A Pattern-Based Approach to Assessment of Delayed Enhancement in Nonischemic Cardiomyopathy at MR Imaging. Radiographics. 2009;29(1):89-103. doi: 10.1148/rg.291085052.

180. Suzuki H, Morita Y, Saito R, Tatebe S, Niihori T, Saiki Y, et al. Detection of Intracellular Histological Abnormalities using Cardiac Magnetic Resonance T1 Mapping in Patients with Danon Disease: A Case Series. Eur Heart J Case Rep. 2021;5(5):ytab145. doi: 10.1093/ehjcr/ytab145.

181. Zhang Y, Zhao R, Yuan Y, Yu Y, Liu B, Li X. Clinical Manifestations and MRI Features of Danon Disease: A Case Series. BMC Cardiovasc Disord. 2023;23(1):397. doi: 10.1186/s12872-023-03356-y.

182. van der Ploeg AT, Reuser AJ. Pompe's Disease. Lancet. 2008;372(9646):1342-53. doi: 10.1016/S0140-6736(08)61555-X.

183. Kishnani PS, Hwu WL, Mandel H, Nicolino M, Yong F, Corzo D, et al. A Retrospective, Multinational, Multicenter Study on the Natural History of Infantile-Onset POMPE disease. J Pediatr. 2006;148(5):671-6. doi: 10.1016/j.jpeds.2005.11.033.

184. Sarah B, Giovanna B, Emanuela K, Nadi N, Josè V, Alberto P. Clinical Efficacy of the Enzyme Replacement Therapy in Patients with Late-Onset Pompe Disease: A Systematic Review and a Meta-Analysis. J Neurol. 2022;269(2):733-41. doi: 10.1007/s00415-021-10526-5.

185. Zhong Y, Zhang W, Fan W. Hypertrophy Cardiomyopathy: A Case of Infantile-Onset Pompe Disease in Cardiac Magnetic Resonance Findings. Heliyon. 2023;9(7):e18330. doi: 10.1016/j.heliyon.2023.e18330.

186. Zhu Y, Liu X, Hu L, Guo Y, Wen L. Cardiovascular Magnetic Resonance Abnormalities in an Infantile-Onset Pompe Disease. Eur Heart J Cardiovasc Imaging. 2025;26(5):935. doi: 10.1093/ehjci/jeaf006.

187. Barker PC, Pasquali SK, Darty S, Ing RJ, Li JS, Kim RJ, et al. Use of Cardiac Magnetic Resonance Imaging to Evaluate Cardiac Structure, Function and Fibrosis in Children with Infantile Pompe Disease on Enzyme Replacement Therapy. Mol Genet Metab. 2010;101(4):332-7. doi: 10.1016/j.ymgme.2010.07.011.

188. Wang W, Zhang X, Lyu J, Yan F, Lou X. Assessing Gene Therapy Efficacy in Infantile-Onset Pompe Disease: Myocardial Native T1 Values of CMR. JACC Case Rep. 2024;29(16):102446. doi: 10.1016/j.jaccas.2024.102446.

189. Boentert M, Florian A, Dräger B, Young P, Yilmaz A. Pattern and Prognostic Value of Cardiac Involvement in Patients with Late-Onset Pompe Disease: A Comprehensive Cardiovascular Magnetic Resonance Approach. J Cardiovasc Magn Reson. 2016;18(1):91. doi: 10.1186/s12968-016-0311-9.

190. Carlier PG, Azzabou N, Sousa PL, Hicks A, Boisserie JM, Amadon A, et al. Skeletal Muscle Quantitative Nuclear Magnetic Resonance Imaging Follow-Up of Adult Pompe Patients. J Inherit Metab Dis. 2015;38(3):565-72. doi: 10.1007/s10545-015-9825-9.

191. Moses SW, Wanderman KL, Myroz A, Frydman M. Cardiac Involvement in Glycogen Storage Disease Type III. Eur J Pediatr. 1989;148(8):764-6. doi: 10.1007/BF00443106.

192. Aksu T, Colak A, Tufekcioglu O. Cardiac Involvement in Glycogen Storage Disease Type IV: Two Cases and the Two Ends of a Spectrum. Case Rep Med. 2012;2012:764286. doi: 10.1155/2012/764286.

193. Ndugga-Kabuye MK, Maleszewski J, Chanprasert S, Smith KD. Glycogen Storage Disease Type IV: Dilated Cardiomyopathy as the Isolated Initial Presentation in an Adult Patient. BMJ Case Rep. 2019;12(9):e230068. doi: 10.1136/bcr-2019-230068.

194. Lyo S, Miles J, Meisner J, Guelfguat M. Case Report: Adult-Onset Manifesting Heterozygous Glycogen Storage Disease Type IV with Dilated Cardiomyopathy and Absent Late Gadolinium Enhancement on Cardiac Magnetic Resonance Imaging. Eur Heart J Case Rep. 2020;4(3):1-6. doi: 10.1093/ehjcr/ytaa078.

195. Wang J, Pu L, Han Y, Chen Y. Glycogen Storage Disease with Massive Left Ventricular Hypertrophy and Increased Native T1: A Case Report. Eur Heart J Case Rep. 2023;7(9):ytad458. doi: 10.1093/ehjcr/ytad458.

196. Borowiec A, Ozdowska P, Rosinska M, Zebrowska AM, Jagiello-Gruszfeld A, Jasek S, et al. Coronary Artery Calcium Score and Other Risk Factors in Patients at Moderate and High Risk of Cancer Therapy-Related Cardiovascular Toxicity. Cardiooncology. 2024;10(1):64. doi: 10.1186/s40959-024-00266-6.

197. van der Steld LP, Rocha MS, Ladeia AMT, Livramento HL, Campos GB, Darrieux FCDC, et al. PRKAG2 Syndrome, a Rare Hypertrophic Cardiomyopathy: A Brazilian Long-Term Follow-Up with Extracardiac Disorders. Einstein. 2024;22:eAO0549. doi: 10.31744/einstein_journal/2024AO0549.

198. Pöyhönen P, Hiippala A, Ollila L, Kaasalainen T, Hänninen H, Heliö T, et al. Cardiovascular Magnetic Resonance Findings in Patients with PRKAG2 Gene Mutations. J Cardiovasc Magn Reson. 2015;17:89. doi: 10.1186/s12968-015-0192-3.

199. Wang J, Li X, Xu Y. Cardiac MR Manifestations in Two Cases of PRKAG2 Mutations in a Chinese Family. Int J Cardiovasc Imaging. 2020;36(8):1527-31. doi: 10.1007/s10554-020-01848-y.

200. Mocumbi AO. Endomyocardial Fibrosis: A form of Endemic Restrictive Cardiomyopathy. Glob Cardiol Sci Pract. 2012;2012(1):11. doi: 10.5339/gcsp.2012.11.

201. Salemi VM, Rochitte CE, Shiozaki AA, Andrade JM, Parga JR, Ávila LF, et al. Late Gadolinium Enhancement Magnetic Resonance Imaging in the Diagnosis and Prognosis of Endomyocardial Fibrosis Patients. Circ Cardiovasc Imaging. 2011;4(3):304-11. doi: 10.1161/CIRCIMAGING.110.950675.

202. Sibley CT, Noureldin RA, Gai N, Nacif MS, Liu S, Turkbey EB, et al. T1 Mapping in Cardiomyopathy at Cardiac MR: Comparison with Endomyocardial Biopsy. Radiology. 2012;265(3):724-32. doi: 10.1148/radiol.12112721.

203. Gonzalez-Bartol E, Cecconi A, Diez-Villanueva P, Olivera MJ, Jimenez-Borreguero LJ, Alfonso F. T1 Mapping in the Assessment of Endomyocardial Fibrosis. Int J Cardiovasc Imaging. 2021;37(1):267-8. doi: 10.1007/s10554-020-01955-w.

204. Ugander M, Oki AJ, Hsu LY, Kellman P, Greiser A, Aletras AH, et al. Extracellular Volume Imaging by Magnetic Resonance Imaging Provides Insights Into Overt and Sub-Clinical Myocardial Pathology. Eur Heart J. 2012;33(10):1268-78. doi: 10.1093/eurheartj/ehr481.

205. Puntmann VO, Carr-White G, Jabbour A, Yu CY, Gebker R, Kelle S, et al. T1-Mapping and Outcome in Nonischemic Cardiomyopathy: All-Cause Mortality and Heart Failure. JACC Cardiovasc Imaging. 2016;9(1):40-50. doi: 10.1016/j.jcmg.2015.12.001.

206. Scolari FL, Garbin HI, Beuren TMA, Matheus FC, Mourilhe-Rocha R, Bittencourt MI. Genetics of the Cardiomyopathies: A Review for the Cardiologist. ABC Heart Fail Cardiomyop. 2024;4(3):e20240047. doi: 10.36660/abchf.20240047.

207. Eda Y, Nabeta T, Iikura S, Takigami Y, Fujita T, Iida Y, et al. Non-Dilated Left Ventricular Cardiomyopathy vs. Dilated Cardiomyopathy: Clinical Background and Outcomes. ESC Heart Fail. 2024;11(3):1463-71. doi: 10.1002/ehf2.14711.

208. Castrichini M, Eldemire R, Groves DW, Taylor MR, Miyamoto S, Mestroni L. Clinical and Genetic Features of Arrhythmogenic Cardiomyopathy: Diagnosis, Management and the Heart Failure Perspective. Prog Pediatr Cardiol. 2021;63:101459. doi: 10.1016/j.ppedcard.2021.101459.

209. Blaszczyk E, Gröschel J, Schulz-Menger J. Role of CMR Imaging in Diagnostics and Evaluation of Cardiac Involvement in Muscle Dystrophies. Curr Heart Fail Rep. 2021;18(4):211-24. doi: 10.1007/s11897-021-00521-2.

210. Topriceanu CC, Al-Farih M, Joy G, Chan F, Webber M, Ilie-Ablachim DC, et al. The Cardiovascular Magnetic Resonance Phenotype of Lamin Heart Disease. JACC Cardiovasc Imaging. 2025;18(6):644-60. doi: 10.1016/j.jcmg.2025.01.004.

211. Lota AS, Hazebroek MR, Theotokis P, Wassall R, Salmi S, Halliday BP, et al. Genetic Architecture of Acute Myocarditis and the Overlap with Inherited Cardiomyopathy. Circulation. 2022;146(15):1123-34. doi: 10.1161/CIRCULATIONAHA.121.058457.

212. Asatryan B, Asimaki A, Landstrom AP, Khanji MY, Odening KE, Cooper LT, et al. Inflammation and Immune Response in Arrhythmogenic Cardiomyopathy: State-of-the-Art Review. Circulation. 2021;144(20):1646-55. doi: 10.1161/CIRCULATIONAHA.121.055890.

213. Ammirati E, Raimondi F, Piriou N, Sardo Infirri L, Mohiddin SA, Mazzanti A, et al. Acute Myocarditis Associated with Desmosomal Gene Variants. JACC Heart Fail. 2022;10(10):714-27. doi: 10.1016/j.jchf.2022.06.013.

214. Bariani R, Rigato I, Cipriani A, Bueno Marinas M, Celeghin R, Basso C, et al. Myocarditis-like Episodes in Patients with Arrhythmogenic Cardiomyopathy: A Systematic Review on the So-Called Hot-Phase of the Disease. Biomolecules. 2022;12(9):1324. doi: 10.3390/biom12091324.

215. Bakogiannis C, Mouselimis D, Tsarouchas A, Papatheodorou E, Vassilikos VP, Androulakis E. Hypertrophic Cardiomyopathy or Athlete's Heart? A Systematic Review of Novel Cardiovascular Magnetic Resonance Imaging Parameters. Eur J Sport Sci. 2023;23(1):143-54. doi: 10.1080/17461391.2021.2001576.

216. Daems JJN, Verwijs SM, van Diepen MA, van Hattum JC, van Luijk RD, Moen MH, et al. Native T1 Mapping Times are Strongly Influenced by Elite Athlete Status. Eur Heart J Cardiovasc Imaging. 2025;26(7):1208-16. doi: 10.1093/ehjci/jeaf123.

217. Graham-Brown MP, McCann GP. T1 Mapping in Athletes: A Novel Tool to Differentiate Physiological Adaptation from Pathology? Circ Cardiovasc Imaging. 2016;9(4):e004706. doi: 10.1161/CIRCIMAGING.116.004706.

218. Prosperi S, Monosilio S, Lemme E, Filomena D, Penza M, Birtolo LI, et al. CMR Native T1 and T2 Mapping in Olympic Athletes: The Influence of Sports Discipline and Sex. Eur Heart J Cardiovasc Imaging. 2024;26(1):89-95. doi: 10.1093/ehjci/jeae247.

219. Görmeli CA, Görmeli G, Yağmur J, Özdemir ZM, Kahraman AS, Çolak C, et al. Assessment of Myocardial Changes in Athletes with Native T1 Mapping and Cardiac Functional Evaluation using 3 T MRI. Int J Cardiovasc Imaging. 2016;32(6):975-81. doi: 10.1007/s10554-016-0866-4.

220. Wu LM, An DL, Yao QY, Ou YZ, Lu Q, Jiang M, et al. Hypertrophic Cardiomyopathy and Left Ventricular Hypertrophy in Hypertensive Heart Disease with Mildly Reduced or Preserved Ejection Fraction: Insight from Altered Mechanics and Native T1 Mapping. Clin Radiol. 2017;72(10):835-43. doi: 10.1016/j.crad.2017.04.019.

221. Tian Z, Jin S, Huo H, Zheng Y, Li Y, Liu H, et al. Myocardial Hypertrophy: The Differentiation of Uremic, Hypertensive, and Hypertrophic Cardiomyopathies by Cardiac MRI. Insights Imaging. 2024;15(1):190. doi: 10.1186/s13244-024-01770-0.

222. Lee H, Park JB, Yoon YE, Park EA, Kim HK, Lee W, et al. Noncontrast Myocardial T1 Mapping by Cardiac Magnetic Resonance Predicts Outcome in Patients with Aortic Stenosis. JACC Cardiovasc Imaging. 2018;11(7):974-83. doi: 10.1016/j.jcmg.2017.09.005.

223. Hwang IC, Kim HK, Park JB, Park EA, Lee W, Lee SP, et al. Aortic Valve Replacement-Induced Changes in Native T1 are Related to Prognosis in Severe Aortic Stenosis: T1 Mapping Cardiac Magnetic Resonance Imaging Study. Eur Heart J Cardiovasc Imaging. 2020;21(6):653-63. doi: 10.1093/ehjci/jez201.

224. Backhaus SJ, Lange T, Beuthner BE, Topci R, Wang X, Kowallick JT, et al. Real-Time Cardiovascular Magnetic Resonance T1 and Extracellular Volume Fraction Mapping for Tissue Characterisation in Aortic Stenosis. J Cardiovasc Magn Reson. 2020;22(1):46. doi: 10.1186/s12968-020-00632-0.

225. Lee SP, Lee W, Lee JM, Park EA, Kim HK, Kim YJ, et al. Assessment of Diffuse Myocardial Fibrosis by using MR Imaging in Asymptomatic Patients with Aortic Stenosis. Radiology. 2015;274(2):359-69. doi: 10.1148/radiol.14141120.

226. Milano AD, Faggian G, Dodonov M, Golia G, Tomezzoli A, Bortolotti U, et al. Prognostic Value of Myocardial Fibrosis in Patients with Severe Aortic Valve Stenosis. J Thorac Cardiovasc Surg. 2012;144(4):830-7. doi: 10.1016/j.jtcvs.2011.11.024.

227. Everett RJ, Treibel TA, Fukui M, Lee H, Rigolli M, Singh A, et al. Extracellular Myocardial Volume in Patients with Aortic Stenosis. J Am Coll Cardiol. 2020;75(3):304-16. doi: 10.1016/j.jacc.2019.11.032.

228. Kwak S, Everett RJ, Treibel TA, Yang S, Hwang D, Ko T, et al. Markers of Myocardial Damage Predict Mortality in Patients with Aortic Stenosis. J Am Coll Cardiol. 2021;78(6):545-58. doi: 10.1016/j.jacc.2021.05.047.

229. Senapati A, Malahfji M, Debs D, Yang EY, Nguyen DT, Graviss EA, et al. Regional Replacement and Diffuse Interstitial Fibrosis in Aortic Regurgitation: Prognostic Implications from Cardiac Magnetic Resonance. JACC Cardiovasc Imaging. 2021;14(11):2170-82. doi: 10.1016/j.jcmg.2021.04.028.

230. Lopes BBC, Kwon DH, Shah DJ, Lesser JR, Bapat V, Enriquez-Sarano M, et al. Importance of Myocardial Fibrosis in Functional Mitral Regurgitation: From Outcomes to Decision-Making. JACC Cardiovasc Imaging. 2021;14(4):867-78. doi: 10.1016/j.jcmg.2020.10.027.

231. Marsan NA, Delgado V, Shah DJ, Pellikka P, Bax JJ, Treibel T, et al. Valvular Heart Disease: Shifting the Focus to the Myocardium. Eur Heart J. 2023;44(1):28-40. doi: 10.1093/eurheartj/ehac504.

232. Edwards NC, Moody WE, Yuan M, Weale P, Neal D, Townend JN, et al. Quantification of Left Ventricular Interstitial Fibrosis in Asymptomatic Chronic Primary Degenerative Mitral Regurgitation. Circ Cardiovasc Imaging. 2014;7(6):946-53. doi: 10.1161/CIRCIMAGING.114.002397.

233. Kitkungvan D, Yang EY, El Tallawi KC, Nagueh SF, Nabi F, Khan MA, et al. Extracellular Volume in Primary Mitral Regurgitation. JACC Cardiovasc Imaging. 2021;14(6):1146-60. doi: 10.1016/j.jcmg.2020.10.010.

234. Kitkungvan D, Yang EY, El Tallawi KC, Nagueh SF, Nabi F, Khan MA, et al. Prognostic Implications of Diffuse Interstitial Fibrosis in Asymptomatic Primary Mitral Regurgitation. Circulation. 2019;140(25):2122-24. doi: 10.1161/CIRCULATIONAHA.119.043250.

235. Guglielmo M, Fusini L, Muscogiuri G, Baessato F, Loffreno A, Cavaliere A, et al. T1 Mapping and Cardiac Magnetic Resonance Feature Tracking In Mitral Valve Prolapse. Eur Radiol. 2021;31(2):1100-9. doi: 10.1007/s00330-020-07140-w.

236. Pavon AG, Arangalage D, Pascale P, Hugelshofer S, Rutz T, Porretta AP, et al. Myocardial Extracellular Volume by T1 Mapping: A New Marker of Arrhythmia in Mitral Valve Prolapse. J Cardiovasc Magn Reson. 2021;23(1):102. doi: 10.1186/s12968-021-00797-2.

237. Sato H. Takotsubo-Type Cardiomyopathy due to Multivessel Spasm. In: Kodama K, Haze K, Hori M, editors. Clinical Aspect of Myocardial Injury: From Ischemia to Heart Failure. Tokyo: Kagaku Hyouronsha; 1990. p. 56-64.

238. Bybee KA, Prasad A, Barsness GW, Lerman A, Jaffe AS, Murphy JG, et al. Clinical Characteristics and Thrombolysis in Myocardial Infarction Frame Counts in Women with Transient Left Ventricular Apical Ballooning Syndrome. Am J Cardiol. 2004;94(3):343-6. doi: 10.1016/j.amjcard.2004.04.030.

239. Citro R, Rigo F, D'Andrea A, Ciampi Q, Parodi G, Provenza G, et al. Echocardiographic Correlates of Acute Heart Failure, Cardiogenic Shock, and In-Hospital Mortality in Tako-Tsubo Cardiomyopathy. JACC Cardiovasc Imaging. 2014;7(2):119-29. doi: 10.1016/j.jcmg.2013.09.020.

240. Vermes E, Berradja N, Saab I, Genet T, Bertrand P, Pucheux J, et al. Cardiac Magnetic Resonance for Assessment of Cardiac Involvement in Takotsubo Syndrome: Do we still Need Contrast Administration? Int J Cardiol. 2020;308:93-5. doi: 10.1016/j.ijcard.2020.03.039.

241. Gil KE, Truong VT, Zareba KM, Varghese J, Simonetti OP, Rajpal S. Parametric Mapping by Cardiovascular Magnetic Resonance Imaging in Sudden Cardiac Arrest Survivors. Int J Cardiovasc Imaging. 2023;39(8):1547-55. doi: 10.1007/s10554-023-02864-4.

242. Aikawa Y, Noguchi T, Morita Y, Tateishi E, Kono A, Miura H, et al. Clinical Impact of Native T1 Mapping for Detecting Myocardial Impairment in Takotsubo Cardiomyopathy. Eur Heart J Cardiovasc Imaging. 2019;20(10):1147-55. doi: 10.1093/ehjci/jez034.

243. Arcari L, Camastra G, Ciolina F, Limite LR, Danti M, Sclafani M, et al. Myocardial Oedema Contributes to Interstitial Expansion and Associates with Mechanical and Electrocardiographic Changes in Takotsubo Syndrome: A CMR T1 and T2 Mapping Study. Eur Heart J Cardiovasc Imaging. 2023;24(8):1082-91. doi: 10.1093/ehjci/jead035.

244. Kozak MF, Redington A, Yoo SJ, Seed M, Greiser A, Grosse-Wortmann L. Diffuse Myocardial Fibrosis Following Tetralogy of Fallot Repair: A T1 mapping Cardiac Magnetic Resonance Study. Pediatr Radiol. 2014;44(4):403-9. doi: 10.1007/s00247-013-2840-9.

245. Broberg CS, Chugh SS, Conklin C, Sahn DJ, Jerosch-Herold M. Quantification of Diffuse Myocardial Fibrosis and its Association with Myocardial Dysfunction in Congenital Heart Disease. Circ Cardiovasc Imaging. 2010;3(6):727-34. doi: 10.1161/CIRCIMAGING.108.842096.

246. Voges I, Raimondi F, McMahon CJ, Ait-Ali L, Babu-Narayan SV, Botnar RM, et al. Clinical Impact of Novel Cardiovascular Magnetic Resonance Technology on Patients with Congenital Heart Disease: A Scientific Statement of the Association for European Pediatric and Congenital Cardiology and the European Association of Cardiovascular Imaging of the European Society of Cardiology. Eur Heart J Cardiovasc Imaging. 2024;25(12):e274-94. doi: 10.1093/ehjci/jeae172.

247. Pagano JJ, Lam CZ. T1 Mapping of the Right Ventricle in Congenital Heart Disease: A Focus on Pediatrics. Pediatr Radiol. 2025;55(11):2368-80. doi: 10.1007/s00247-025-06278-3.

248. Riesenkampff E, Luining W, Seed M, Chungsomprasong P, Manlhiot C, Elders B, et al. Increased Left Ventricular Myocardial Extracellular Volume is Associated with Longer Cardiopulmonary Bypass Times, Biventricular Enlargement and Reduced Exercise Tolerance in Children after Repair of Tetralogy of Fallot. J Cardiovasc Magn Reson. 2016;18(1):75. doi: 10.1186/s12968-016-0290-x.

249. Haggerty CM, Suever JD, Pulenthiran A, Mejia-Spiegeler A, Wehner GJ, Jing L, et al. Association between Left Ventricular Mechanics and Diffuse Myocardial Fibrosis in Patients with Repaired Tetralogy of Fallot: A Cross-Sectional Study. J Cardiovasc Magn Reson. 2017;19(1):100. doi: 10.1186/s12968-017-0410-2.

250. Chen CA, Dusenbery SM, Valente AM, Powell AJ, Geva T. Myocardial ECV Fraction Assessed by CMR Is Associated With Type of Hemodynamic Load and Arrhythmia in Repaired Tetralogy of Fallot. JACC Cardiovasc Imaging. 2016;9(1):1-10. doi: 10.1016/j.jcmg.2015.09.011.

251. Yim D, Riesenkampff E, Caro-Dominguez P, Yoo SJ, Seed M, Grosse-Wortmann L. Assessment of Diffuse Ventricular Myocardial Fibrosis Using Native T1 in Children with Repaired Tetralogy of Fallot. Circ Cardiovasc Imaging. 2017;10(3):e005695. doi: 10.1161/CIRCIMAGING.116.005695.

252. Rao S, Tseng SY, Pednekar A, Siddiqui S, Kocaoglu M, Fares M, et al. Myocardial Parametric Mapping by Cardiac Magnetic Resonance Imaging in Pediatric Cardiology and Congenital Heart Disease. Circ Cardiovasc Imaging. 2022;15(1):e012242. doi: 10.1161/CIRCIMAGING.120.012242.

253. Shehu N, Meierhofer C, Messroghli D, Mkrtchyan N, Martinoff S, Ewert P, et al. Diffuse Fibrosis is Common in the Left, But Not in the Right Ventricle in Patients with Transposition of the Great Arteries Late after Atrial Switch Operation. Int J Cardiovasc Imaging. 2018;34(8):1241-8. doi: 10.1007/s10554-018-1338-9.

254. Broberg CS, Valente AM, Huang J, Burchill LJ, Holt J, van Woerkom R, et al. Myocardial Fibrosis and its Relation to Adverse Outcome in Transposition of the Great Arteries with a Systemic Right Ventricle. Int J Cardiol. 2018;271:60-5. doi: 10.1016/j.ijcard.2018.04.089.

255. Kato A, Riesenkampff E, Yim D, Yoo SJ, Seed M, Grosse-Wortmann L. Pediatric Fontan Patients are at Risk for Myocardial Fibrotic Remodeling and Dysfunction. Int J Cardiol. 2017;240:172-7. doi: 10.1016/j.ijcard.2017.04.073.

256. Ramachandran P, Serai SD, Veldtman GR, Lang SM, Mazur W, Trout AT, et al. Assessment of Liver T1 Mapping in Fontan Patients and its Correlation with Magnetic Resonance Elastography-Derived Liver Stiffness. Abdom Radiol. 2019;44(7):2403-8. doi: 10.1007/s00261-019-01990-9.

257. Lange C, Reichert MJE, Pagano JJ, Seed M, Yoo SJ, Broberg CS, et al. Increased Extracellular Volume in the Liver of Pediatric Fontan Patients. J Cardiovasc Magn Reson. 2019;21(1):39. doi: 10.1186/s12968-019-0545-4.

258. Yang D, Li X, Sun JY, Cheng W, Greiser A, Zhang TJ, et al. Cardiovascular Magnetic Resonance Evidence of Myocardial Fibrosis and its Clinical Significance in Adolescent and Adult Patients with Ebstein's Anomaly. J Cardiovasc Magn Reson. 2018;20(1):69. doi: 10.1186/s12968-018-0488-1.

259. Aly S, Seed M, Yoo SJ, Lam C, Grosse-Wortmann L. Myocardial Fibrosis in Pediatric Patients with Ebstein's Anomaly. Circ Cardiovasc Imaging. 2021;14(3):e011136. doi: 10.1161/CIRCIMAGING.120.011136.

260. Giertzsch T, Jerosch-Herold M, Schneider P, Voges I, Gabbert DD, Wegner P, et al. Non-Invasive Tissue Characterization in Children and Young Adults with Aortic Coarctation-an MRI-Based Prospective Study. Cardiovasc Diagn Ther. 2025;15(2):375-87. doi: 10.21037/cdt-24-497.

261. Hajjar LA, Costa IBSDSD, Lopes MACQ, Hoff PMG, Diz MDPE, Fonseca SMR, et al. Brazilian Cardio-Oncology Guideline - 2020. Arq Bras Cardiol. 2020;115(5):1006-43. doi: 10.36660/abc.20201006.

262. Cardinale D, Colombo A, Bacchiani G, Tedeschi I, Meroni CA, Veglia F, et al. Early Detection of Anthracycline Cardiotoxicity and Improvement with Heart Failure Therapy. Circulation. 2015;131(22):1981-8. doi: 10.1161/CIRCULATIONAHA.114.013777.

263. Farolfi A, Melegari E, Aquilina M, Scarpi E, Ibrahim T, Maltoni R, et al. Trastuzumab-Induced Cardiotoxicity in Early Breast Cancer Patients: A Retrospective Study of Possible Risk and Protective Factors. Heart. 2013;99(9):634-9. doi: 10.1136/heartjnl-2012-303151.

264. Jafari F, Safaei AM, Hosseini L, Asadian S, Kamangar TM, Zadehbagheri F, et al. The Role of Cardiac Magnetic Resonance Imaging in the Detection and Monitoring of Cardiotoxicity in Patients with Breast Cancer after Treatment: A Comprehensive Review. Heart Fail Rev. 2021;26(3):679-97. doi: 10.1007/s10741-020-10028-y.

265. Giusca S, Korosoglou G, Montenbruck M, Geršak B, Schwarz AK, Esch S, et al. Multiparametric Early Detection and Prediction of Cardiotoxicity using Myocardial Strain, T1 and T2 Mapping, and Biochemical Markers: A Longitudinal Cardiac Resonance Imaging Study During 2 Years of Follow-Up. Circ Cardiovasc Imaging. 2021;14(6):e012459. doi: 10.1161/CIRCIMAGING.121.012459.

266. Hong YJ, Park HS, Park JK, Han K, Park CH, Kim TK, et al. Early Detection and Serial Monitoring of Anthracycline-Induced Cardiotoxicity using T1-mapping Cardiac Magnetic Resonance Imaging: An Animal Study. Sci Rep. 2017;7(1):2663. doi: 10.1038/s41598-017-02627-x.

267. da Silva Costa IBS, Assunção BMBL, Cruz CBBV. Pavani AVB, Pereira J, Buccheri V et al. Cardiac Magnetic Resonance with Myocardial Strain as a Predictor of Anthracycline-Induced Cardiotoxicity in Patients with Lymphoma: A Prospective Multimodality Study. Cardio-Oncology. 2026. doi: 10.1186/s40959-026-00540-9.

268. Altaha MA, Nolan M, Marwick TH, Somerset E, Houbois C, Amir E, et al. Can Quantitative CMR Tissue Characterization Adequately Identify Cardiotoxicity during Chemotherapy?: Impact of Temporal and Observer Variability. JACC Cardiovasc Imaging. 2020;13(4):951-62. doi: 10.1016/j.jcmg.2019.10.016.

269. Tong X, Li VW, Liu AP, So EK, Chan Q, Ho KK, et al. Cardiac Magnetic Resonance T1 Mapping in Adolescent and Young Adult Survivors of Childhood Cancers. Circ Cardiovasc Imaging. 2019;12(4):e008453. doi: 10.1161/CIRCIMAGING.118.008453.

270. Mohamed AA, Elmancy LY, Abulola SM, Al-Qattan SA, Ibrahim MIM, Maayah ZH. Assessment of Native Myocardial T1 Mapping for Early Detection of Anthracycline-Induced Cardiotoxicity in Patients with Cancer: a Systematic Review and Meta-analysis. Cardiovasc Toxicol. 2024;24(6):563-75. doi: 10.1007/s12012-024-09866-1.

271. Musella F, Librera M, Sibilio G, Boccalatte M, Tagliamonte G, Cavaglià E, et al. Cardiovascular Magnetic Resonance Parametric Techniques to Characterize Myocardial Effects of Anthracycline Therapy in Adults with Normal Left Ventricular Ejection Fraction: A Systematic Review and Meta-Analysis. Curr Probl Cardiol. 2024;49(7):102609. doi: 10.1016/j.cpcardiol.2024.102609.

272. Li X, Shen H, Peng Y, Miao Z, Tu C, Zhang X, et al. The Additional Value of Myocardial T1ρ Mapping to T1 and T2 Mapping for Predicting Subsequent Cancer Therapy-Related Cardiac Dysfunction in Breast Cancer Patients who Received Anthracyclines with/without Trastuzumab. Eur J Radiol. 2024;181:111755. doi: 10.1016/j.ejrad.2024.111755.

273. Wang T, Ouyang B, Tang L, Li L, Liu Y. Myocardial Extracellular Volume Derived from Contrast-Enhanced Chest Computed Tomography in Longitudinal Evaluation of Cardiac Toxicity in Patients Treated with Immune Checkpoint Inhibitors. Quant Imaging Med Surg. 2024;14(4):3107-20. doi: 10.21037/qims-23-850.

274. Ricco A, Slade A, Canada JM, Grizzard J, Dana F, Gharai LR, et al. Cardiac MRI utilizing late Gadolinium Enhancement (LGE) and T1 Mapping in the Detection of Radiation Induced Heart Disease. Cardiooncology. 2020;6:6. doi: 10.1186/s40959-020-00061-z.

275. Ntusi NAB, Piechnik SK, Francis JM, Ferreira VM, Matthews PM, Robson MD, et al. Diffuse Myocardial Fibrosis and Inflammation in Rheumatoid Arthritis: Insights from CMR T1 Mapping. JACC Cardiovasc Imaging. 2015;8(5):526-36. doi: 10.1016/j.jcmg.2014.12.025.

276. Muser D, Chahal AA, Selvanayagam JB, Nucifora G. Clinical Applications of Cardiac Magnetic Resonance Parametric Mapping. Diagnostics. 2024;14(16):1816. doi: 10.3390/diagnostics14161816.

277. Guo Q, Wu LM, Wang Z, Shen JY, Su X, Wang CQ, et al. Early Detection of Silent Myocardial Impairment in Drug-Naive Patients with New-Onset Systemic Lupus Erythematosus: A Three-Center Prospective Study. Arthritis Rheumatol. 2018;70(12):2014-24. doi: 10.1002/art.40671.

278. Wang Z, Tang X, Hang C, Gao H, Yang J, Han Y, et al. Differences in Myocardial Involvement between New Onset and Longstanding Systemic Lupus Erythematosus Patients Assessed by Cardiovascular Magnetic Resonance. Eur J Radiol Open. 2024;14:100623. doi: 10.1016/j.ejro.2024.100623.

279. Ntusi NA, Piechnik SK, Francis JM, Ferreira VM, Rai AB, Matthews PM, et al. Subclinical Myocardial Inflammation and Diffuse Fibrosis are Common in Systemic Sclerosis--A Clinical Study using Myocardial T1-Mapping and Extracellular Volume Quantification. J Cardiovasc Magn Reson. 2014;16(1):21. doi: 10.1186/1532-429X-16-21.

280. De Luca G, Palmisano A, Campochiaro C, Vignale D, Cavalli G, Bruno E, et al. Cardiac Magnetic Resonance in Systemic Sclerosis Myocarditis: The Value of T2 Mapping to Detect Myocardial Inflammation. Rheumatology. 2022;61(11):4409-19. doi: 10.1093/rheumatology/keac098.

281. Terrier B, Dechartres A, Gouya H, Ben Arfi M, Bérézne A, Régent A, et al. Cardiac Intravoxel Incoherent Motion Diffusion-Weighted Magnetic Resonance Imaging with T1 Mapping to Assess Myocardial Perfusion and Fibrosis in Systemic Sclerosis: Association with Cardiac Events From a Prospective Cohort Study. Arthritis Rheumatol. 2020;72(9):1571-80. doi: 10.1002/art.41308.

282. Greulich S, Mayr A, Kitterer D, Latus J, Henes J, Steubing H, et al. T1 and T2 Mapping for Evaluation of Myocardial Involvement in Patients with ANCA-Associated Vasculitides. J Cardiovasc Magn Reson. 2017;19(1):6. doi: 10.1186/s12968-016-0315-5.

283. Huber AT, Bravetti M, Lamy J, Bacoyannis T, Roux C, de Cesare A, et al. Non-Invasive Differentiation of Idiopathic Inflammatory Myopathy with Cardiac Involvement from Acute Viral Myocarditis using Cardiovascular Magnetic Resonance Imaging T1 and T2 Mapping. J Cardiovasc Magn Reson. 2018;20(1):11. doi: 10.1186/s12968-018-0430-6.

284. Huang L, Tao Q, Zhao P, Ji S, Jiang J, van der Geest RJ, et al. Using Multi-Parametric Quantitative MRI to Screen for Cardiac Involvement in Patients with Idiopathic Inflammatory Myopathy. Sci Rep. 2022;12(1):9819. doi: 10.1038/s41598-022-13858-y.

285. McAllister HA Jr. Primary Tumors and Cysts of the Heart and Pericardium. Curr Probl Cardiol. 1979;4(2):1-51. doi: 10.1016/0146-2806(79)90008-2.

286. Cresti A, Chiavarelli M, Glauber M, Tanganelli P, Scalese M, Cesareo F, et al. Incidence Rate of Primary Cardiac Tumors: A 14-Year Population Study. J Cardiovasc Med. 2016;17(1):37-43. doi: 10.2459/JCM.0000000000000059.

287. Kim RJ, Wu E, Rafael A, Chen EL, Parker MA, Simonetti O, et al. The Use of Contrast-Enhanced Magnetic Resonance Imaging to Identify Reversible Myocardial Dysfunction. N Engl J Med. 2000;343(20):1445-53. doi: 10.1056/NEJM200011163432003.

288. Gulati A, Jabbour A, Ismail TF, Guha K, Khwaja J, Raza S, et al. Association of Fibrosis with Mortality and Sudden Cardiac Death in Patients with Nonischemic Dilated Cardiomyopathy. JAMA. 2013;309(9):896-908. doi: 10.1001/jama.2013.1363.

289. Paolisso P, Bergamaschi L, Angeli F, Belmonte M, Foà A, Canton L, et al. Cardiac Magnetic Resonance to Predict Cardiac Mass Malignancy: The CMR Mass Score. Circ Cardiovasc Imaging. 2024;17(3):e016115. doi: 10.1161/CIRCIMAGING.123.016115.

290. Bonnes J, Brink M, Nijveldt R. How to Evaluate Cardiac Masses by Cardiovascular Magnetic Resonance Parametric Mapping? Eur Heart J Cardiovasc Imaging. 2023;24(12):1605-7. doi: 10.1093/ehjci/jead221.

291. Nasser SB, Doeblin P, Doltra A, Schnackenburg B, Wassilew K, Berger A, et al. Cardiac Myxomas Show Elevated Native T1, T2 Relaxation Time and ECV on Parametric CMR. Front Cardiovasc Med. 2020;7:602137. doi: 10.3389/fcvm.2020.602137.

292. Yue P, Xu Z, Wan K, Tan Y, Xu Y, Xie X, et al. Multiparametric Mapping by Cardiovascular Magnetic Resonance Imaging in Cardiac Tumors. J Cardiovasc Magn Reson. 2023;25(1):37. doi: 10.1186/s12968-023-00938-9.

293. Caspar T, El Ghannudi S, Ohlmann P, Ohana M, Gangi A, Germain P. Characterization of an Intra-Cardiac Melanoma Metastasis by Magnetic Resonance T1 and T2 Mapping. Int J Cardiovasc Imaging. 2016;32(10):1543-4. doi: 10.1007/s10554-016-0939-4.

294. Ciliberti P, Bordonaro V, Curione D, Perazzolo A, Ciancarella P, Santangelo T, et al. Additional Value of Cardiac Magnetic Resonance Parametric Mapping in Tissue Characterization of Common Benign Paediatric Cardiac Tumours. Eur Heart J Cardiovasc Imaging. 2024;26(1):161-8. doi: 10.1093/ehjci/jeae187.

295. Haider I, Ullah H, Fatima M, Karim MS, Haq FU, Majid A, et al. Tissue Characterization of Benign Cardiac Tumors by Cardiac Magnetic Resonance Imaging, a Review of Core Imaging Protocol and Benign Cardiac Tumors. Front Cardiovasc Med. 2023;10:1009411. doi: 10.3389/fcvm.2023.1009411.

296. Saba SG, Bandettini PW, Shanbhag SM, Spottiswoode BS, Kellman P, Arai AE. Characterization of Cardiac Masses with T1 Mapping. J Cardiovasc Magn Reson. 2015;17(Suppl 1):Q32. doi: 10.1186/1532-429X-17-S1-Q32.

This is an open-access article distributed under the terms of the Creative Commons Attribution License